CHALMERS
UNIVERSITY OF TECHNOLOGY

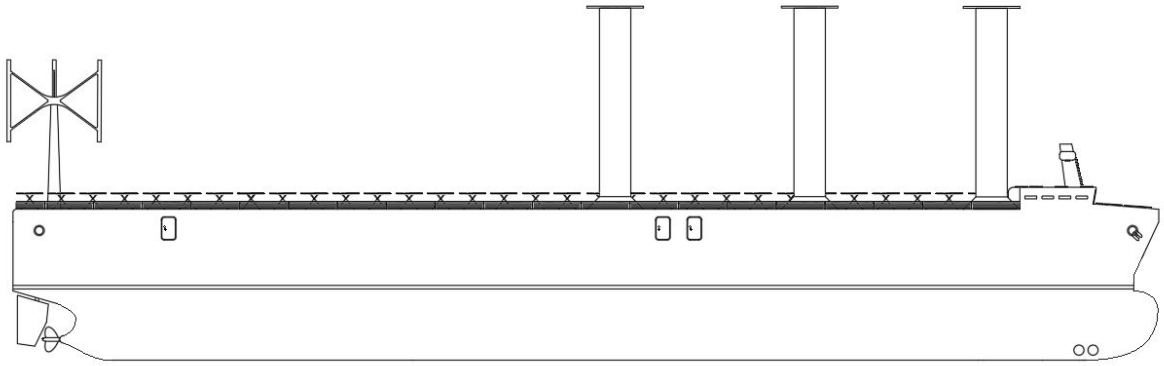

Concept development of a fossil free operated cargo ship

Master's thesis in the International Master´s Programme Naval Architecture and Ocean Engineering

ENRIC JULIÀ LLUIS

Department of Mechanics and Maritime Sciences
CHALMERS UNIVERSITY OF TECHNOLOGY
Gothenburg, Sweden 2019
Master's Thesis 2019/54

MASTER'S THESIS IN THE INTERNATIONAL MASTER'S PROGRAMME IN NAVAL ARCHITECTURE AND OCEAN ENGINEERING

Concept development of a fossil free operated cargo ship

ENRIC JULIÀ LLUIS

Department of Mechanics and Maritime Sciences

Division of Marine Technology

CHALMERS UNIVERSITY OF TECHNOLOGY

Göteborg, Sweden 2019

Concept development of a fossil free operated cargo ship
ENRIC JULIÀ LLUIS

Master's Thesis 2019/54
Department of Mechanics and Maritime Sciences
Division of Marine Technology
Chalmers University of Technology
SE - 412 96 Göteborg
Sweden
Telephone: + 46 (0)31 772 1000

Cover: Side drawing of the fossil free ship concept

Printed by Chalmers Reproservice

Göteborg, Sweden 2019

Concept development of a fossil free operated cargo ship
Master's Thesis in the International Master's Programme in Naval Architecture and Ocean Engineering
ENRIC JULIÀ
Department of Mechanics and Maritime Sciences
Division of Marine Technology
Chalmers University of Technology

Abstract

The reduction of air pollution caused by shipping is of increasing interest. IMO has implemented regulations regarding the contents of sulfides and nitrates in fossil fuels, and also established a long-term proposal to reduce the GHG emissions. The shipping industry has started a process of transition towards cleaner fuels.

This thesis takes one step further by studying the feasibility of a ship concept operating 100% free of fossil fuels, using renewable energy accessible at sea, with all the difficulties in its predictability. The main objective is to develop a simulation tool that can be used to predict the feasibility of a concept ship with a renewable hybrid power system, in each moment of a journey.

The thesis starts with an exhaustive study of technologies and renewable systems available in the market. The most promising renewable propulsion systems and electric energy generators are numerically defined to be implemented in the simulation. A hybrid system is found to be the best choice, with Flettner rotors, a wind propulsion system that generates thrust with a relatively low requirement of energy, as well as photovoltaic solar panels and wind turbine generators for electric production. Finally, numerical methods are integrated into a simulation model that evaluates all renewable technologies.

Simulations are performed for three different routes: from Rotterdam to Houston, Rio de Janeiro to Gothenburg and Los Angeles to Shanghai. The journeys are defined according to real weather conditions data. The results from the analysis give relevant information about the ship journey (time and speed) and the energy balance of the systems.

Results show that in regions with high-intensity winds, the ship speed is high, but the renewable generators onboard cannot supply sufficient energy for the Flettner rotors. On the other hand, for low wind speeds, the ship velocity is small with a surplus of energy generation.

The thesis demonstrates the functionality of the concept on some of the routes, with a high dependency on the weather conditions. It opens the way for future studies to keep the relationship between energy consumption and energy production in balance.

Keywords: CO_2 emissions, photovoltaic panels, ship concept, wind-assisted propulsion, wind turbines.

Table of Contents

Abstract I
Table of Contents III
Preface V
Nomenclature VII
1 Introduction 1
1.1 Background and Motivation of Study 1
1.2 Regulations 2
1.3 Objective and Goals 3
1.4 Assumptions and Delimitations 4
1.5 Outline of the Thesis 5
2 Literature Review 7
2.1 Renewable Propulsion Systems 7
2.1.1 Wind Propulsion 7
2.1.2 Wave Energy 8
2.2 Energy Generation Systems 9
2.2.1 Solar Energy 9
2.2.2 Wind Power 10
2.3 Energy Storage Systems 10
2.4 Ship Concepts 11
2.4.1 Neoline 11
2.4.2 E/S Orcelle 12
2.4.3 NYK Super Eco-Ship 2050 13
2.4.4 E-Ship 1 14
2.5 Evaluation 14
3 Methodology and Feasibility Study 17
3.1 Wind Propulsion 17
3.2 Solar Photovoltaic Energy Production 22
3.2.1 Methodology study of the system 23
3.2.2 Results and discussion for solar photovoltaic system 27
3.3 Wind Turbine Power Generation 33
3.3.1 Methodology study of the wind turbine generator 34
3.3.2 Results and discussion of wind turbine generator 34
3.4 Results and Conclusions 35

4 Concept Design 37
4.1 Ship Considerations 37
4.1.1 Arrangement 37
4.1.2 The electric consumption of the ship 39
4.2 Choice of Routes 39
4.2.1 Rotterdam to Houston 40
4.2.2 Rio de Janeiro to Gothenburg 41
4.2.3 Los Angeles to Shanghai 42
4.3 Concept Simulation 43
4.3.1 Route configuration 43
4.3.2 Flettner rotor wind propulsion 43
4.3.3 Electric power generation 46
5 Results and Discussion 47
5.1 Rotterdam – Houston 47
5.2 Rio de Janeiro – Gothenburg 51
5.3 Los Angeles – Shanghai 54
6 Conclusions 59
7 Future Work 61
8 References 63
Appendix A: Results of simulations from Rotterdam to Houston 67
Appendix B: Results of simulations from Houston to Rotterdam 69
Appendix C: Results of simulations from Rio de Janeiro to Gothenburg 71
Appendix D: Results of simulations from Gothenburg to Rio de Janeiro 74
Appendix E: Results of simulations from Los Angeles to Shanghai 77
Appendix F: Results of simulations from Shanghai to Los Angeles 80

Preface

This thesis is part of the requirements for the master's degree at Chalmers University of Technology, Göteborg, and has been carried out at the Division of Marine Technology, Department of Mechanics and Maritime Sciences, Chalmers University of Technology between January and June of 2019.

First, I would like to thank the supervisor of this master thesis, Fabian Tillig, for offering me the opportunity to participate in such an ambitious project directly related to his study. Also, for the time, advice, and help that he provided me throughout the process.

I want to thank as well to the examiner of this project, Professor Jonas Ringsberg for the support and advice offered during the research that has helped me as an additional guide in the development of my thesis.

Finally, I want to note the support and encouragement from my family and friends without which I could not have done this thesis.

Göteborg June 2019

Enric Julià

Nomenclature

List of Acronyms

ECA	Emission Control Area
EEDI	Energy Efficiency Design Index
EEOI	Energy Efficiency Operational Index
GHG	Greenhouse Gases
IMO	International Maritime Organization
MARPOL	International Convention for the Prevention of Pollution for Ships
MBM	Marked Based Measurements
MEPC	Marine Environmental Protection Committee
WACC	Weighted Average Cost of Capital

List of Unit Abbreviations

deg	degrees
kg	kilograms
kW	kilowatt
kWh	kilowatt-hours/year
m	meters
N	newtons
s	seconds

1 Introduction

The introductory chapter provides a general overview of the challenges the marine sector and the society are facing. In this chapter, the main objectives, delimitations and a general description of the process are defined.

1.1 Background and Motivation of Study

The use of renewable energy for ship propulsion is not a new idea. Until the 19th century, the primary propulsion method was wind energy. With the steam engine revolution, marine technology was reinvented with more trustable and powerful technologies, that set aside the sails in the world of sea transport. The technology evolved, and from the first coal, different fossil fuels appeared in the marine industry (Casson, 1964). Nowadays, driven by rising fuel costs, emission regulations and the changing climate, there is a need to return to those original renewable energy sources (Harrould-Kolieb, 2008).

Transportation is one of the pillars of globalization, and marine transport constitutes the most significant part of the cargo volume. In 2017, global sea trade reached 10.7 billion tones (Zhang 2016 and Hoffmann et al. 2017), corresponding to over 90% of the total global transport volume (Harrould-Kolieb, 2008). Almost all of today's cargo ships are powered by fossil fuel. Fossil fuels provide an outstanding energy density, but at the same time cause high emissions of CO_2, NO_x, and SO_x, all of which contribute to climate change. As an example, between 2007 and 2012, the annual consumption of fossil fuels was between 250 and 325 million tons, resulting in yearly CO_2 emissions of about 740-795 million tons (Atkinson et al., 2018). In 2012, shipping accounted for 2.7% of the global CO_2 emissions, and predictions say that this will increase by 150-250% until 2050 (Margaritou and Tzannatos, 2018). A reduction of greenhouse gas emissions is required, and policies and initiatives for the marine industry to become more sustainable are now under evaluation for the global framework (Hoffmann et al., 2017).

During the last decades, innovations for the reduction of some pollutant gasses, as NOx or Sox, have been introduced. New fuels, with lower contents of sulfurs, scrubbers for the exhaust gasses on vessels or internal modification of marine engines with recirculation of exhaust gasses are examples (Margaritou and Tzannatos, 2018). However, the above solutions do not reduce CO_2 emissions.

According to IMO, it is necessary to reduce the CO_2 emissions between 70 and 100% until 2050, compared to the levels in 2008, and the resurgence of renewable energies in the marine industry is a promising solution (Kam, 2019). For now, those technologies are still under investigation, and the effectivity of a pure renewable system is not proved. However, some initiatives have been already developed and implemented for hybrid systems.

1.2 Regulations

In 1973, IMO created the convention MARPOL, for the need of international understanding for prevention of contaminant practices. MARPOL are regulations to prevent pollution at sea by, e.g., oil, noxious liquid substances, harmful substances carried packaged, sewage, garbage and air pollution. (Becker, 1997). Air pollution regulations started to appear in MARPOL's discussion in 1980, and it was in 1991 when it was introduced on the MEPC conversation (Kam, 2019). The pressure from the shipping industry was high enough for the non-incorporation of GHG on the regulations (Kam, 2019). MEPC established a division between the air pollution gasses like ozone, nitrogen oxide and sulfur dioxide, cause of acid rain and ozone depletion; and gasses that cause climate change, e.g., carbon dioxide. The annex regarding air pollution was finally incorporated in 1997 (MEPC, 2005)(Kam, 2019). In the first instance, MARPOL created regulation 13 for the control of NOx emissions of Marine Diesel Engines. Implementation was gradual, starting in 2005 (Kam, 2019). For the same implementation date, the convention elaborates limitations on SOx contents in fuels. Emissions were restricted to levels under 4.5% in any case, and under 1.5% in Emission Control Areas (ECA's) (MEPC, 2005 and Kam, 2019).

In 2009, MEPC set some non-mandatory measures applicable for the shipping industry to promote its regulations. Three measures were proposed: The Energy Efficiency Design Index (EEDI), the Energy Efficiency Operational Indicator (EEOI) and Ship Efficiency Management Plan (SEEMP) and finally, the Market-based measurement (MBMs) (Kam, 2019).

- EEDI is a technical prevention measure and expresses the amount of emitted CO_2 per cargo tones per mile. The EEDI dictates a reduction of GHG emissions of new ships, forcing the evolution of new vessels towards more environmentally friendly technologies. It became mandatory for newbuilding orders from January 2013 (Lee and Nam, 2017 and IMO, 2018b).
- EEOI and SEEMP are measures established for existing ships to operate with lower emissions. Elaborated as a recommendation instead of a regulation, it also helped to redesign the transport tasks in a more efficient way. It has an operational perspective and a corresponding character of enforcement for the challenge of GHG emissions reduction (Lee and Nam, 2017).
- MBMs are defined to promote lower ship emissions. It is based on a system of incentive and penalizations, depending on the GHG emissions efficiency (Lee and Nam, 2017).

After the Copenhagen Climate Change Conference in 2009, and the Paris Agreement in December 2015, some members of the United Nations established steps to mitigate the impact of the contamination and climate change. A maximum increment of the average temperature of 2ºC and a global cooperation requirement from the parties involved to implement policies of emission reduction for 2020 were agreed upon (United Nations, 2010). Moreover, pressure from South Pacific and European member states did pursuit IMO to adopt strategies for GHG mitigation on the 70th session of the MEPC held in 2016 (Kam, 2019).

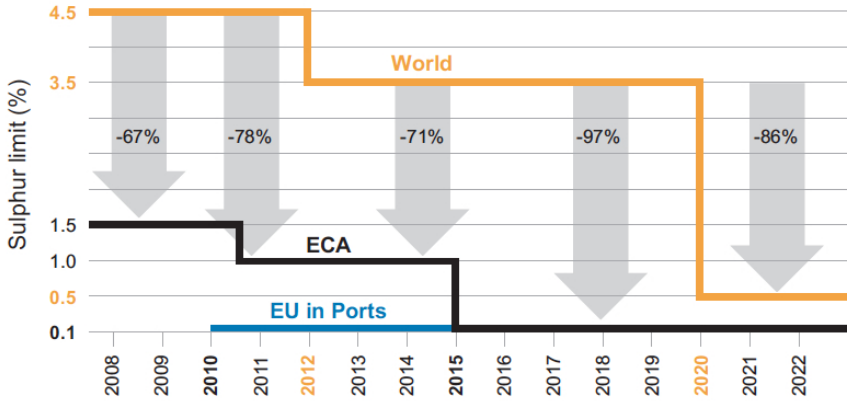

Figure 1.1: Sulphur Limits timeline (Hong Liang, 2017)

In the 70th session of MEPC, a reinforcement on regulations about Sulphur content for fuel oil was decided. The committee reduced the limit from 3.5 to 0.5% (Clark, 2018). With the already existing limitations in ECA's, and port authority's rules that limit the Sulphur content of the berthed ships, this new limit made a significant change of the Sulphur emissions in shipping. On the other hand, there wasn't any relevant actuation on GHG emissions that year, and the strategy was postponed for 2018 (Kam, 2019).

In 2018, the plan was to reduce the GHG emissions to 50% of the 2008 values, by 2050. Some participants, as European Union representants and the Marshall Islands, showed a high interest and commitment, targeting at a reduction of between 70 and 100%. Different phases were established: short-term from 2018 to 2023, mid-term from 2023 to 2030 and long-term after 2030, starting the implementation of regulations from 2023 (Kam, 2019).

Tasks for the first stage of the strategy according to (Kam, 2019) and (IMO, 2018a):

- National plans purpose
- Research on the establishment of new systems
- Ports enabling the infrastructure to encourage new technologies
- Study on new zero carbon emission fuels for shipping
- Analyzing the costs of the latest technologies
- Cooperate towards a common goal of technical development

1.3 Objective and Goals

The aim of this thesis is the design and study of a concept ship purely powered and operated with renewable energies. The main objective is to promote a sustainable transition of the shipping industry by providing an assessment of the feasibility to operate a cargo ship with the elimination of fossil fuels

The following goals were defined for the thesis work:

- Study of the different existing technologies for renewable energy purposes on vessels.

- Development of numerical simulation models to evaluate and compare the most feasible renewable technologies for the thesis
- Integration of renewable systems into a numerical model to simulate the concept ship design, including the energy consumption and generation depending on the renewable sources to evaluate self-sufficiency of the system.
- Definition of routes to prove the viability of the concept
- Simulate journeys to demonstrate the applicability of the concept ship

1.4 Assumptions and Delimitations

Renewable energy is a vast field of research in constant development, and specifically in the marine sector has been one of the most relevant subjects to study during the last years. The first challenge is to limit the study areas of the thesis establishing the delimitations and assumptions of the project.

- In-depth hull design and detailed general arrangement are set aside to favor the development of an overall power and propulsion concept.
- The adaptation of renewable technologies is limited. It is assumed that the installation of the system on a ship is not modifying the essential characteristics of the technology established by the manufacturer.
- The renewable sources are limited to three: wind, waves, and solar. This limitation is established based on the previous studies that give higher viability to those renewable sources.
- Regarding renewable power systems, there is a big range of manufacturers that can provide a technology adaptable for our concept, and an exhaustive comparison would exceed the time limit. Characteristics of systems are defined in the scope of the available technologies in the market.
- Risk assessments and applicable regulations are not contemplated assuming those as assessments for later stages on the design.
- On the journey simulations, the weather condition is limited to monthly average global data with a precision of 1 degree of longitude and latitude. It is assumed that the weather condition remains constant in the square defined by the latitude and longitude being modified each month.
- In Chapter 3, the initial ship resistance used is calculated by interpolation from the results of ShipCLEAN software for intervals of 5º of wind angle and 5 knots of wind speed.
- In Chapter 4, for the final calculations of ship resistance, weather input parameters are defined by wind speed and angle, wave height, current speed and direction, and water temperature and depth. Although, because of the high computational power to simulate a full route with all those variables, weather input values are reduced to wind speed and direction, wave height is deduced from wind characteristics as an approximation, currents are neglected, water temperature set as 19ºC and water depth set as high depth in all the route.
- An essential aspect of the concept design is the requirement of low electric consumption. The ship is assumed without crew for operation at sea to reduce electrical

consumption. In this way, the power consumption from habitability systems is eliminated.

- Renewable energy technologies are installed mainly on the weather deck. It is assumed that the concept ship will have clearance in to fit the required renewable technologies

1.5 Outline of the Thesis

This section gives an overview of the structure of the thesis.

Table 1.1: Outline of the thesis work

Chapter	Title	Pages	Description
2	Literature Review	8-16	It is a research study of the different technological advances to implement renewal energies in the shipping industry. It also identifies the essential parameters to succeed in the goals of the thesis.
3	Methodology and Feasibility Study	17-36	It identifies the opportunities of the systems by the development of individual numerical models that provide initial results of energy balance.
4	Concept Design	37-46	This chapter designs a single numerical model that englobe the different chosen systems. It also defines a ship type and motivates the election of three different routes. Finally, the ship is simulated.
5	Results and Discussion	47-58	This section evaluates the results of the simulation of the journey results of time and ship speed and considering the final power balance of the propulsion system requirements and including an estimation of the total power consumption of the vessel.
6	Conclusions	59	This section summarizes the main findings of the results concluding with an outcome of the thesis.
7	Future work	60	The final chapter gives ideas and relevant topics to evaluate and study in the future.

2 Literature Review

The purpose of the literature review is to get essential insights, to simulate and provide an honest evaluation of the feasibility of a concept ship driven and powered by renewable energies. The literature study focuses on propulsion and power generation systems using renewable energy that could be used on a commercial vessel at sea.

Since the primary objective of this thesis is to avoid fossil fuels and to achieve an unlimited range of the ship, the employed propulsion methods must use energy sources available at sea, e.g., wind or wave energy. Other sources of energy as solar radiation cannot produce thrust directly. Instead, those can provide electrical power that is used for onboard systems or as electrical propulsion. The power generation from renewable energy sources is not constant, thus it is necessary to analyze the possible options to store the surplus of renewable energy on board the ship. Finally, a review of different existing green ship concepts that use the mentioned technologies for similar or the same goal as the thesis are presented.

2.1 Renewable Propulsion Systems

This section analyses different technologies to provide propulsion from wind and/ or waves.

2.1.1 Wind Propulsion

During the last decades, numerous studies on energy saving solutions promoted the idea of establishing more sustainable propulsion in the marine industry (Lan et al. 2015, Bøckmann 2015, Bockmann and Steen, 2011 and Hou et al., 2018). Wind power is one of the most relevant examples. However, on merchant ships its implementation has experienced difficulties as the increment of the initial costs of the installation, additional workload and risks for the crew and the variability of performance depending on the wind conditions (Atkinson et al., 2018). In Atkinson et al., (2018), a general overview of sails for modern vessels is provided. Different factors affecting the decision if wind propulsion could be implemented, are discussed.

Wind propulsion contemplates different possibilities. Some of these technologies, as the proposals from Leloup et al. (2016) and Wood et al. (2013), analyze the feasibility of kites by considering different possible flight modes and generating an algorithm that optimizes the flight condition for maximum thrust, showing potential savings of up to 50% for winds of about 15 m/s. Wood et al. (2013), compared Flettner rotors and kites as a propulsive system to reduce fuel consumption, concluding that for both cases wind is contributing to the power requirement of the vessel with a relevant reduction on the fuel consumption and emissions. Talluri et al. (2018) developed a techno-economic analysis of the implementation of Flettner rotors compared with other (fossil fuel-based) technologies underlining that the benefits of installing rotors are highly dependent on the weather conditions on the ship's route and social parameters as the CO2 emission taxation. Kramer (2016) compared Flettner rotors and Wing sails considering thrust, drag and lift, analyzing its efficiency in terms of energy savings depending on the number of sails, and if those are retractable. The results of the paper give a general understanding of the forces on a ship depending on the sails settings as well as the optimization of the keel area and the required rudder angle to maximize the efficiency. Bøckmann (2015)

considers wing sails as a part of the propulsion system for a ship powered with renewable energies. In the study, it is assumed that the best distribution is along the centerline of the vessel and that the interaction between wing sails can be neglected.

Tillig et al. (2019) developed the software ShipCLEAN. A numerical simulation model to give an accurate result of the resistance and power requirements of a ship using wind propulsion systems. The model considers the forces from the wind, waves, and currents, and provides solutions for 1 and 4 DOF. The studies by Tillig et al. (2019) and Tillig and Ringsberg (2018) show the potential of wind-assisted propulsion for merchant ships. Even though it contemplates the system as a methodology of fuel-saving, it can be restated for a concept without fuel consumption, as done in the present thesis.

2.1.2 Wave Energy

Waves are typically seen as a source of added resistance of ships at sea. However, the use of wave energy for thrust generation has been a topic of interest during a long time.

The first documented system for wave energy propulsion is Vroman, from the United States of America patent register. It was registered on November 1858 and describes a system of fins on the hull that produce thrust from the sea waves. Modern technologies have not gone far from those first designs (Bøckmann, 2015). Improvements are mainly focused on increasing efficiency by modifying the foils angle of attack (Bøckmann, 2015). Jakobsen (1981) studied the control of the angle of attack for wave foils as well as the optimal location of the center of rotation to minimize the resistance of the foils. Additional studies like Politis and Politis (2014) proved the effectivity of an active pitch foil controller in comparison with other methods. As an example of the technology, in 2008 Yutaka Tanao designed the wave-powered catamaran “Suntory Mermaid II”. Figure 2.1 shows the system of wave foils installed in the bow of the ship

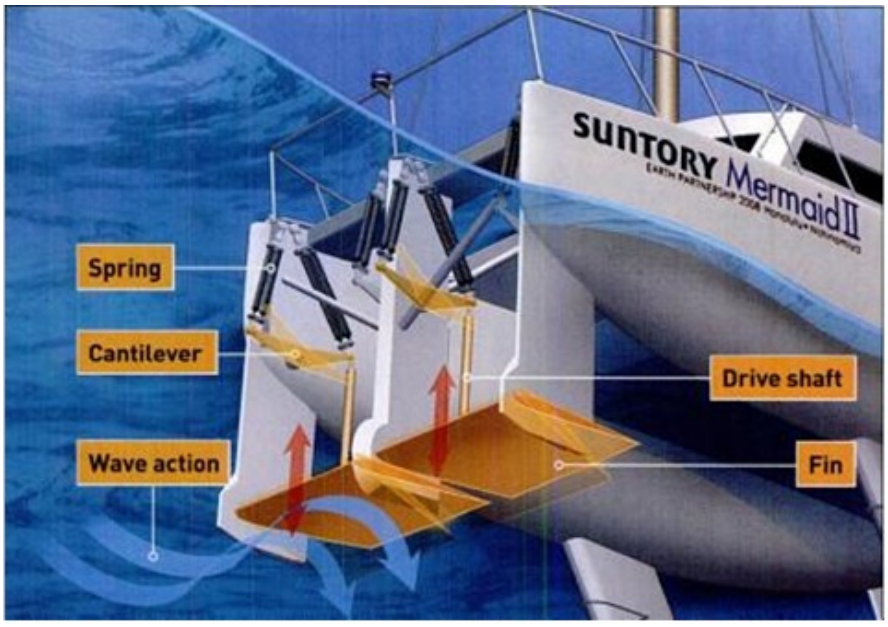

Figure 2.1: Wave foils powered catamaran "Suntory Mermaid II" (Bøckmann, 2015)

Bøckmann (2015) studied, in a theoretical and experimental way, how foils attached to the underwater structure of the ship can give thrust with the heave and roll motions of the vessel. Results from the study show a reduction in fuel consumption from 2 to 15% in regular North Sea waves, reaching fuel savings in the range of 29 – 50% in head seas, with notable reduction of ship motions. Bøckmann, Yrke et al. (2018) evaluate the same technology from a commercial perspective with a project to implement a system of retractable wave foils in a 100m long ship concluding with a functional foil able to reduce the fuel consumption. Riley (2015), studied wave foils for the unmanned prototype ship "ReVolt" designed by the classification society DNV-GL with relevant findings of the reduction of CAPEX costs dependents on wave parameters as height, peck, and heading angle, but also depending on the ship speed.

In summary, wave energy is a promising source of energy for ships. From the previous research projects, it proves that the energy savings in all cases are higher than 20% and reaching theoretical values of about 60%. Since the thrust of the wave foils highly depend on the heave and pitch motion, it is crucial to determine the RAO of the ship under investigation. However, an accurate prediction of the RAO requires a high amount of knowledge of the hull shape of a vessel and extensive computation. Due to the limitations of this thesis, wave propulsion is not included in the concept.

2.2 Energy Generation Systems

This section presents an analysis of possibilities to generate electrical energy from renewal energy sources at sea. Solar and wind power proved to be the most promising technologies taking into account the vessel's characteristics as those technologies produce electric current without interfering with the ship operation (Balcombe et al. 2019 and Rezaie et al., 2011). In the following sections, some of the most relevant findings from previous studies are presented.

2.2.1 Solar Energy

Solar applications on ships is a well-studied subject for the reduction of emissions, as it is shown in Yu et al. (2015) and Lan et al. (2015). As an example, in Yu et al. (2015) results show that the installation of 2000 m^2 solar systems on a vessel can reduce the overall commercial costs up to 12.1%. The performance of a solar power system can be estimated using the position on the earth and employing numerical models to determine the solar radiation intensity based on the earth's rotation around the sun (Vieira da Rosa, 2005). Moreover, weather conditions can be included by employing historical data from each location on the planet, to estimate the irradiation at a specific point on the earth (Yu et al., 2015).

The tilted angle of solar panels and tracking systems are discussed in Tröster and Schmidt (2012) and Yu et al. (2015). Slanted panels increase the efficiency for a specific orientation; however, in a moving structure, the direction of the groups are continuously modified by the ship heading. In this case, the tilt of the panels has to be supported by a tracking system (Tröster and Schmidt, 2012). While arranging solar panels on deck, shadowing effects, as well as free space margin in between the groups, must be respected, while ensuring efficient use of the available space (Yu et al., 2015).

2.2.2 Wind Power

Wind turbines convert the kinetic energy of the wind into electric power, which can be used for both, propulsion and on board systems (Clarson and Nilsson, 2015). Modeling and Dinkova (2006), validate the use of wind to produce electrical energy on ships focusing on horizontal wind turbines. In the paper, a societal analysis about how this new technology is perceived for the possible stakeholders is included. In 2014, Stena Teknik AB developed the scale model of a tanker ship shown in Figure 2.2 to estimate the influence of the wind turbine on the ship's maneuverability and power consumption. Results showed savings in fuel consumption of about 10% for real route conditions (Clarson and Nilsson, 2015).

Figure 2.2: AirMAX scaled model with wind turbine (Clarson and Nilsson, 2015)

Compared to horizontal axis turbines, a vertical axis turbine provides advantages for the implementation on board a ship, e.g., the unnecessary yaw orientation (Kim and Yaakob, 2016 and Bockmann and Steen, 2011). Kim and Yaakob (2016), evaluated the installation of a vertical axis wind turbine on a ship, including an assessment of the stability, arrangement on deck, costs, and electrical loads. Results show about 38% reduction in fuel oil consumption in real-life conditions. Regarding stability parameters, the research analyses the possible effects of the wind turbine in the worse possible conditions with a maximum heel of 1 degree. Finally, from a techno-economical perspective, the project is viable with a total economical return after 16 years of use, considering all costs.

Finally, in Bockmann and Steen (2011), the fuel-saving of wing sails and wind turbines of the same area are compared. Results show a potential saving of 33.1% when using wind turbines to produce electrical energy that is used for propulsion. As a comparison, wing sails provided a fuel saving of 31.8%.

2.3 Energy Storage Systems

Energy generation systems from renewable energies can generate large amounts of power at times but are highly reliant on the weather conditions. This uncertainty creates the need to maximize power generation in favorable conditions and use energy storage systems to preserve the energy for times of low power production.

An energy storage system allows the conservation of energy. In the marine sector, this technology is not yet established but is starting to appear as a solution for specific design and

operational conditions, e.g. hybrid ferries. Batteries are the most common system to store energy. Hesse et al. (2017) offer a guide with all relevant information about the Li-Ion cells. It ranges from the fundamental equations for the design of systems through a review of advantages that Li-ion cells offer compared other batteries. Andersson et al. (2018) designed a concept of RoPax ship to travelling a medium distance course from Gothenburg (Sweden) to Frederikshavn (Denmark). Some highlights of this concept are the possibility to distribute the cell modules around the structure of the hull to avoid spaces like the engine room. Also, in Andersson et al. (2018), a charging system is conceptualized to recharge about 70% of the battery capacity during the short times in port. Hou et al., (2018) present a paper on hybrid systems of batteries combined with flywheels or ultracapacitors to store the surplus power from the electric generators and smooth the power load. The study concludes that hybrid systems with batteries and fly-wheels are beneficial for batteries since they reduce high currents.

An additional energy storage solution considered in some projects is hydrogen. In Platzer et al. (2014) the possibility to use the excess of electric power from renewable energies to convert seawater into hydrogen is studied. The idea of this research is to analyze the technology for installation in a sailing ship. Results show a total production for the hydrogen system of 119.4 m^3/h hydrogen and 59.7 m^3/h oxygen for a purposed catamaran ship of 119 m length. The project concludes that the technology is viable as a method to generate hydrogen as an energy storage product.

2.4 Ship Concepts

2.4.1 Neoline

The Noeline project is an example of a concept ship with a new transportation methodology to face the challenge of GHG emission reduction. Neoline is a 136m RoRo ship to be operating on the route St-Nazaire, Bilbao, Charleston, Baltimore, Sant-Piere & Miquelon St-Nazaire with two round trips per month (Neoline, 2019).

The goal of the project is to create a RoRo vessel with renewable energies as the primary source of power to minimize emissions. The project is structured in two phases that are targeted to be finished in 2020 and 2030, respectively. For 2020, the goal is to overcome the current regulatory limits and to reduce fuel consumption by about 80-90%.

Figure 2.3: Neoline ship (Neoline, 2019)

To reach this goal, the primary source of propulsion is soft sails with an area of 4200 m^2. The vessel is also equipped with a shore connection and a battery pack. As auxiliary and back up power, a marine fuel-oil engine is installed (Neoline, 2019).

Facts, why the project can succeed in the merchant ship market, are according to Neoline (2019):

- Competitiveness of a system not depending on the bunker market increasing the stability of the cost.
- A Proper ship size allows the ship to operate faster with less required systems.
- The Focus on the route planning allows a reliable schedule.
- A reduction of emissions will improve the corporate social responsibility strategy and also will give a positive image identity and social value.

For this thesis, Neoline represents proof of the feasibility of sails as the primary propulsion system of cargo vessels.

2.4.2 E/S Orcelle

The project "E/S Orcelle" started in 2005 for the company Wallenius Wilhelmsen with the aim to design a versatile car carrier, powered by renewable energies available at sea (Wallenius Wilhelmsen, 2005).

The primary sources of power are wind, solar and wave, with a hydrogen fuel cell as a back-up. Wind energy is used as a propulsive source with a system of three rigid sails with about 1400m^2 of sail area each (Wallenius Wilhelmsen, 2005). Solar power is used for electricity generation with the installation of solar panels located in the rigid sail surface with a total surface about 800m^2 on each sail with an approximate energy output of about 2500kW (Wallenius Wilhelmsen, 2005). Twelve fins about 210m^2 each define a system that creates propulsion and electric power from wave energy (Wallenius Wilhelmsen, 2005 and Sáiz and López, 2007). Finally, as an additional source of energy, hydrogen fuel cells system with output energy of about 10000kW are installed (Wallenius Wilhelmsen, 2005). Hydrogen would not

just be another energy source; it would also be used as an energy storage system, with an electrolyzer that converts electrical energy from the renewable energies into hydrogen (Wallenius Wilhelmsen, 2005).

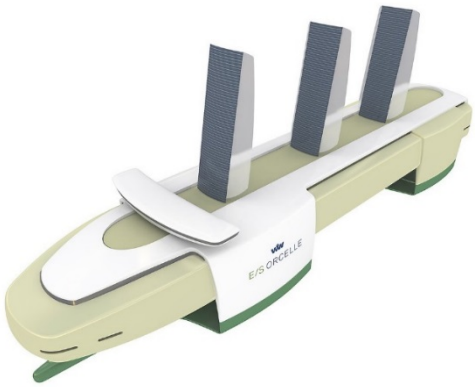

Figure 2.4: E/S Orcelle (Wallenius Wilhelmsen, 2005)

The project "E/S Orcelle" is relatively old in terms of renewable energy systems for ships, but it is highly relevant for new designs and this thesis because of the different technologies integrated into the concept.

2.4.3 NYK Super Eco-Ship 2050

The super Eco-Ship 2050 is one of the most recent projects from the Korean company NYK. The ship does not rely on sails as propulsion technology but focuses on propulsion using energy from hydrogen and solar power.

Hydrogen stands for about 80% of the total energy production and is stored onboard in 1900 m^3 tanks (NYK Grup, 2018). Additionally, a solar power system, composed of 9000 m^2 of solar panels, covers about 15% of the ship's power demand (NYK Grup, 2018). Hydrogen can be produced using solar electricity by electrolysis if there is surplus power generation (NYK Grup, 2018).

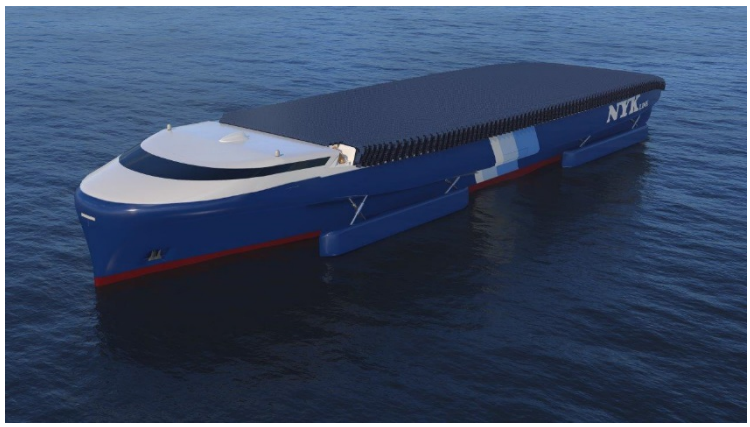

Figure 2.5: NYK Super Eco-Ship 2050 (NYK Grup, 2018)

The Super Eco-Ship 2050 is of interest for this thesis since it proves the value of solar power for ships at sea and the feasibility of hydrogen as an energy storage system.

2.4.4 E-Ship 1

The E-ship 1 is a RoLo ship built for the German wind turbine manufacturer Enercon (Rutkowski, 2017). The 130m long vessel is equipped with 4 Flettner rotors and standard screw propellers for propulsion (Rutkowski, 2017). The four rotor sails, each 27m high and 4 m in diameter, are estimated to provide a total fuel saving of 25% (Rutkowski, 2017).

Figure 2.6: E-Ship 1 (Rutkowski, 2017)

Even though this project is not as ambitious as the previous, E-Ship 1 is one of the most impressive projects with Flettner rotors as wind-assisted propulsion. The project proves the viability of Flettner rotors for marine propulsion.

2.5 Evaluation

Table 2.1 presents the most feasible systems technologies to generate power from renewable energy sources. Because of the timing limitations of the thesis, the implementation of some viable technologies to the concept ship is postponed to future work.

Table 2.1: Technologies to evaluate the concept

Technology	Figure*	Comment
Wind turbine		Wind turbines are a reliable source of energy at sea. This system can complement wind propulsion by covering wind angles that sails are not operative.
Solar Panel		It is a vital source of energy at sea. PV efficiency is low in comparison with the power coming from the sun; however, the production is relevant enough to be considered for the concept ship.

Wave foils		It is technology highly depending on the sea state. It has significant benefits for low ship speeds. It is helpful as a complementary system to another power.
Wing sails		It is dependent on the wind, and it can produce a considerable amount of energy for propulsion. Requires complementary systems for trimming and its use reduce the effectivity of the PV system on the deck
Flettner rotor	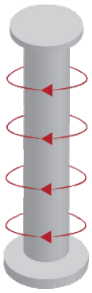	It is dependent on the wind, and it is advantageous to respect wing sails because it requires less space, and is used in a more straightforward way for the crew
Batteries		It is the most efficient way to store electrical energy. Costs for this system are high and requires space. Security is an essential element to consider for these systems, and the charging systems is another a matter to solve.
Hydrogen		Hydrogen fuel cells represent a promising technology due to its high power output and the possibility to produce hydrogen using renewable energy sources. However, energy requirements, safety and costs are challenges to overcome.

3 Methodology and Feasibility Study

Chapter 3presents the numerical models developed to evaluate and define technologies chosen in Chapter3. The mathematical modelis created open and generic to make it applicable for different ships and routes. Results from this chapter present the applicability of the system to the concept ship.

The basis for the evaluation of the concept ship is the ShipCLEAN simulation model (Tillig et al., 2019). The usability of the systems is proved by the comparison of the power generated, with the requirements of a real ship. The resistance is calculated for the high blockage hull “MRTanker3”, and thrust forces of Flettner rotors and wing sails are evaluated by ShipCLEAN. Basic parameters of the ship used for the research are specified in Table 3.1, the resistance curve is shown in Figure 3.1.

Table 3.1: Dimensions "MRTanker3" (Tillig et al. 2019)

Dimension	Value	Unit
LOA	183	m
Draft	11	m
Breadth	32,2	m
Displacement	50610	t

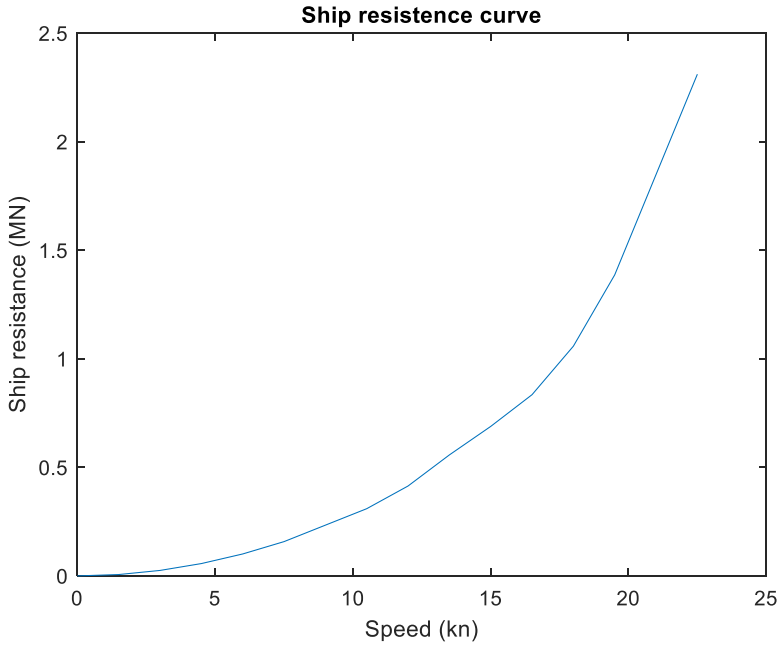

Figure 3.1: Speed-Resistance relation "MRTanker3"(ShipCLEAN)

3.1 Wind Propulsion

The methodology study of wind as a propulsion method considers Flettner rotors and Wing sails as the most plausible options to install and operate on commercial ships. Different

configurations for both systems are analyzed to evaluate the forces generated in different wind conditions. The purpose of this initial analysis is to study the capacity of the system and the achievable speeds. A balance of generated force and ship resistance with the relation of speed – resistance of the vessel from Figure 3.1 defines this result for 1 DOF. Assumptions for this analysis are:

i. Constant wind speed and direction
ii. Resistance calculated for 1 DOF neglecting the resistances from side forces.

Although the limitations create uncertainties into the final results, the results offer a general idea of the potential power generation of the system.

According to Tillig et al. (2019), there are some interaction effects when more than one Flettner rotor is installed on a ship, although these interaction effects can give an advantage compared to a single rotor. The interaction of different wing sails reduces the total thrust coefficient (Choi et al., 2013). However, as the effect of the hull concentrates the wind currents into the sail surfaces, increasing its efficiency, interaction properties between wing sails are not considered (Tillig et al., 2019).

Calculations of the force generated from sails are done using the equation (3.1) for both systems.

$$F_x = C_t * A * n * \frac{\rho}{2} * AWS^2 \qquad (3.1)$$

C_t is the thrust coefficient of the sail. It represents a relation value of the force produced with the area of the sail and the wind characteristics. A is the sail area. For the wing sail, it is the plane projection, and for the Flettner rotors, it is the projection of the cylinder. n is the total number of sails. ρ is the density of the air equal to 1.25 kg/m^3. AWS is the apparent wind speed.

Dimensions of the evaluated Flettner rotors and Wing sails are represented in Table 3.2. In the analysis, relevant forces are the thrust and side force. Those coefficients are taken from the software ShipCLEAN and are dependent on the angle of the apparent wind.

Table 3.2: Sails dimensions (ShipCLEAN)

Type of sail	Dimensions (sail area)
Flettner Rotor	150 m^2
Wing Sail	1800 m^2

Figure 3.2 and 3.3 show the thrust coefficient and side force coefficient of the sails, depending on the wind angle. It is remarkable that for both, the most efficient wind direction is between 90º - 120º, considering 0º as head winds, 90º as side winds and 180º stern winds. Flettner rotors have its maximum thrust generation for side winds with a thrust coefficient notably higher than wing sails; however, after the maximum in 90º, the thrust coefficient decreases fast to zero. Wing sails have lower thrust coefficients in comparison with Flettner rotors, i.e., it requires more sail area for the same thrust. The curve shows that from the zero force on headwinds, the thrust coefficient grows to the maximum in winds about 100º, but after the peak, the reduction for stern winds doesn't affect the final thrust.

For Flettner rotors, side forces require special attention. Its maximum appears for wind angles with minimum thrust. A critical situation with unfavorable wind angle conditions could create an excessive drift of the ship. For wing sails, the highest side forces are caused for the quarter winds, with its maximum for an angle of 45º. On this case, the excessive heave could occur as well, but as the side forces are proportionally lower than the thrust, the drift would be lower.

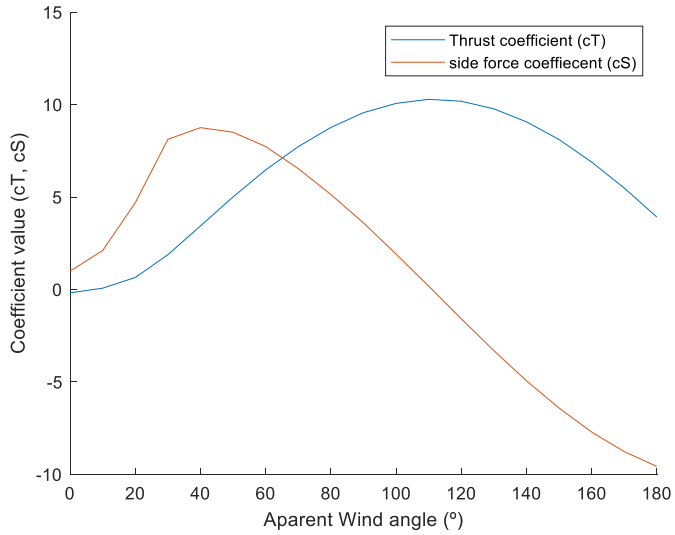

Figure 3.2: Coefficients for Flettner Rotor 150 m^2

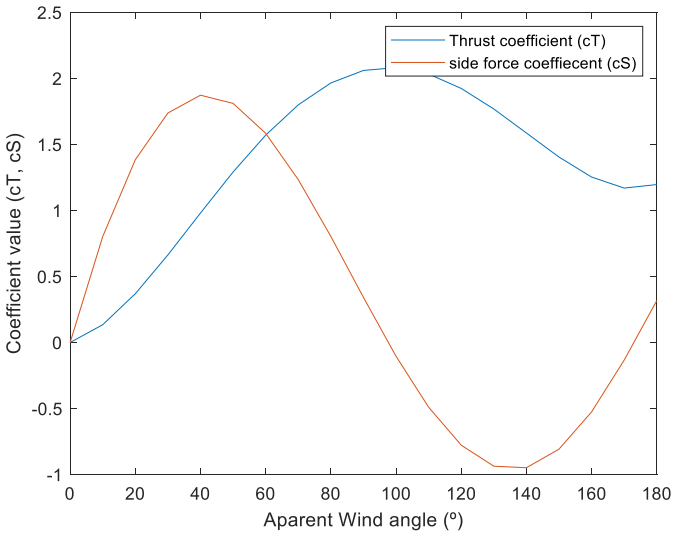

Figure 3.3: Coefficients for Wing Sail 1800 m^2

As the ship velocity and true wind speed are mutually dependent, the calculation of the final ship speed requires an iterative process. The first step is to find the apparent wind speed that the ship is facing depending on the real weather conditions. Starting with zero initial ship speed, the force balance between the ship resistance and the thrust produced by the sails give a new ship velocity. Movement modifies the apparent wind speed and angle, and the vessel speed is

recalculated. By iterations on this calculation, the process continues until the equilibrium is found.

The results presented give relevant information about the efficiency of the systems in different conditions. The efficiency of the rotors depends on three input parameters; the true wind speed, the true wind angle, and the number of sails. Data is modified gradually to show a range of results.

The thrust from Flettner rotors is dependent on the wind speed and the speed of rotation. In this paper, it is assumed that the rotational speed of the cylinders is always optimal for maximum efficiency of the system.

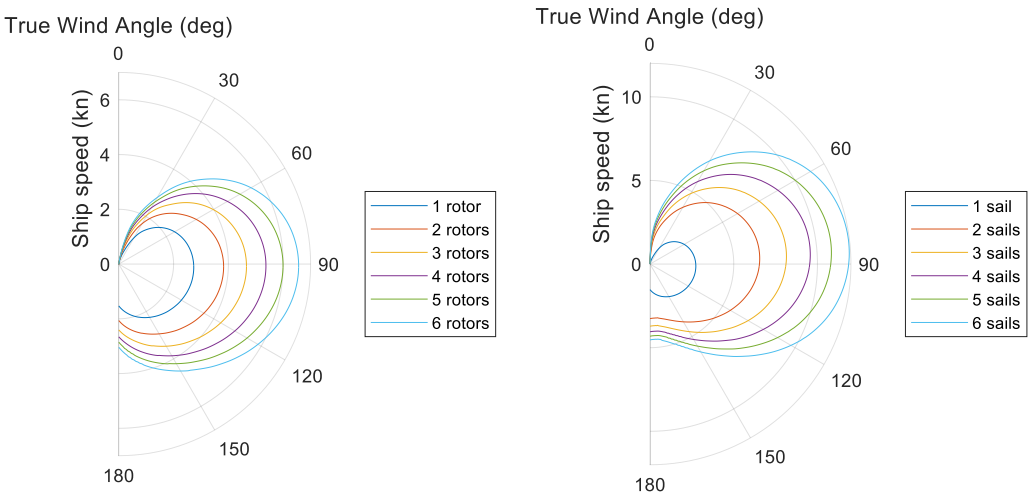

Figure 3.4: Ship speed for 5 m/s wind speed for Flettner rotors (left) and Wing Sails (right)

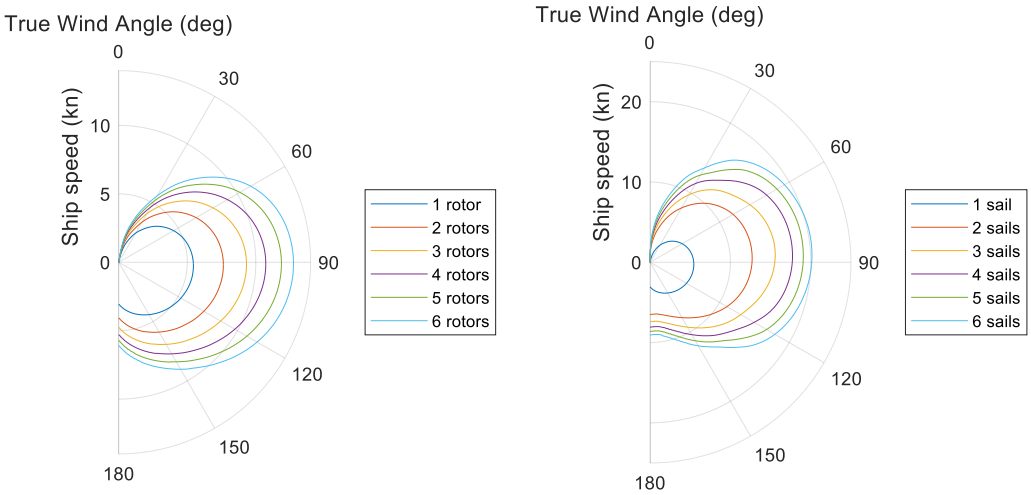

Figure 3.5: Ship speed for 10 m/s wind speed for Flettner rotors (left) and Wing Sails (right)

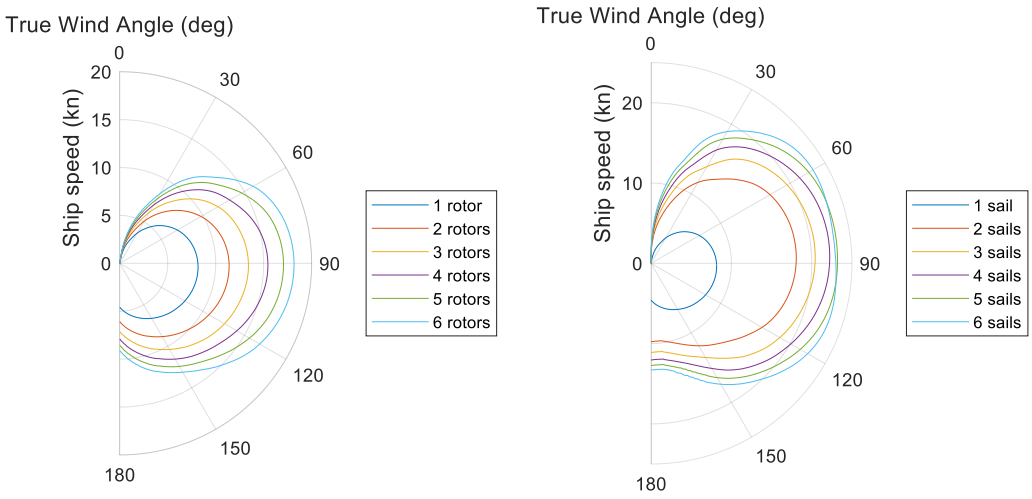

Figure 3.6: Ship speed for 15 m/s wind speed for Flettner rotors (left) and Wing Sails (right)

Results from Figure 3.4, Figure 3.5 and Figure 3.6 show that for the same wind and number of sails, with the previously mentioned specifications, the resultant speed with Wing sails is higher than with Flettner rotors. Maximum rates are coincident for wind angles close to 90 degrees. For wing sails, it is relevant that for the case on 15 m/s wind speed, when the number of sails increases from 4 to 6, the increasing of ship speed is not significant; and that for stern winds, more sails don't produce essential benefits.

The power required for the rotation of the sails is a significant parameter for the selection of the system to use. A power requirement curve, from Tillig et al. (2019) is also expressed by a power coefficient depending on the wind angle. As Figure 3.7 shows, the optimal rotation for constant wind speed is not proportional to the ship velocity. With a comparison between speed and rotation power, the most favorable wind angle is between 100º and 150º, where the velocity reaches its maximum with lower energy requirement. From 150º to stern wind, the speed is reduced, but with an increase of power requirement. Finally, from 0º to 80º, the energy required grows proportionally with the velocity. Figure 3.7 is an example of six rotors and 5 m/s wind speeds. The relation from Figure 3.7 is the same independently of the number of rotors or wind speed.

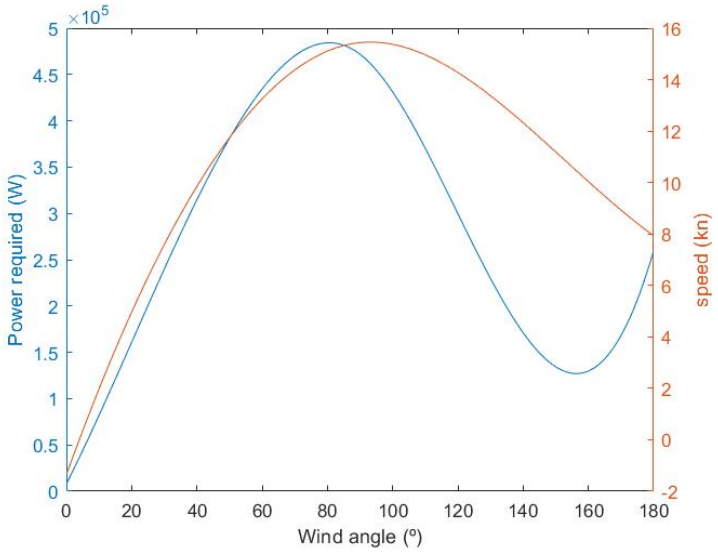

Figure 3.7: Comparison Rotor Power - Wind Angle for six rotors and 5 m/s of AWS

Additional considerations of the wind propulsion method to install on the ship are presented.

- The number of sails is a parameter to consider if the systems are not foldable. In Kramer (2016), it is evaluated for a fixed route different configurations with a different number of Flettner rotors, and the result shows that due to the effect of the wind resistance on the sails there are some situations where increasing the number of rotors reduce the energy savings because of the wind resistance.
- The space required on the main deck and the shadows created will have relevance for the election on the system. Section 3.2.1 take out the importance of solar power. Then it would be necessary to analyze the effects implement one or other method for PV energy generation.
- The practical use of the sails is an essential characteristic for a cargo ship to reduce crew requirements; in this case, the automation required for wing sails creates a challenge in comparison with Flettner rotors.
- Flettner rotors is a system that requires energy to develop its function. It is an essential consideration for a ship that needs to generate its power.

Results and considerations give uncertainty about the selection of the sail-assisted propulsion system. Focusing on the practicality, to simplify the operation and in the reduction of space required and shadow effect, Flettner rotors are analyzed for the concept ship. Although as the wing sails seem to be a system with potential, it will be considered for future work.

3.2 Solar Photovoltaic Energy Production

In Yu et al. (2015) and Lan et al. (2015) the feasibility of solar power applications in sea transport is demonstrated. In chapter 3.2, findings from the literature study are used to elaborate on a numerical model. The model is developed to find the electrical energy production for a coordinate on the globe, date of the year, and a time of the day.

3.2.1 Methodology study of the system

The simulation analyzes the power produced by a photovoltaic installation. Equations to define the PV (photovoltaic) power generation are described by Yu et al. (2015), Vieira da Rosa (2005) and Lan et al. (2015). The generic power equation is defined by (3.2).

$$P_{PV(t)} = \eta_{pv} * A_{pv} * I_{(t)} \quad (3.2)$$

In (3.2) η_{pv} is the efficiency of the PV generator, A_{pv} is the total area and$I_{(t)}$ is the solar radiance.

The input of area is fitted according to the equation (3.3) with the total system dimensions as the sum of the photovoltaic surfaces of all solar panels. n, l, w are the number of generators, the length of each of them and its width.

$$A_{pv} = n * l * w \quad (3.3)$$

Equation (3.4) defines the PV efficiency. It is characterized by reference efficiency $\eta_{ref.}$ determined by the manufacturer, the efficiency of the tracking systemη_{track} and parameters dependent on the working temperature of the system as the temperature coefficient β that depends on the material of the cell, the cell reference temperature T_{ref} and cell temperature T_c.

$$\eta_{pv} = \eta_{ref.} * \eta_{track.} * (1 - \beta * (T_c - T_{ref})) \quad (3.4)$$

The efficient cell temperature is obtained by the equation (3.5). It comes from the ambient temperature T_a, the normal operating cell temperature $NCOT$ and the irradiation that the solar panels are receiving $I_{(t)}$.

$$T_c = T_a + ((NCOT - 20)/800 * I_{(t)} \quad (3.5)$$

The irradiation is a variable parameter that defines the amount of power from the sun that the cells receive. It depends on the weather conditions and the perpendicularity between the rays and the surface of the panel. Equation (3.6) specifies the calculation of the irradiation received by the system. It is expressed as a sum of I_B, I_D, I_R that denotes the direct radiation, the sky radiation, and the ground reflected radiation respectively.

$$I = I_B + I_D + I_R \quad (3.6)$$

However, it can also be expressed as in equation (3.7) where the different intensities are dependent on $I_{B,N}$ as normal direct radiation on a surface perpendicular to the sun rays. In the formula, the different intensities are calculated based on the temporal parameters ρ and χ that are the Albedo or reflection index and the zenith angle.

$$I = I_{B,N} * \left(\cos(\theta) + cos^2\left(\frac{\phi}{2}\right) * \sin(\chi) + \rho * \cos(\chi) * sin^2\left(\frac{\phi}{2}\right) \right) \quad (3.7)$$

In this study case, ρ is set as a constant with a value of 0.2 (Yu et al., 2015 and Andrews and Pearce, 2013). θ, ϕ are the incidence angles that represent the relation of the angle between the board and the solar rays, (Vieira da Rosa, 2005 and Lan et al., 2015).

Matching χ equal to θ, we can get both from Equation (3.8) defined by δ, λ and α as declination angle, latitude and hour angle.

$$\theta = \chi = cos^{-1}(\sin(\delta) * \sin(\lambda) + \cos(\delta) * \cos(\lambda) * \cos(\alpha)) \quad (3.8)$$

Equation (3.9) defines the declination angle. It is a consequence of the inclination of the rotation axes of the earth going from -23,44 to 23,44 depending on the season of the year. d represents the day of the year starting from the first of January.

$$\delta = 23.44 * \sin\left(360 * \left(\frac{d - 80}{365.25}\right)\right) \quad (3.9)$$

Hour angle denotes the angle of rotation of the earth starting at midnight. Equation (3.10) calculate it based on the LST (Local Standard Time).

$$\alpha = \frac{360}{24} * (\mathrm{LST} - 12) \quad (3.10)$$

Local Standard Time is the correction of time, depending on the astronomical position of the sun in the sky. It depends on LT and TC as local time and the time correction factor, and it is represented by Equation (3.11)

$$\mathrm{LST} = \mathrm{LT} + \frac{TC}{60} \quad (3.11)$$

The time correction factor is the variation in minutes due to the difference between the theoretical meridian for the local time and the exact location. Equation (3.12) shows its dependency on L_{LOCAL}, $LSTM$, and EOT. Meaning respectively, local longitude, local standard time meridian and equation of time

$$\mathrm{TC} = 4 * (L_{LOCAL} - \mathrm{LSTM}) + \mathrm{EOT} \quad (3.12)$$

Local standard time meridian is the reference meridian used to calculate the local time of the studied location. Equation (3.13) define it in the function of the T_{ZONE} referred to time zone.

$$\mathrm{LSTM} = 15 * T_{ZONE} \tag{3.13}$$

The equation of time is a tool to correct the irregularities caused by the eccentricity of earth orbit or the inclination of the earth rotation. Equation (3.14) shows that it depends on the parameter B:

$$\mathrm{EOT} = 9.87 * \sin(2 * \mathrm{B}) - 7.53 * \cos(\mathrm{B}) - 1.5 * \sin(\mathrm{B}) \tag{3.14}$$

Finally, B is defined in Equation (3.15). It is a parameter specified by the day of the year starting on the first of January.

$$\mathrm{B} = 360 * (\mathrm{d} - 81)/364 \tag{3.15}$$

The numerical model has two input groups. The first is related to the definition of the system arrangement and the PV generator election. The size and the number of panels are parameters that change according to the available space on the ship from Table 3.1, and the efficiency depends on the PV panel used. The second input is associated with the location of the system. The input parameters are the local solar irradiations, the weather conditions, and the cosmological parameters about the movement of the earth around the sun. On the first group, input values are stable during time as the only factor that can change is the temporary deterioration. Instead, on the second, those are changing continuously because of the irregularity of weather conditions and positions.

The availability of space on the ship for solar panels evaluates two different situations. One condition considering that 80% of the weather deck is the total PV surface and another where this area is reduced to 40%. The total deck surface is assumed to be 4800 m^2 according to the ship dimensions.

The parameters of the PV generators used on the system are from the model "X-Series: X21-460-COM DC" from the producer SUNPOWER. As Figure *3.8* and Table 3.4 show, solar panels have a surface of 2.16 m^2 and an efficiency of 22%.

The inclination of the panels is a beneficial method to increase solar production for PV systems. The orbit of the sun around the earth has an angle that reduces production during mid-day. By adding a tilde inclination or a tracking system, the efficiency would increase. In this system, instead, because of the uncertainty of the concept routes, adding a fixed angle could produce problems for specific courses (Tröster and Schmidt, 2012). For this reason, the tilde is not considered for the PV solar system of the concept.

Diversity of locations define the range of possible results that the system offers. Input location selection is done according to two different parameters; the weather conditions and the annual variation of irradiation depending on the season. The locations where the studies have been carried out and the motivation of the coordinates are shown in table Table 3.3.

Table 3.3: Locations of consideration for PV system

Region	**Global coordinates**	**Weather conditions**	**Annual variation of irradiation**
North Sea	56º, 2º	It is a region with hard winds and low solar intensity	It has high variation because of the distance to Ecuador line.
Arabian Sea	13º, 64º	It is a region with low winds and high solar intensity	It has small variation because of the proximity of Ecuador line.
South African Republic Coast	-42º, 25º	It is a region with mid-low winds and medium solar intensity	It has medium-high variation because of the distance to Ecuador line.

- In the North Sea (56º, 2º)
- In the Arabian Sea (13º, 64º)
- Near the South African Republic Coast (-42º, 25º).

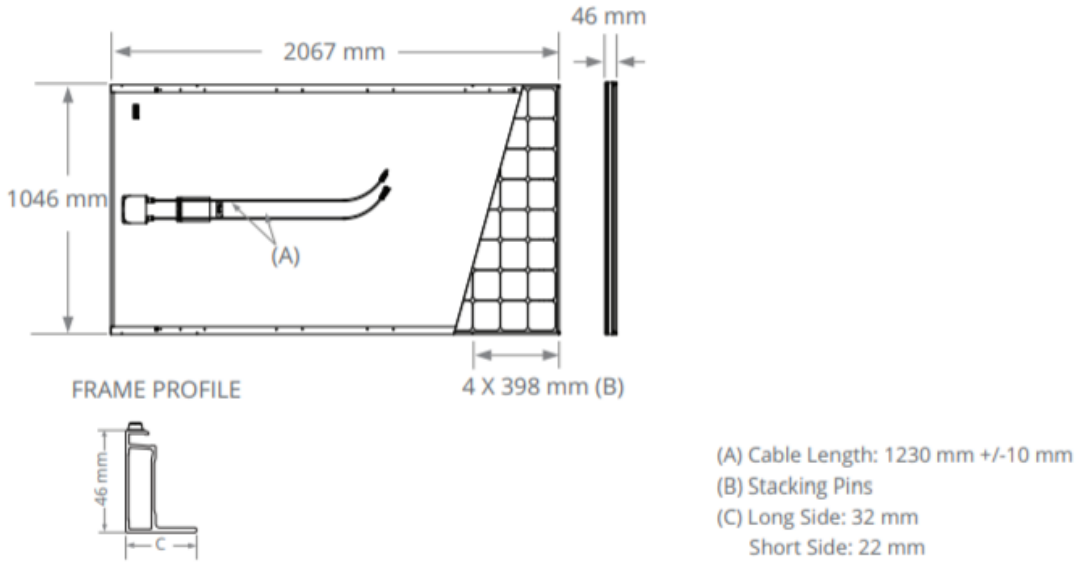

Figure 3.8*: Solar panel dimensions (www.sunpower.com)*

Table 3.4: Solar Panels Data (www.sunpower.com)

ELECTRICAL DATA (SPR-X21-460-COM)	
Nominal Power	460 W
Power Tolerance	+5/0%
Panel Efficiency	21.3%
Rated Voltage (Vmpp)	77.3 V
Rated Current (Impp)	5.95 A
Open-Circuit Voltage (Voc)	90.5 V
Short-Circuit Current (Isc)	6.39 A
Max. System Voltage	1500 V IEC & 1500 V UL
Maximum Ser	15 A
Power Temp. Coef.	-0.29% / ºC
Voltage Temp. Coef	-223.2 mV /ºC
Current Temp. Coef.	2.9 mA / ºC

3.2.2 Results and discussion for solar photovoltaic system

3.2.2.1 Case 1: 40% of the weather deck with PV panels in the North Sea (56º, 2º)

Figure 3.9 and Figure 3.10 presents a full year data of results for two situations with 880 and 1780 panels, resulting in 1903 m^2 and 3849 m^2 of PV surface respectively.

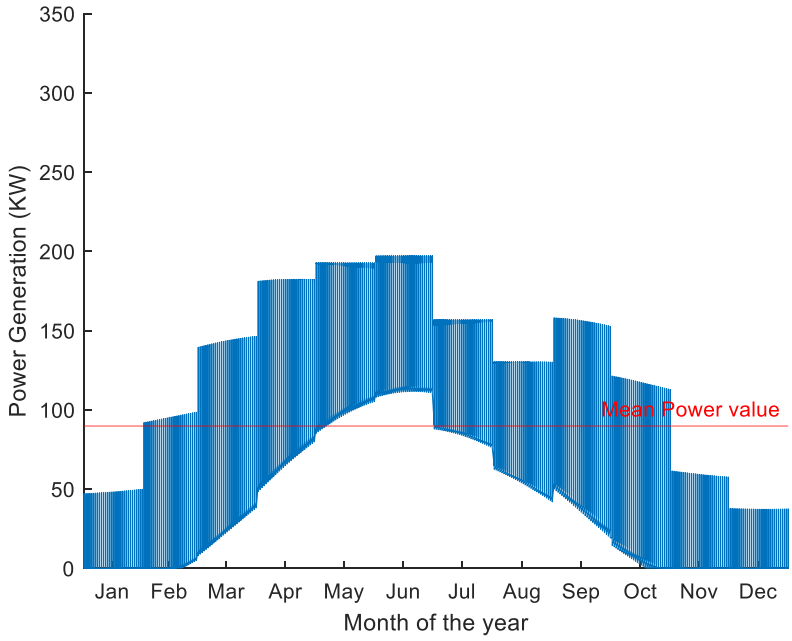

Figure 3.9: Year power generation in the North Sea for 1780 solar panels

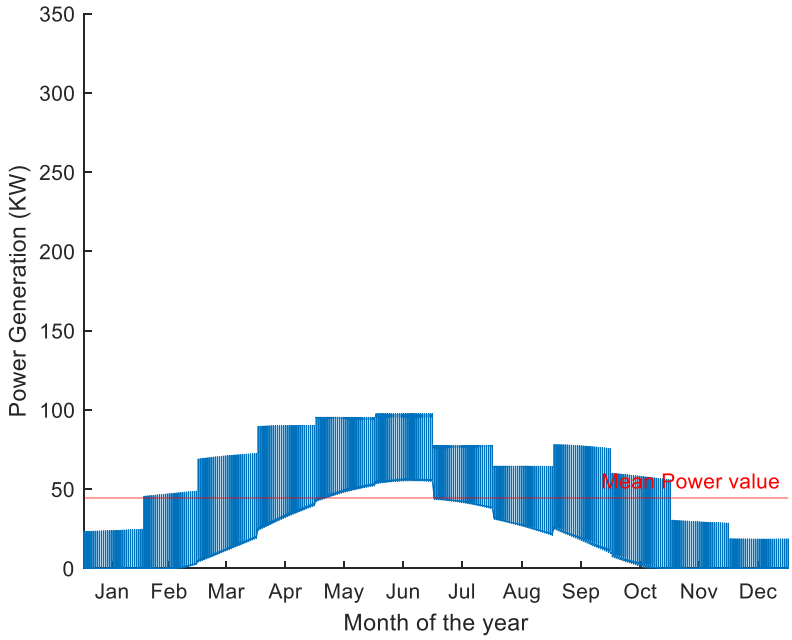

Figure 3.10: Year power generation in the North Sea for 880 solar panels

Both graphs represent the same geographical situation with a variation in the total area of PV panels. As equation (3.2) demonstrate, values increase proportionally with the PV area. The tendency of the figures shows differences between summer and winter production, typical characteristic for ubications far from the equator line.

The irregularities in the graph shape are caused by the data used in the calculations. Final intensity received by the PV panels depends on the angle of the solar rays on the surface and the average solar intensity depending on cloudiness, pressure, or temperature. The solar intensity is defined in a monthly average in this thesis; then the power production is changing twelve times during the year.

Figure 3.9 and Figure 3.10 show three different areas. In winter the output is the lowest. During the month of January, fluctuation goes from 0 to approximately 25kW for 880 panels and from 0 to 50kW for 1780 panels. Summer is the season with the best production. There is energy generation during day and night. Maximum power is on 16th of June reaching values of 97 kW for 880m^2 and 197kW for 1780 panels.

Figure 3.11 represents a power comparison between the daily production depending on the season. The left graph represents summer production and the right graph winter production for the installation of 1780 solar panels in the North Sea. The summer graph is for the 1st of June and winter graph for the 1st of January.

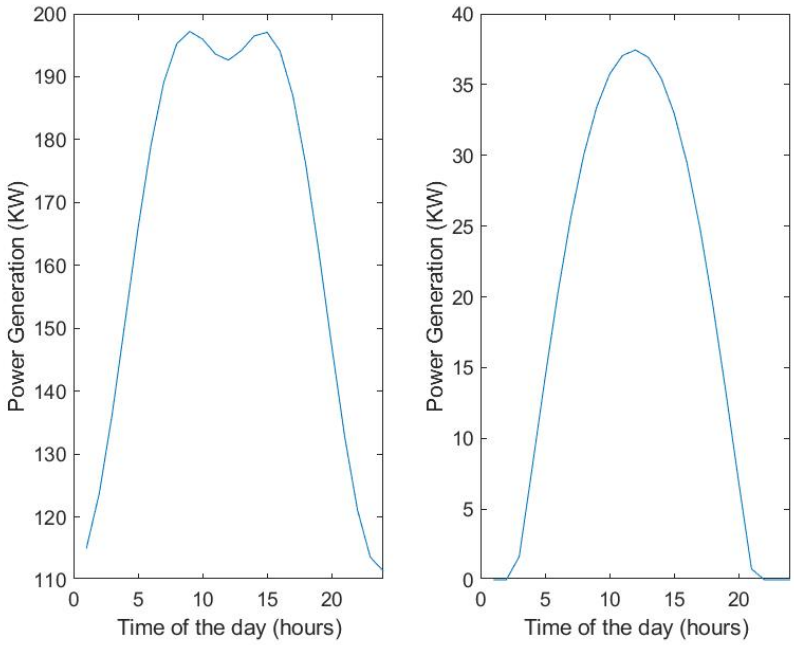

Figure 3.11: Comparison between Summer(left) and Winter(right) daily power generation in the North Sea

Between the graphs shown in Figure 3.11, it is possible to compare a daily power fluctuation for summer and winter radiation. In both cases, there is an increasing level corresponds to the sunrise, the top maximum radiation for the period where the sun is up in the sky, the sunset where the radiation decreases and the night where the radiation is very low or inexistent. An interesting point to see is the "M profile" that the graph has during the maximum radiation period with a valley coincident with the mid-day. As it is mentioned above, it is because the sun course in the sky does not follow a circle perpendicular to the PV. Then, there are two peaks of maximum production.

If the daily production of the two cases is compared, the summer fluctuation has a more extended period of maximum output, with a short night and the lowest value above 45 kW. Instead, the operation during the winter season would give longer nights with periods without energy production, and the maximum energy production is reduced to values under 40 kW.

3.2.2.2 Case 2: 40% of the weather deck with PV panels in the Arabian Sea (13º, 64º)

Figure 3.12 and Figure 3.13 show the energy generation fluctuation for one year of the two system dimensions exposed above for the coordinates 13º longitude, 64º latitude located in the Arabic sea.

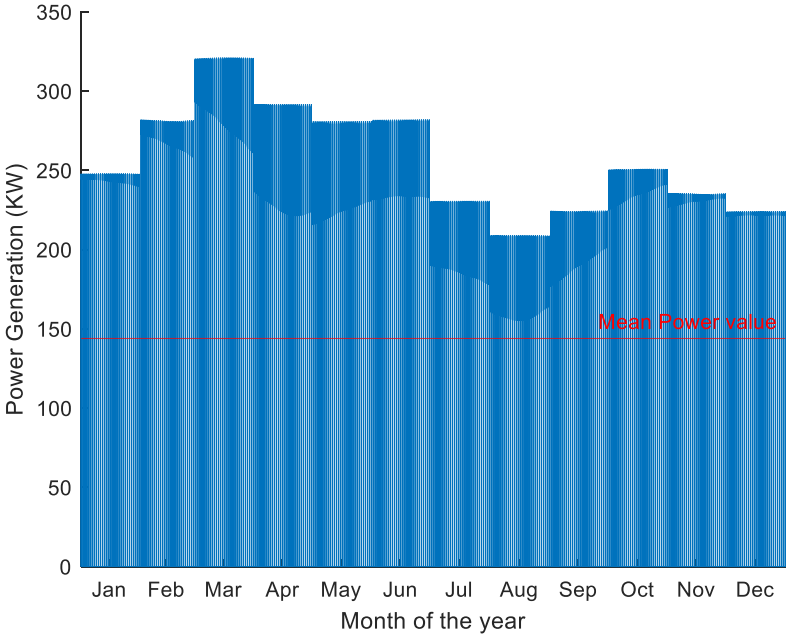

Figure 3.12: Year power generation in the Arabic Sea for 1780 solar panels

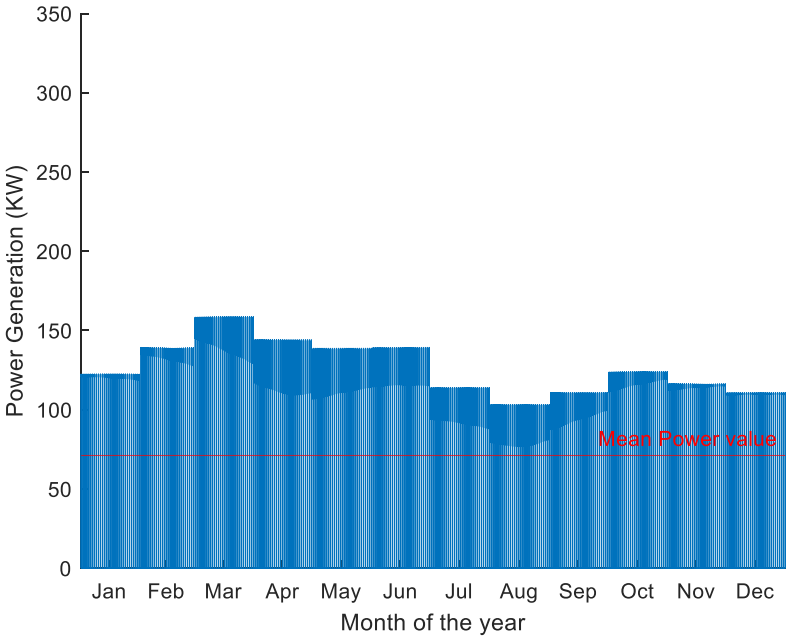

Figure 3.13: Year power generation in the Arabic Sea for 880 solar panels

The proximity to the equator gives a more regular pattern of production all year with much lower fluctuations depending on the season. For this second case, the maximum yearly

variations go from a minimum generation during August to maximum output in March. Maximum power supplied is in this case 159 kW for 880 panels and 321kW for 1780.

Figure 3.14 represents the daily power fluctuations for 1780 solar panels on summer in the left hand and winter on the right side in the Arabic sea.

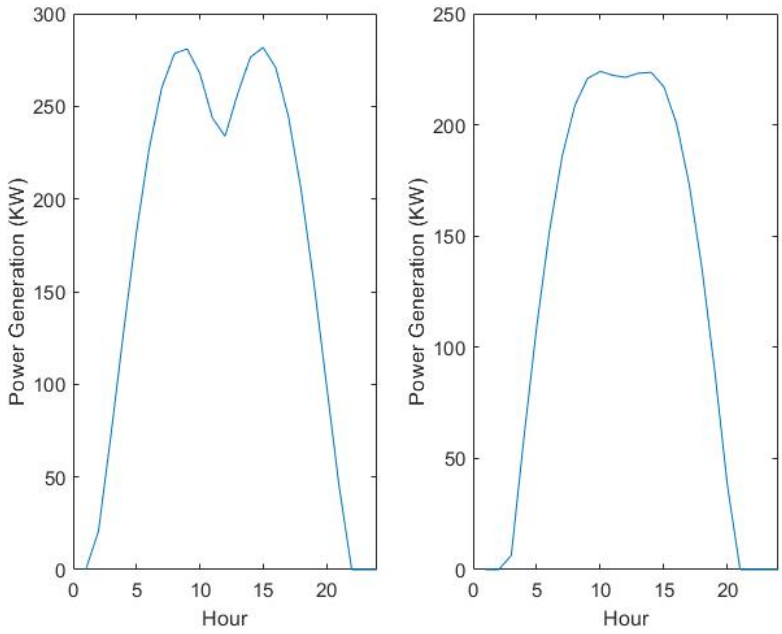

Figure 3.14: Comparison between Summer(left) and Winter(right) daily power generation in the Arabic Sea

Difference between summer and winter power generation is not relevant in this localization. Production shape for both situations similar. For both cases, the maximum energy outputs go between 200 kW and 300 kW. During the night, there is no production at any time of the year. The differences between the two conditions is a slightly higher production during summer that increments the “M profile”.

3.2.2.3 Case 3: 40% of the weather deck with PV panels in South African Coast (-42º, 25º)

Figure 3.15 and Figure 3.16 represents a full year data of results for situations with 880 and 1780 panels, respectively.

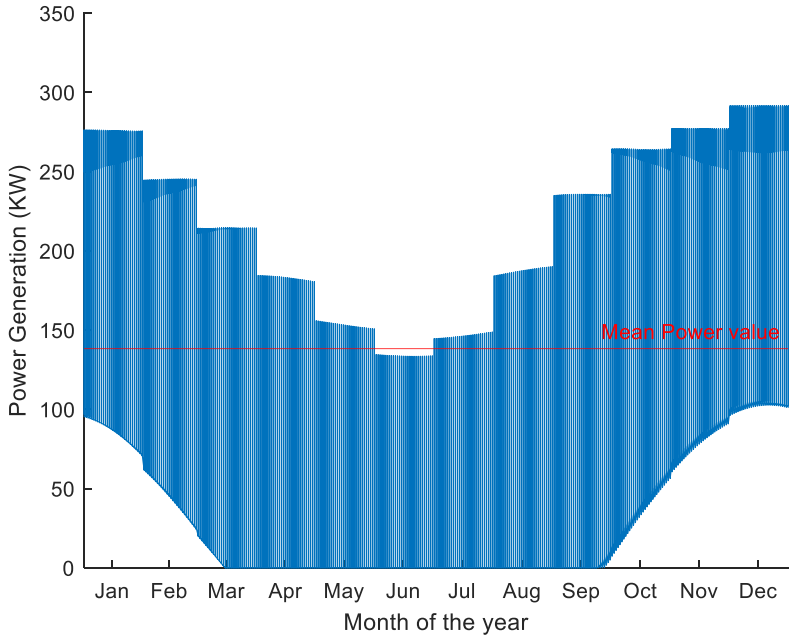

Figure 3.15: Year power generation in the Arabic Sea for 1780 solar panels

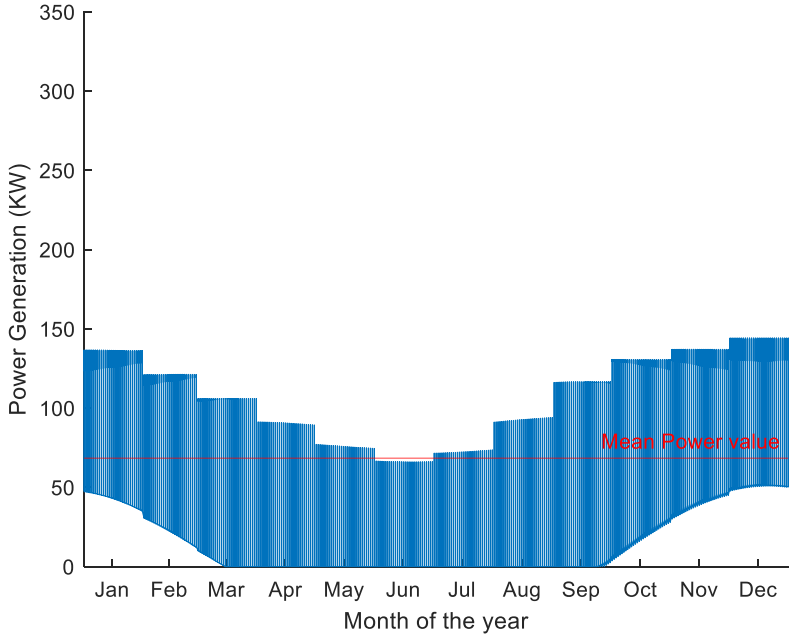

Figure 3.16: Year power generation in the Arabic Sea for 880 solar panels

The difference in shape on this graph is because the location is in the southern hemisphere. As Figure 3.15 and Figure 3.16 show, in this case, the maximum production is during the month

of December with an output of 292 kW for 1780 solar panels, and 144 kW for the 880 solar panels.

Figure 3.17 represents the daily power fluctuations for 1780 solar panels on the South African coast. Summer is represented on the right hand and winter on the left. Although the dates are the same as in 3.2.2.1 and 3.2.2.2, for this case as the location is in the southern hemisphere, winter season is in June and the summer in January.

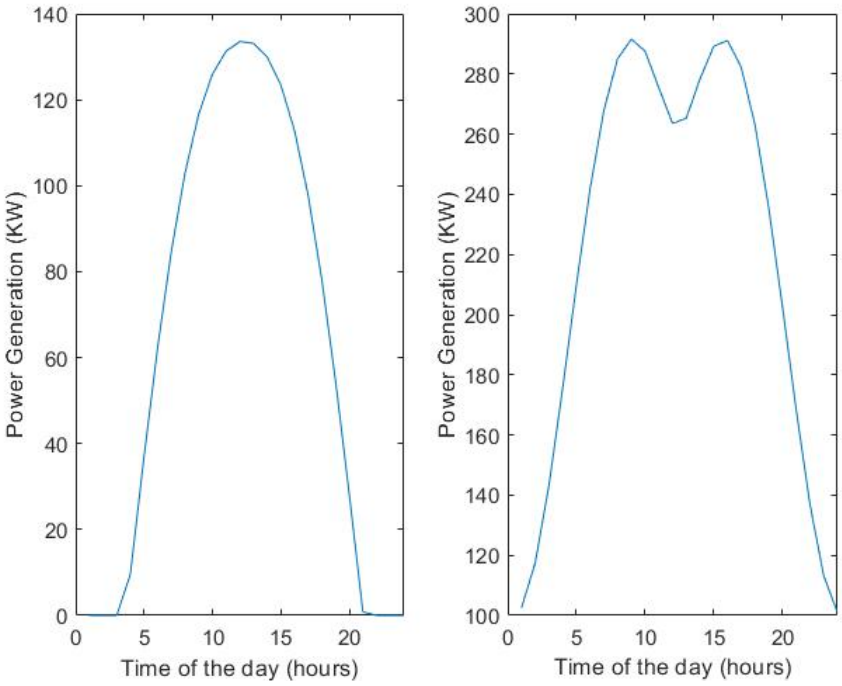

Figure 3.17: Comparison between Summer(right) and Winter(left) daily power generation in the South African Coast

Figure 3.17 shows that the production is continuous during summer, with short nights where the energy production stays above 50 kW. As in case 1, “M profile” appear during summer months. During winter, there are extended periods of the night without any electrical output with peaks of power about 130 kW at mid-day.

3.3 Wind Turbine Power Generation

As a part of the electrical generation systems, wind turbines are supposed to contribute to the power supply of the systems onboard. Among the different possibilities of wind power generation, the vertical axis wind turbine has some advantages compared to the others to install on a ship. It does not require an orientation system to adapt to the constant changing of wind direction. The electrical generator of the turbine is installed into a floor-level, i.e., it would avoid high altitude labors. Finally, vertical axis turbines have a better weigh arrangement in terms of stability, an essential characteristic of a floating structure (Kim and Yaakob, 2016).

3.3.1 Methodology study of the wind turbine generator

For the analyses of the wind turbine, data comes from the manufacturer, D'Ambrosio and Medaglia (2010) and Kim and Yaakob (2016). The rotor is a "VAWT 200 kW" from the manufacturer "VerticalWind AB". Relevant technical specifications are shown in Table 3.5.

Table 3.5: Vertical wind turbine technical specifications (D'Ambrosio and Medaglia 2010)

Data	Unit
Number of blades	3
Height of the tower	40 m
Rotor diameter	26 m
Length of blades	24 m
Nominal Power	200 kW
Nominal Wind speed	12 m/s
Minimum wind speed	3 m/s
Cut-off wind speed	22 m/s
Power coefficient (Cp)	0.314
The efficiency of the generator (η)	0.95

Some critical parameters of the wind turbine systems are:

- Wind speed limit or cut-off wind speed: It is the maximum allowed wind speed to run the generators for security reasons.
- Nominal speed: It is the maximum rotational speed that the propeller run. The propeller can resist harder winds; however, the output continues to be the same.
- Minimum wind speed: It is the minimum wind required for the turbine to generate.

Using the above parameters and with the equation (3.16), it is possible to establish a relation of electric power production depending on the apparent wind speed. It is defined by v as the apparent wind speed in m/s, A as the Area of the turbine blades, Cp as the power coefficient, ρ as the density of the air and η that is the efficiency of the generator.

$$P = 0.5 * Cp * \rho * \eta * A * v^3 \tag{3.16}$$

The area of the turbine blades is defined with the equation (3.17), with the length of the blades, H_{blades} and the turbine diameter, D_{rotor}.

$$A = H_{blades} * D_{rotor} \tag{3.17}$$

3.3.2 Results and discussion of wind turbine generator

With the data from Table 3.2 and Equation (3.16), the power for a range of wind speeds from 0 to 25 m/s can be calculated, the result is shown in Figure 3.18. The figure shows that the energy productions start with the minimum wind speed corresponding to 3 m/s. The production follows the Equation (3.16) up to the nominal wind speed at 12 m/s. From 12 m/s the output

is maintained stable at 200 kW until the cut-off point at 23 m/s when the rotation stops for safety reasons.

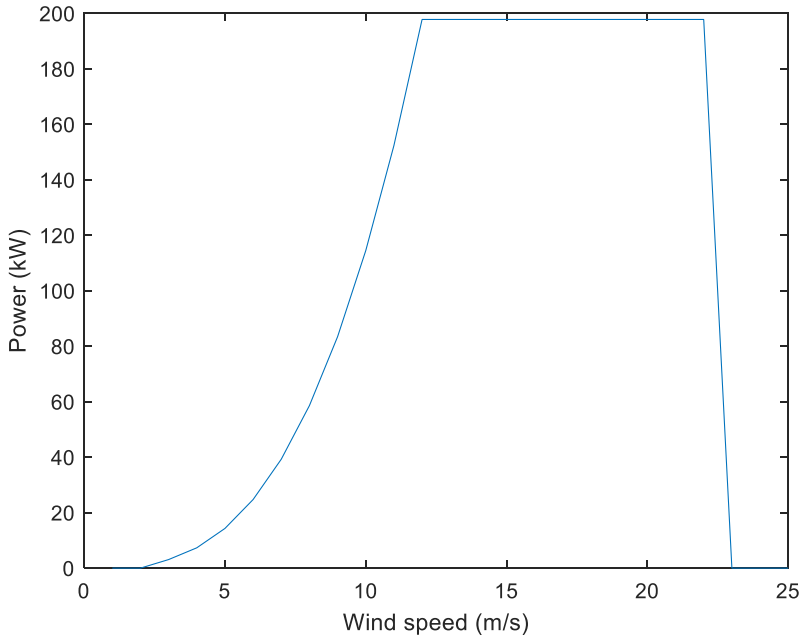

Figure 3.18: Wind turbine power

Apart from the production rates depending on the wind, some other parameters are considered to determine the usability of the system in the ship concept:

- The space required: The system has a big sweeping range that creates incompatibility with other structures on the weather deck.
- Height Limitations: The total height of the structure creates limitations in some routes with air draft restrictions.
- Stability: The side forces can create some problems of security in extreme circumstances.
- Added resistance: The balance between the energy generated and the added air resistance need to be analyzed.

3.4 Results and Conclusions

Chapter 3 studied four different technologies to install in a renewable-powered vessel to prove its viability and to develop a numerical model to use as a tool to evaluate systems and to implement in a final simulation. For the propulsion of the vessel, two wind propulsion systems are considered and compared, Flettner rotors and Wing sails. Also, for the electric production onboard electrical photovoltaic panels, and wind turbine generators are evaluated.

The study of the wind propulsion systems is done for a wing sail of 1800 m^2 of sail area and a Flettner rotor of 150 m^2 of cylinder section. The renewable systems are calculated to be installed on an example high blockage ship.

Both systems have the potential to be installed on the concept vessel. Wing sails, with a larger area, produce higher speeds for the same number of sails and don't require power to generate propulsion. Flettner rotors need less space to be installed, have better performance regarding stability, and have reduced operational requirements. Focusing on the criteria of practicality and simplicity of the ship, Flettner rotors will be used.

Regarding PV generators, simulation establish the electrical production for three different locations and two different panel distribution on each point in the map. Results give notable fluctuations of production in the high latitudes and stability in low latitudes. Although the total electric generation is depending on the weather conditions, it is concluded from the results that the production is efficient enough to be included for the concept ship.

Finally, wind turbines are analyzed based on data from previous studies of vertical axis models. Some points to consider for this technology are the total power production, the space required, the height limitations, the stability of the turbine, and the added resistance. The conclusion gives viability to the system as it can produce a high production rate, and the other considerations are proved not to negligible, according to Kim and Yaakob (2016).

4 Concept Design

4.1 Ship Considerations

An optimum selection of a ship and the correct arrangement of the systems on board is an essential step to define the requirements to accomplish later on the simulations. It is necessary to analyze the pros and cons of the design and go for the best option.

The most crucial challenge for the ship is the energy limitations that renewable sources have. The combination of lower energy production, in comparison with fossil fuel, and the intermittency in power production, limits the vessels speed. An unacceptable condition that creates uncertainties for the market for high-value goods, unless in an excess of fleet capacity (Balcombe et al., 2019). The best option is to go for ships that do not require high speeds. Low-value goods market is the best option, i.e., freight with a relatively low price concerning volume (Korinek and Sourdin, 2009).

Renewable energy systems require spaces on open structures. Merchant ships that need to allocate the cargo or handling equipment on the weather deck create a limitation for those technologies. Sufficient deck space is necessary to install the systems without interfering on loading or unloading operations.

The ship used for this study is a high-blockage cargo ship. It is not designed for the specific purpose of the concept because it would go far from the goal of the thesis. Energy sources on board consist of a hybrid system with electric power production by photovoltaic cells and wind turbines, and a wind propulsion system with Flettner rotors. Renewable energy systems are installed on the weather deck; it is assumed that the space required for the installation is available and is not compromising the operation of the ship.

The ship is designed with the assumption that crew is not required to operate it because of two main reasons: (i) Reducing the costs of crew helps to make the concept more profitable, even with low speeds. (ii) Avoiding the crew energy demand, e.g. for hoteling, the final energy consumption is reduced.

An element on the vessel to be reassessed is the superstructure. In conventional ships, it rises vertically, resulting in the highest point. However, in a renewable concept, this structure would block the wind. As it is an unmanned vessel, the superstructure is reduced to a bridge to take control of the vessel in case of an emergency. It is located forwards since then the interaction with the Flettner rotors is the most favorable.

4.1.1 Arrangement

The final energy production, as well as the thrust generated, is hardly dependent on the distribution of the systems on the vessel.

From Section3, the most feasible option according to results for propulsion was six Flettner rotors. Distribution of the rotors is equally in both sides, with three in port and three in starboard. A point to discuss for the arrangement of the rotors is the center of forces where the thrust is applied. If the position is far aft, the yaw moment is too high to be compensated by the rudder. It is necessary to allocate the rotors forward to avoid this situation. Figure 4.1 shows

a top view sketch presenting the distribution of the rotors on the open deck. Those are located forward in the ship with the thrust force at 75% Lpp from AP.

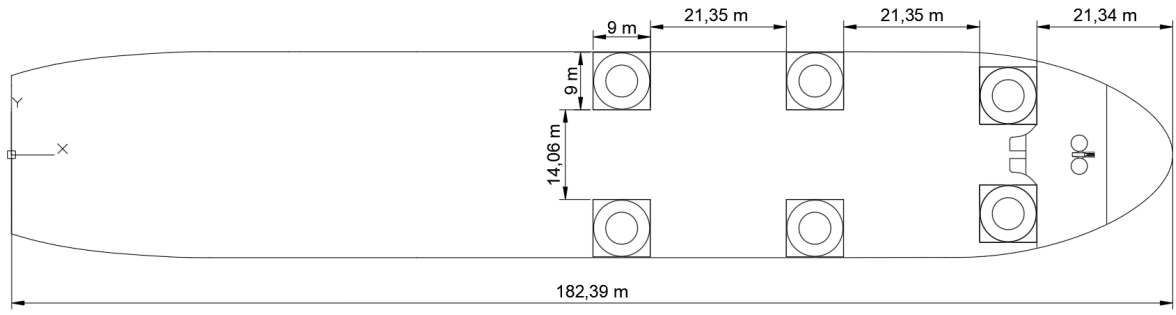

Figure 4.1: Top view of the Flettner wind propulsion installation

Vertical wind turbines are located in the aft of the ship. Flettner rotors generate maximum propulsive force for side wind conditions, but with head or stern winds, the power is reduced or neglected (Tillig et al., 2019). Turbines are installed in the aft of the ship because of its interferences creates a lower effect for the rotors. Also, as the distance between turbines and rotors is considerable, the interaction of wind from rotors is small (Tillig et al., 2019). Two wind turbines are installed according to Figure 4.2 in a position to not exceed the beam of the ship and with clearance for the swept areas of the blades between them.

Figure 4.2: Top view of the wind power installation

The rest of the weather deck surface is used for the installation of solar panels. As Figure 4.3 shows, there are 1564 PV generators distributed in groups of 2 lines going from port to starboard. The distribution considers margins between photovoltaic groups to enable maintenance and reparation. The panels are mounted in a structure at 2.59 m above the deck surface to allow the access and for machinery space. The characteristics of the groups are presented in Figure 3.8 and Table 3.4.

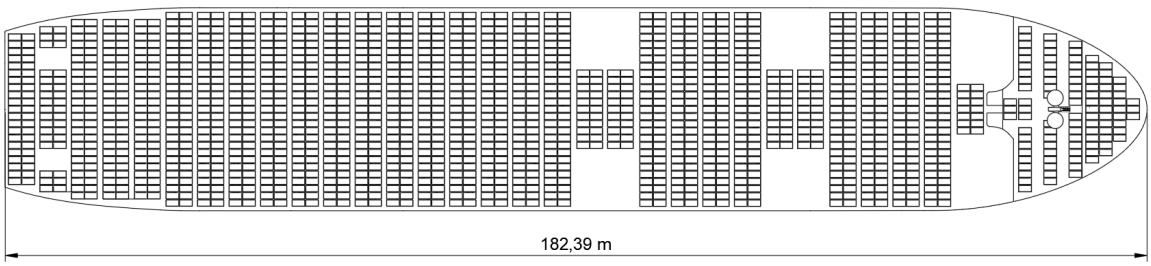

Figure 4.3: Top view of PV installation

Figure 4.4 shows the bridge of the ship. It is located in the fore of the vessel. As Figure 4.3 shows, the roof of the bridge is designated to the installation of communication systems and additional solar panels.

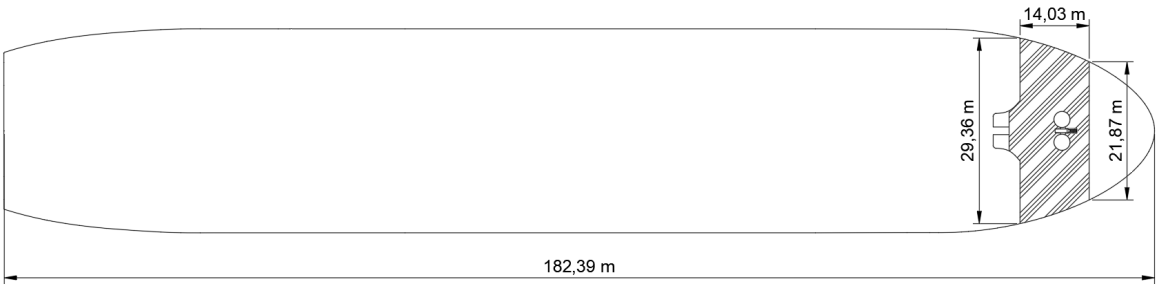

Figure 4.4: Top view of the superstructure

4.1.2 The electric consumption of the ship

Some devices and electrical systems are indispensable for the operation of the vessel. The objective of this section is to find an estimation of the electrical consumption when the ship is at sea.

There are two different electric consumption considered:

i) When the ship is at sea
ii) During maneuvering.

For the sailing condition, Flettner rotors are the only propulsive system considered. Many electrical loads of conventional vessels are designated to the habitability systems as for the water treatments or hotel loads. As the ship is unmanned; loads designated to the habitability of the vessel are eliminated. Emergency energy systems are not considered. The electric consumption is assumed to be for propulsion, navigation systems, power management system devices, and other required cargo systems onboard. From Kusuma and Pratama (2017) and NýOrka and Marina (2017), it is set that the energy demand for those systems is between 37 kW to 145 kW for a ship with similar dimensions. The fluctuation range is notable because of the uncertainties that the concept has concerning the cargo of the vessel or the undefined equipment on board. It is assumed that the electric consumption is 70 kW keeping it constant for all the routes.

In maneuvering condition, the ship is assumed to have an output power of 80kW (Andersson et al., 2018). Moreover, considering that this situation is maintained for a period of one hour, in the energy balance there is an extra output power of 80 kWh.

4.2 Choice of Routes

As the performance of the ship is dependent on the environmental condition, the selection of the route is crucial to see the usability of the concept and to evaluate which courses are the most and the least favorable.

Two parameters are considered to choose the routes. The first is the viability of the system regarding the weather condition like wind, solar radiation, and sea state. And the second is about the density of trade between the ports of the route.

There are three different evaluated routes. In all cases, the analysis is for the round trip, to increase the situations being assessed. Courses are:

i) Rotterdam to Houston
ii) Rio de Janeiro to Gothenburg
iii) San Francisco to Shanghai.

The routes in the numerical model are defined by a series of waypoints fixed by longitude and latitude.

Wind data, used for a waypoint in the sea, remains constant during a full month because of the average monthly data, and solar radiation intensity modifies with the daytime. The starting dates are defined to study a diversity of weather conditions. Houston – Rotterdam, starts the 1st of January, Rio de Janeiro - Goteborg the 1st of August, and the transpacific course from Los Angeles to Shanghai is set to begin the 1st of April. About the daily timing factor, all three trips start at 7 a.m. local time.

4.2.1 Rotterdam to Houston

This route constitutes the bond between some of the primary ports form the European Union and the East Coast of the United States of America. Houston is one of the most important ports for the exportation of grain to the rest of the world. For bulk carriers, these routes are carried out frequently. It is a relevant point for the study of the concept (Hoffmann et al., 2017).

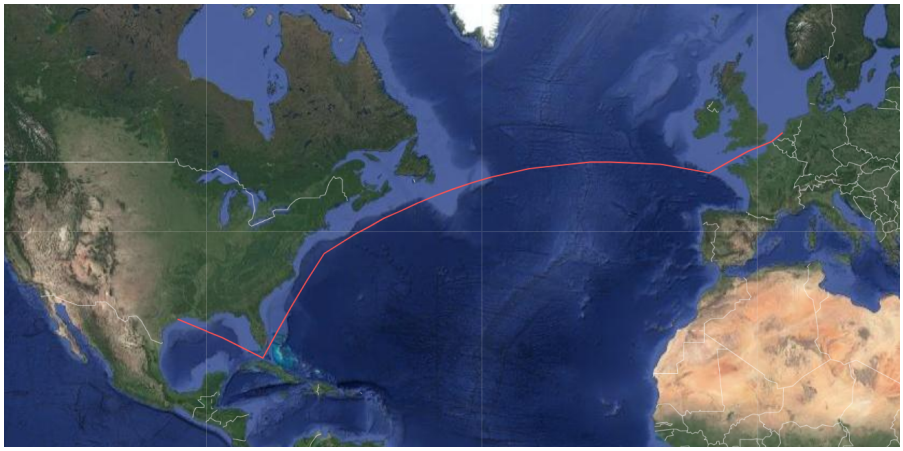

Figure 4.5: Route Rotterdam - Houston

The journey starts in Rotterdam. The ship goes throw the English Channel, and when it arrives at the Atlantic Ocean, the vessel crosses it with a constant latitude to the northern United States coast. Finally, it sails down close to the coast and enters the Mexican Gulf through Straits of Florida to reach Houston Port. The total distance is about 5096 nautical miles. Table 4.1 shows the coordinate points on the map.

Table 4.1: Route Rotterdam to Houston starting day 1 of the year

Point in the map	Latitude	Longitude
Rotterdam	52º	4º
English Strait	51,2º	2,2º
North Atlantic 1	47,9º	-7.8º
North Atlantic 2	38,3º	-70,8º
Florida Strait	23,8º	-80.9º
Houston	29,5º	-94,9º

Meteorologically, the interest of the route is on the areas that the ship is circulating. Winds and currents in this region follow for the North Atlantic Gyre. This phenomenon occurs as a consequence of the increasing of air temperature in the equator; then it goes clockwise to the north getting colder and arriving at the African Coasts. The result creates a different priority of routes depending on the direction.

4.2.2 Rio de Janeiro to Gothenburg

Brazil has 25.8% of the global market in iron, and it also has a remarkable production in raw products as the sugar cane (Hoffmann et al., 2017). Gothenburg, on the other hand, is the most crucial port to distribute gods around the Scandinavian peninsula. The route Rio de Janeiro – Goteborg is represented as a vital union for importation-exportation of a diversity of products from South America to the North of Europe.

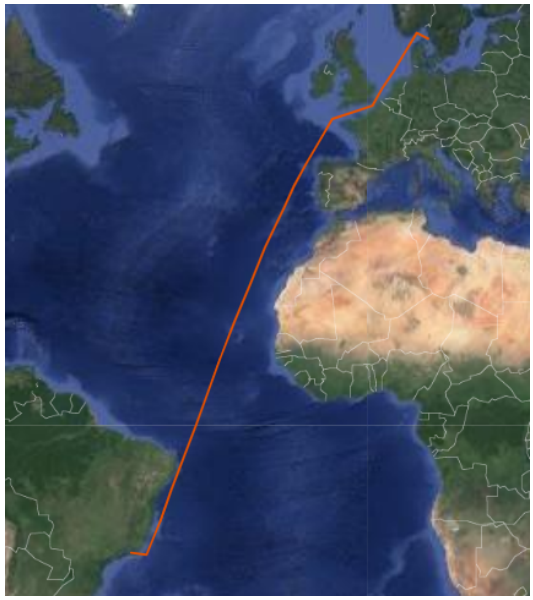

Figure 4.6: Route Rio de Janeiro – Gothenburg

The journey, with a distance of 5784 nautical miles, goes from the South Atlantic to the North Atlantic in a diagonal directly to the Celtic Sea. Then through the English Channel to the North Sea crossing the Skagerrak Strait, arriving in Gothenburg.

Table 4.2: Route Rio de Janeiro to Gothenburg starting the day 213 of the year

Point in the map	Latitude	Longitude
Rio de Janeiro	-22,9º	-43,1º
South Atlantic Sea	-23,3º	-40,5º
Nord Atlantic Sea	40,0º	-6,4º
English Strait	50,5º	1,0º
Skagerrak Strait	58,2º	9,3º
Gothenburg	57,7º	11,3º

Interests on weather conditions for this case is the diversity of global winds that the route goes throw. The journey starts in a zone affected by the South Sea Gyre, and then, it enters the Southern trade winds. The equator line is the worse situation as winds are shallow. Moreover, in the northern hemisphere area, the course faces front winds and the North Atlantic Gyre.

4.2.3 Los Angeles to Shanghai

Commercially, Shanghai and Los Angeles ports can be considered as a connection of the main importation – exportation points for the two economic global powers. The route is not predominated for dry bulk, instead elaborated products are more relevant in this trade. However, the interest is in the frequency of transit that exists between them.

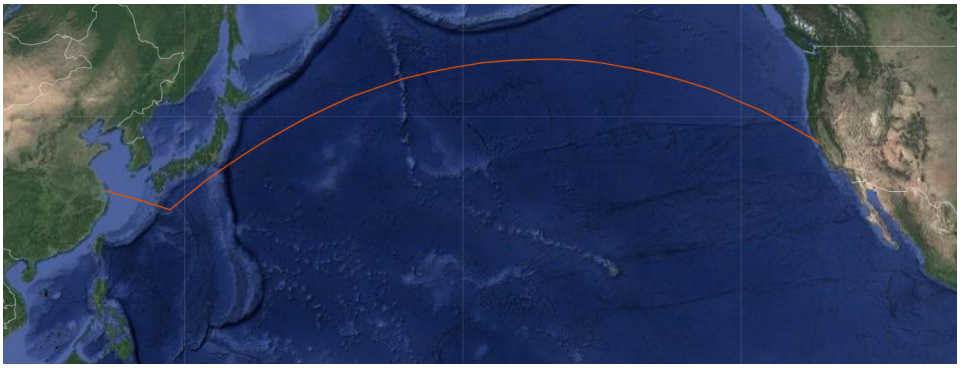

Figure 4.7: Route San Francisco - Shanghai

The route goes directly from Los Angeles harbor, with a constant latitude to the Philippine Sea in the South of Japan. Entering into the Oriental Asian Sea, the course goes through the Hangzhou Bay to Shanghai. The total distance of the course is about 5869 nautical miles.

Table 4.3: Route San Francisco – Shanghai starting day 91 of the year

Point in the map	Latitude	Longitude
Los Angeles	33,7º	-118,3º
Philippine Sea	28,8º	132,6º
Gothenburg	31,3º	122,3º

This simulation is a study of a transpacific course. The route is mostly going along the 30th parallel. This latitude goes throw the westerlies winds, which possibly creates differences between the eastbound and westbound journey.

4.3 Concept Simulation

Chapter 4.3 considers all energy sources that the ship receives for specific points and analyze the technologies individually implemented on board the vessel. For the simulation of the concept, all systems need to unify into an extensive numerical simulation that offers the sailing condition and the energy situation of the concept ship for a defined route.

4.3.1 Route configuration

The chosen route must be validated with real data from the places where the ship is in each moment. This data comes from the NASA database "POWER Data Access Viewer" (NASA, 2019). The information from this source gives a monthly mean value of different weather conditions for any point of the earth with a precision of one degree of longitude and latitude. The input data for the simulations is the solar intensity, the Albedo index, temperature data at sea level as well as wind speed and direction. As parameters depend on the period of the year and daily time, a starting temporal parameter with a date and time of the trip is set for the study.

The course is defined in the simulation by joining the coordinates of all waypoints. Each section is treated separately and divided into equidistant points; the ship responses are evaluated individually.

Environmental data is provided with a precision of one degree; thus, the distance between coordinates must be less than 60 nautical miles corresponding to the distance between consecutive degrees.

The process to calculate the instantaneous condition of the ship starts with an initial point. This point is described with global coordinates and a polar direction of the line to the next point. The process begins by finding the surrounding weather condition that the ship faces. Those are used as the input value to calculate the speed, power consumption, and power generation. Then, the results are used to determine the time that takes for the vessel to arrive at the next point in the route and the power balance during this leg. New coordinates define a new position, and the actualized input values are redefined. The process continues for the different sections until the end of the route.

4.3.2 Flettner rotor wind propulsion

In the pre-study of the wind propulsion systems, the ship is considered to sail without any drift, an assumption that reduced the accuracy of the result. In the concept design, results are reconsidered by using the code from ShipCLEAN software for 4 DOF to calculate the resistance and the thrust generated by the Flettner rotors. ShipCLEAN, apart from the wind speed and angle used on the pre-study, uses other parameters as wave height and direction, current speed and direction, water temperature and sea depth, which result in a more accurate prediction of the ship‘s response(Tillig et al., 2019). For the study case, the parameters are

simplified to afford the computational power required. As it is mentioned in Section 4, from the wind speed and angle, the wave height and direction is estimated; sea current is not considered, the temperature is assumed constant at about 19ºC and sea depth set to 2000 meters.

The numerical model calculates all the forces applied on the ship, and the equilibrium of forces results in the resistance for 4 DOF. The side forces generate drift in the vessel´s movement. As the purpose is to adjust the drift for the route requirements, the calculation establishes the necessary rudder and keel forces for the wind correction angle to follow the desired course (Tillig et al., 2019). The result is a final speed based on the equilibrium between the total resistance and the sail thrust.

To work in an affordable range of time the study needs to avoid estimating the response in each point in time with the 4DOF function of ShipCLEAN. The solution is to work with tabulated data, i.e. interpolating precalculated results for the actual wind speed and angle.

Figure 4.8 presents the resulting ship speeds of the concept ship with 6 Flettner rotors. As discussed in Section 3.1, the plot affirms that:

- The winds that give more thrust are always those coming from the sides of the vessel
- Winds coming from angles between 60 and 300 degrees (i.e. head winds) offers low or negligible forces on the ship
- For stern winds, there is relevant decreasing on thrust and increasing of resistance due to high side forces.

In terms of efficiency, it is beneficial to sail in certain apparent wind angles and avoid others. As an example, in a route with head winds, it would be impossible to go straight ahead since the ship cannot sail straight against the wind. On the other hand, on journeys with side winds, the straight line is the fastest way. VMG (Velocity Made Good) represents the speed towards the target, which is used to calculate the time to travel between two points and which considers tacking angles.

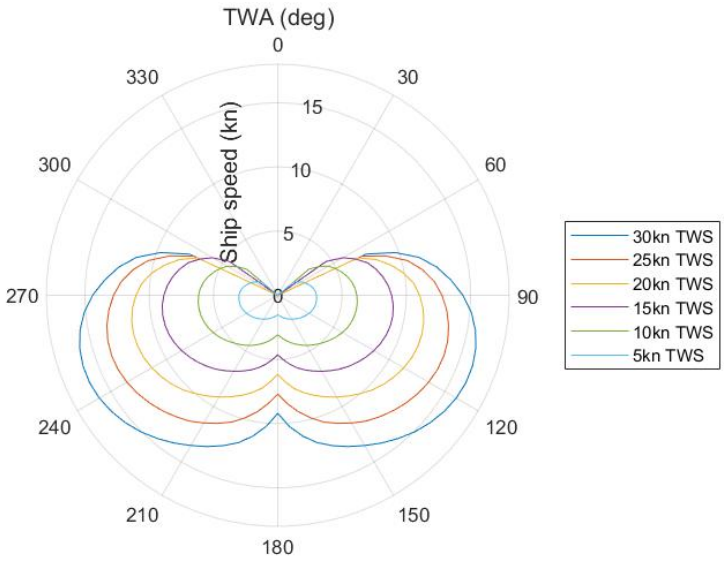

Figure 4.8: Polar plot of ship speed depending on wind angle and speed

4.3.2.1 Velocity Made Good

The purpose of the VMG (velocity made good) is to give a reference speed for the ship to move the straight-line between two points. In a sailing vessel, for some courses navigating with wind angles different from those experienced on the direct course is beneficial. For these cases, the final route is longer than the straight line. As the optimal distances depend on the directions of the wind, VMG is referred to the straight-line distance that a ship has traveled divided by the elapsed time. To sail the most efficient route, the use of an algorithm for VMG optimization is necessary.

Input information for the VMG algorithm is the true wind speed, the true wind angle and the polar angle of the course.

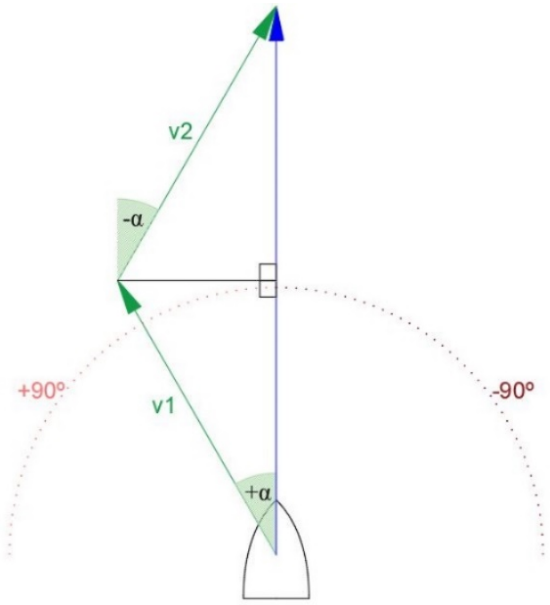

Figure 4.9: VMG sketch

The process starts with a definition of different wind angles estimate the 4 DOF solution. As it is sketched in Figure 4.9, the angle deviation must always be higher than -90 degrees and lower than 90 degrees from the ship's heading. Angles from 90 to 0 degrees are referred to the port direction and from 0 to -90 degrees for starboard directions. The range of deviations will be split into steps of one degree, and speeds are calculated for each of the angles.

The 180 possible angles are evaluated individually, but as the ship travels the same distance for port and starboard deviation, the resultant VMG from a situation as Figure 4.9 is calculated with the Equation (4.1)

$$VMG = \frac{cos(\alpha) * v1 + cos(\alpha) * v2}{2} \tag{4.1}$$

Finally, from the different results, the highest VMG gives the best deviation angles for a weather condition, and the resultant speed is used to calculate the journey results.

4.3.3 Electric power generation

Electrical power is generated onboard the ship by means of PV generators and the wind turbines. General numerical models include both, individual simulations from sections 3.2 and 3.3, for solar panels and wind turbines, respectively. The challenge is to estimate the total power generated for those systems. It is assumed that at sea, results of power production stay constant until the next point in the route, the total power generated is the instantaneous production multiplied by the time elapsed.

5 Results and Discussion

This section is divided into two parts, a journey evaluation, and an energy balance. The journey evaluation consists of an analysis of the VMG of the ship according to the wind conditions on each part of the route. Today, similar high blockage ships are traveling at around 15 knots (McKenna et al., 2012). It is assumed that the market accepts up to 50% speed reduction for an entirely renewable-powered ship. Tus, the minimum target velocity for the vessel is 8 kn.

Flettner rotors have advantages in terms of simplicity for operation and space requirement. However, at the same time the power consumption to rotate the cylinders has to be covered. Thus, the second part is an analysis of the balance between power generated and consumed, first considering only the power necessary for the rotors and secondly also including onboard systems.

5.1 Rotterdam – Houston

Table 5.1 shows the total time needed for the journey, according to the simulation.

Table 5.1: Timing of route Rotterdam - Houston

Distance	5096 nautical miles
Time Rotterdam – Houston	24 days 3 hours
Time Houston – Rotterdam	18 days 22 hours

Wind speeds and angles along the route are presented in Figure 5.1 for the journey from Rotterdam to Houston, in Figure 5.2 for the return trip, from Houston to Rotterdam.

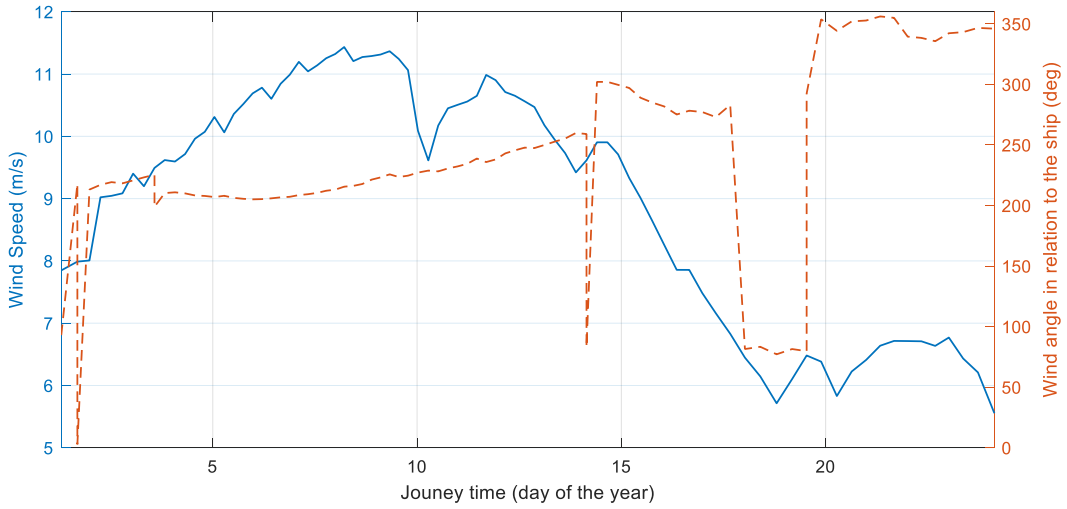

Figure 5.1: Wind speeds and angles for the route from Rotterdam to Houston

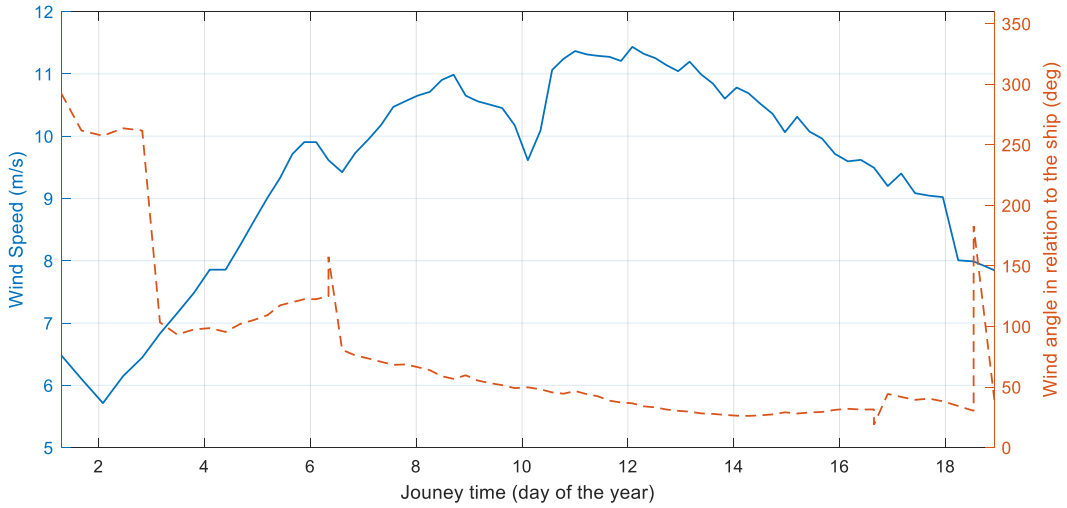

Figure 5.2: Wind speeds and angles for the route from Houston to Rotterdam

In Figure 5.1, the wind angles remain almost constant in the first part of the trip, at a value between 200º and 300º. Wind speeds fluctuate between 8 and 12 m/s. These conditions are optimal for thrust generation and result in high ship speeds. In the last part of the journey, from day 19, the wind speed is reduced to 6-7 m/s, and the wind angle get close to 0º (i.e. head winds), thus becoming worse for the wind propulsion system.

The return trip, shown in Figure 5.2, starts with low wind speeds, around 6 m/s, while it later increases to about 8-11 m/s Wind angles at the start are around 300º, and are later changing to 40º.

Figure 5.3 and Figure 5.4 show the estimated ship speed and the energy generation outputs as well as the energy required on the route Rotterdam to Houston and Houston to Rotterdam, respectively. The instantaneous energy balance considers the energy production from renewable energy systems and the demand from the Flettner rotors. In Figure 5.3, positive values represent that there is more power generated than consumed, while negative values represent for the opposite situation.

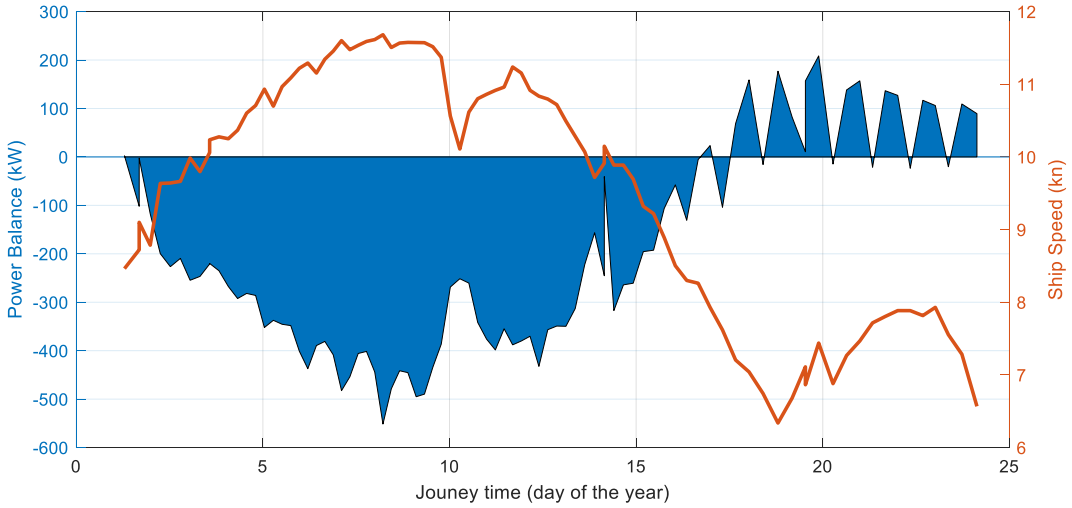

Figure 5.3: Energy Balance and Ship speed from Rotterdam to Houston

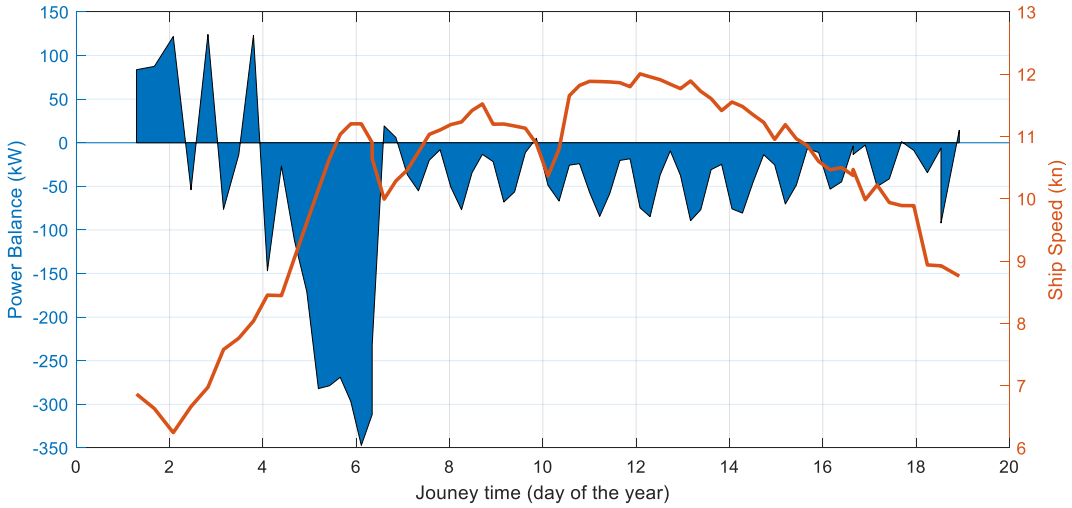

Figure 5.4: Energy Balance and Ship speed from Houston to Rotterdam

According to the results, on the Rotterdam-Houston route the ship experiences an energy deficiency. Both legs of the round trip have an average VMG of 9.7 knots. These journey speeds are competitive, considering the innovative character of the concept. On the outward journey, shown in Figure 5.3, the energy balance is negative for the major part of the journey, reaching a maximum additional energy requirement of about 550 kW. In the last leg of the trip, the speed is reduced and also the power requirements. For these parts, the simulation shows positive energy balances. In Figure 5.4, it can be seen that the conditions are preferable in the return trip. The route starts with slight positive balances, and with increasing wind speeds, the consumption gets negative with values fluctuating mainly from 0 kW to -80 kW.

A comparison between the two journeys, shows that for the same wind speed there is a notable difference in power consumption of the Flettner rotors. This difference is caused by the difference in wind angle, as power consumption increases for headwinds.

Figure 5.5 and Figure 5.6 represent the accumulated power at each moment of a ship journey. Both figures illustrate the energy balance between the energy produced by the renewable systems and the energy demand for two separate cases. A first case, represented in blue, considers the power request from the Flettner rotors operation; and a second case, in red, includes the energy request from Flettner rotors and all electrical systems onboard. Figure 5.5 represents the route from Rotterdam to Houston and Figure 5.6 from Houston to Rotterdam.

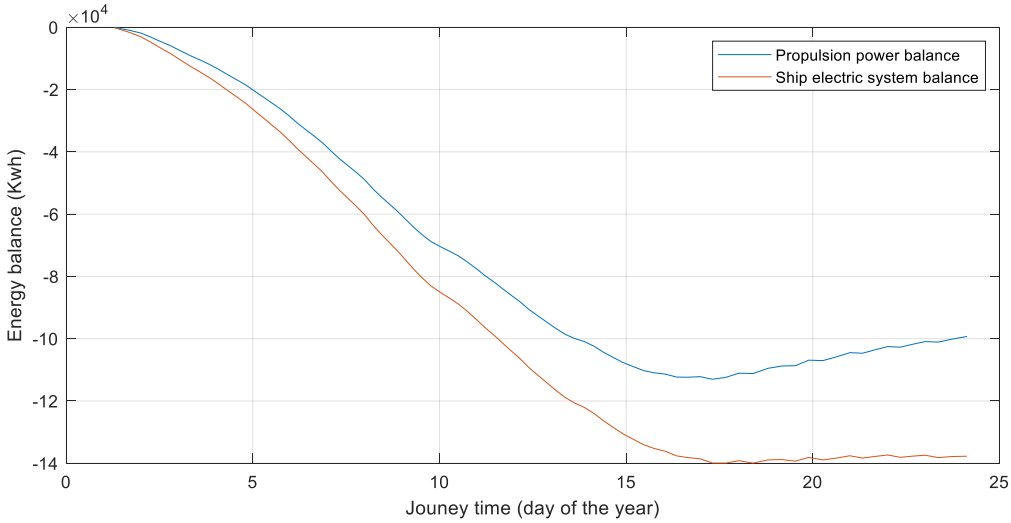

Figure 5.5: Accumulated energy from Rotterdam to Houston

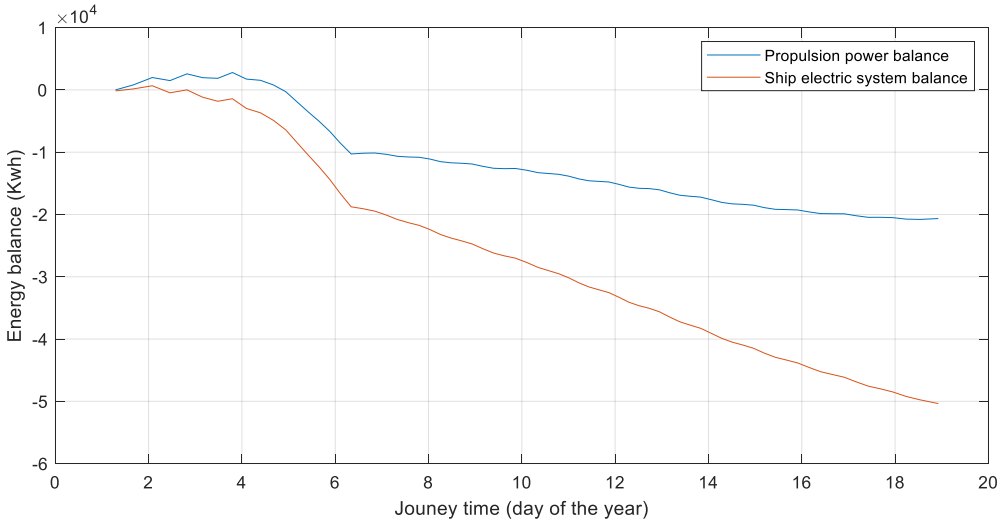

Figure 5.6: Accumulated energy from Houston to Rotterdam

The accumulated power balance always stays in negative values for both routes, independently of the electric power demand considered. It can be seen in Figure 5.5, that both energy balances have a similar shape, reaching a total energy demand of 99289 kWh, only considering the propulsive energy and 137740 kWh for the overall energy balance. For the return trip, Figure 5.6 shows that, due to the lower power demand for propulsion, results are significantly better. The balance reaches a total deficit of 20656 kWh for the propulsion energy balance and 50362 kWh for the total energy balance.

Results shown in Figures 5.1 - 5.6 and Appendix A-B prove this route as unfeasible using the systems evaluated. Moreover, the simulation shows the that it is important to consider the idea of installing an additional source of power to afford the extra power requirements.

5.2 Rio de Janeiro – Gothenburg

Table 5.2 shows the total time needed for the journey.

Table 5.2: Timing of route Rio de Janeiro - Gothenburg

Distance	5784 nautical miles
Time Rio de Janeiro - Gothenburg	36 days 6 hours
Time Gothenburg - Rio de Janeiro	36 days 13 hours

The wind speeds and angles along the route are in Figure 5.7 for the journey from Rio de Janeiro to Gothenburg, and in Figure 5.8 form the return trip from Gothenburg to Rio de Janeiro.

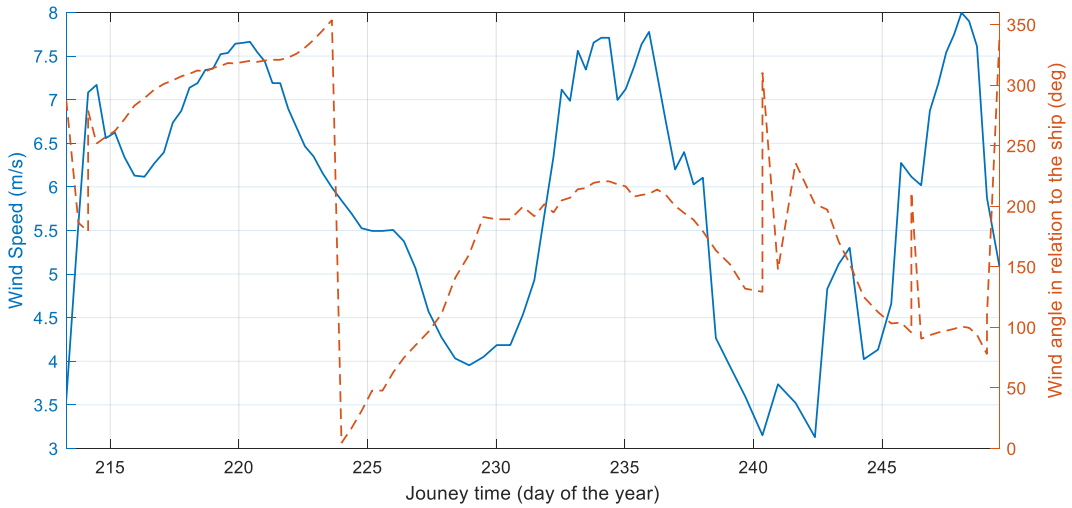

Figure 5.7: Wind speeds and angles for the route from Rio de Janeiro to Gothenburg

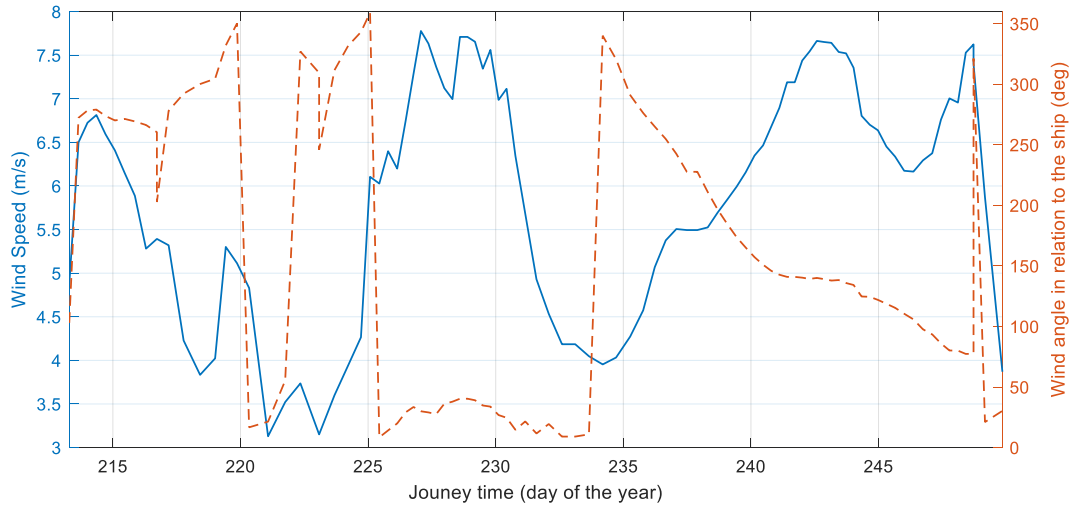

Figure 5.8: Wind speeds and angles for the route from Gothenburg to Rio de Janeiro

Figure 5.7 and Figure 5.8 show variable weather conditions for both journeys. In Figure 5.7, it is shown that the wind speeds fluctuate from 4 to 8 m/s, with wind angles between 100º and 250º, for most of the journey. On the return trip, shown in Figure 5.8,the wind speed fluctuates from 3 m/s to 7.5 m/s, with wind angles close to 0º (i.e. head wind) for the first half of the journey. The second part, from the day 234 of the year, the wind angle is constant at around 90º.

Results for the ship speed and the instantaneous energy balance for the route from Rio de Janeiro to Gothenburg are shown in Figure 5.9 and for the return trip the results are shown in Figure 5.10.

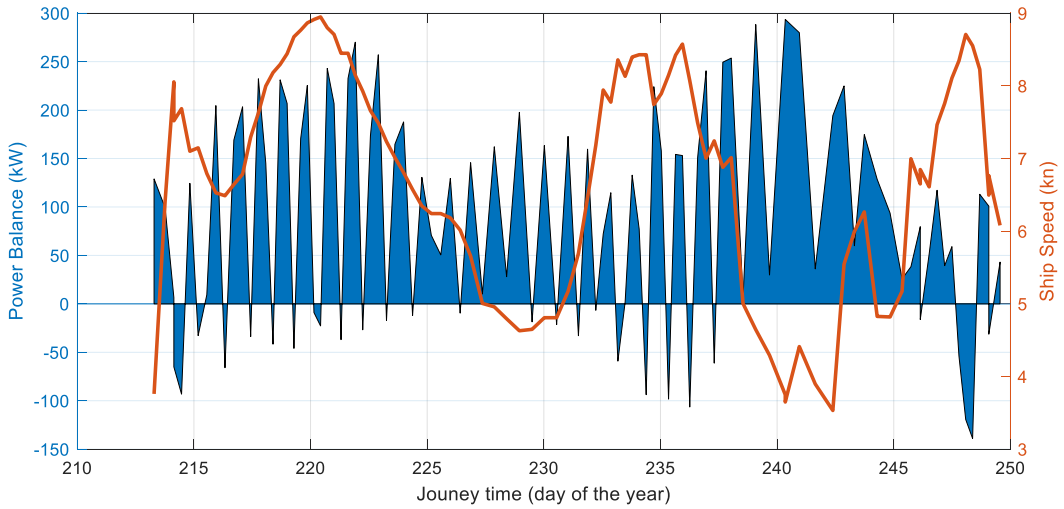

Figure 5.9: Energy Balance and Ship speed from Rio de Janeiro to Gothenburg

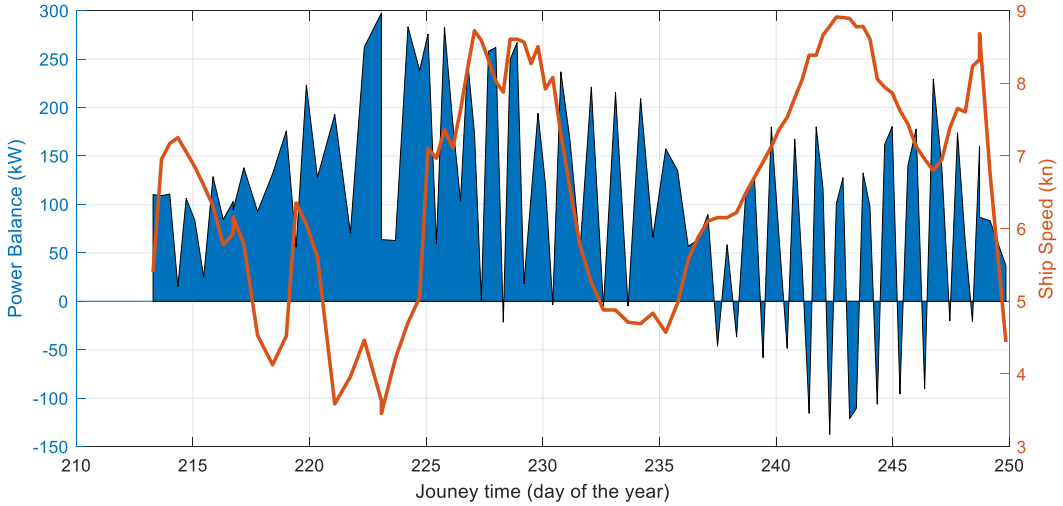

Figure 5.10: Energy Balance and Ship speed from Gothenburg Rio de Janeiro

Both routes, from and to Gothenburg seem to be feasible concerning the instantaneous energy balance, as shown in Figure 5.9 and Figure 5.10. For both trip, excess power is available with maximums instantaneous values above 200 kW. The ship's speed fluctuates from 3 to 9 kn for both trips, with an average VMG of 6.86 kn for Rio de Janeiro - Gothenburg trip and 6.79 kn for Gothenburg - Rio de Janeiro.

Figure 5.11 and Figure 5.12, compare the accumulative electric power considering the energy required for propulsion systems in blue and for all-electric systems of the ships in red. Figure 5.11 is the route from Rio de Janeiro to Goteborg and Figure 5.12 from Goteborg to Rio de Janeiro.

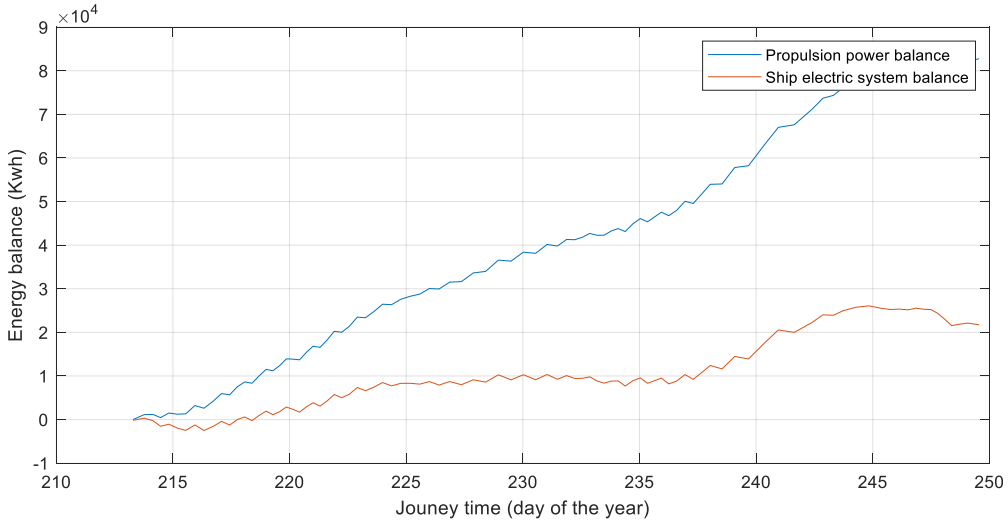

Figure 5.11: Accumulated energy from Gothenburg to Rio de Janeiro

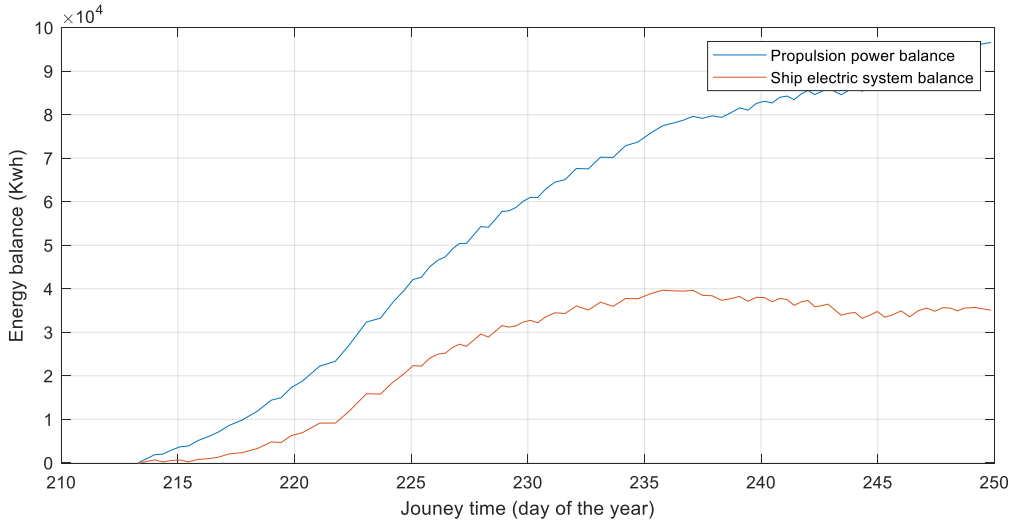

Figure 5.12: Accumulated energy from Rio de Janeiro to Gothenburg

In Figure 5.11, only considering the propulsion power demand, an energy surplus of 82756 kWh is accumulated over the journey. For the balance including loads for the electric systems onboard, a final energy surplus of 21749 kWh is reached. In Figure 5.12, for the return trip, 96580 kWh are accumulated when only considering the propulsion systems and 35079 kWh when considering all systems.

For this route, as Figures 5.7 - 5.12 and Appendix C-D show, the resulting energy balances prove high feasibility of the concept However, the average speeds stay well below the target speed of 8 kn. Thus, it would be interesting to use the surplus of electrical power to generate thrust by means of electric propulsion in order to increase the average speed along the journey.

5.3 Los Angeles – Shanghai

Simulation results for the total time required for the journey are shown in Table 5.3.

Table 5.3: Timing of route Los Angeles - Shanghai

Distance	5869 nautical miles
Time Los Angeles – Shanghai	36 days 1 hour
Time Shanghai – Los Angeles	36 days 0 hours

Wind speeds and wind angles along the route from Los Angeles to Shanghai are presented in Figure 5.13, and in Figure 5.14 for the return trip from Shanghai to Los Angeles.

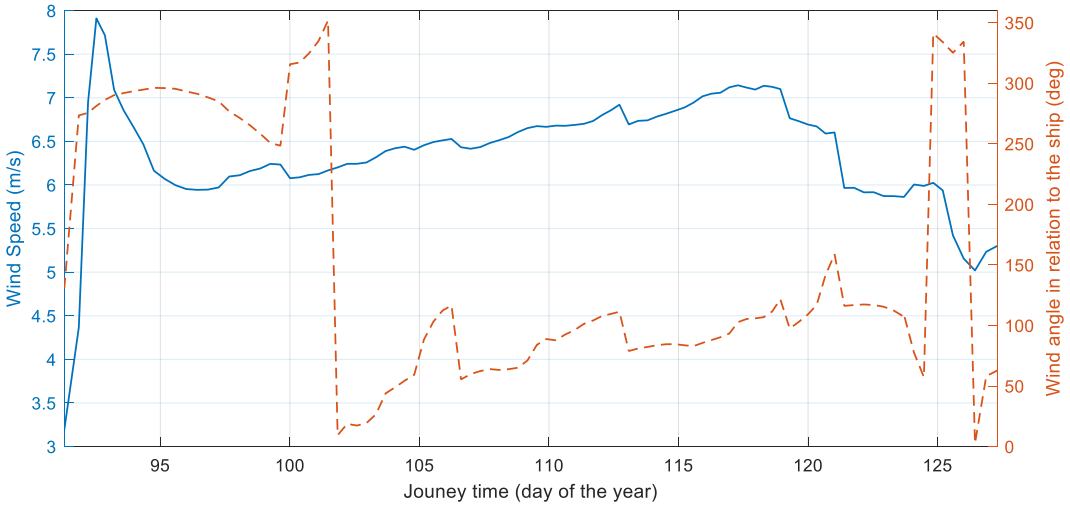

Figure 5.13: Wind speeds and angles for the route from Los Angeles to Shanghai

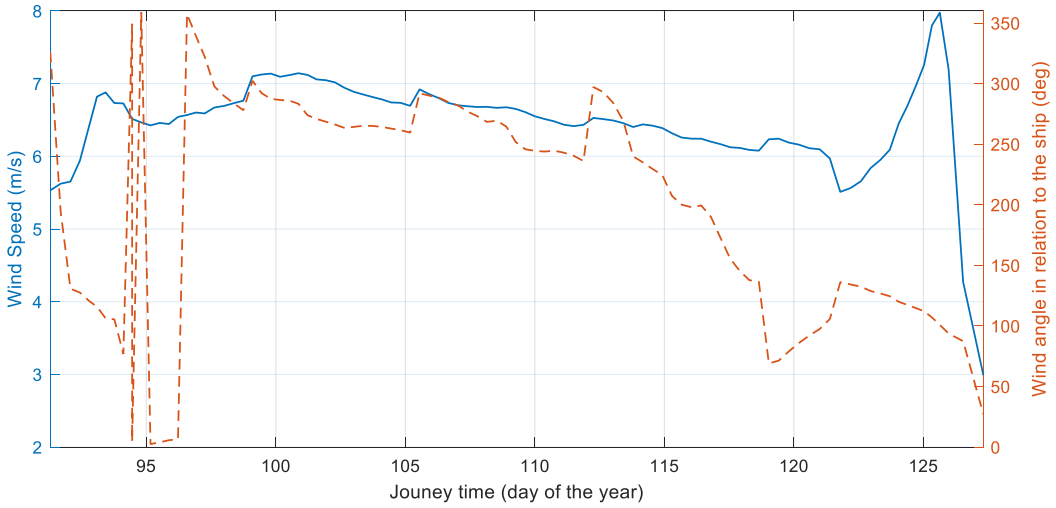

Figure 5.14: Wind speeds and angles for the route from Shanghai to Los Angeles

The above Figures show constant wind speeds during most of the journey. In Figure 5.13, close to the American coast, the wind speed is about 3 m/s with a peak of 8 m/s, and it stabilizes for most of the journey between 6 m/s and 7 m/s. Close to the Philippine Sea at the end of the trip, the wind speed is reduced to 5 m/s. Wind angles stay constant at about 250º in the first part of the route, and after the day 102 of the year, the wind angles change to values about 100º, remaining stable.

Figure 5.14 show stable wind speeds between 5.5 m/s and 7 m/s during most of the journey. Although, for the last leg close to the American coast, the speed is reduced to values about 3 m/s. The wind angles for this route start with values about 100º, entering into the Pacific Ocean the ship faces a period with head winds of 0º. Finally, the wind angles change to a value between 300º and 50º.

Simulation results for the ship speed and instantaneous energy balance for the journey from Los Angeles to Shanghai are shown in Figure 5.15 and in Figure 5.16 for the journey from Rotterdam to Houston and from Houston to Rotterdam.

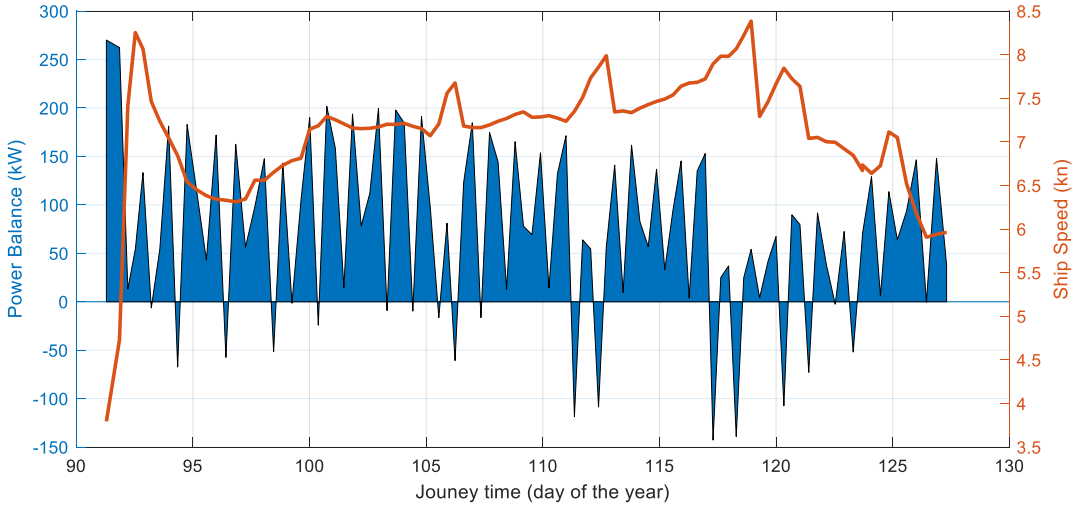

Figure 5.15: Energy Balance and Ship speed from Los Angeles to Shanghai

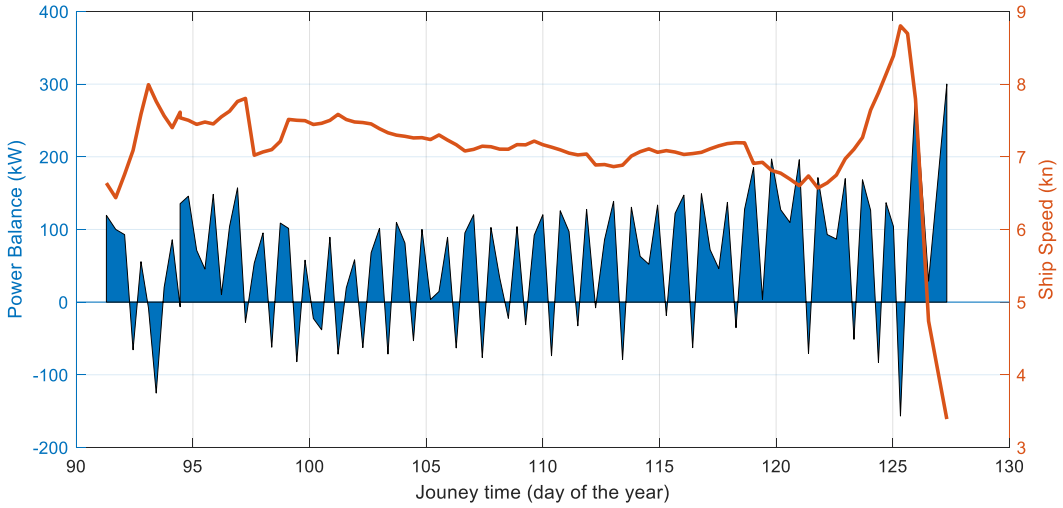

Figure 5.16: Energy Balance and Ship speed from Shanghai to Los Angeles

Results show that the average ship speed is 7.13 kn for the journey Shanghai – Los Angeles and 6.79 kn for the return trip Los Angeles - Shanghai.

The energy balance for the first route, shown in Figure 5.15, stays positive throughout most of the trip. In Figure 5.16, a similar result is shown for the return trip.

It is remarkable that the results show stable ships speeds and energy balances throughout both journeys, thus proving the concept reliable on this route. However, the average ship speed is lower than the target speed of 8 kn.

Figure 5.17 and Figure 5.18 compare the accumulative electric power considering the energy required for propulsion systems in blue and for all-electric systems of the ships in red. Figure 5.17 is the route from Los Angeles to Shanghai, and Figure 5.18 from Shanghai to Los Angeles.

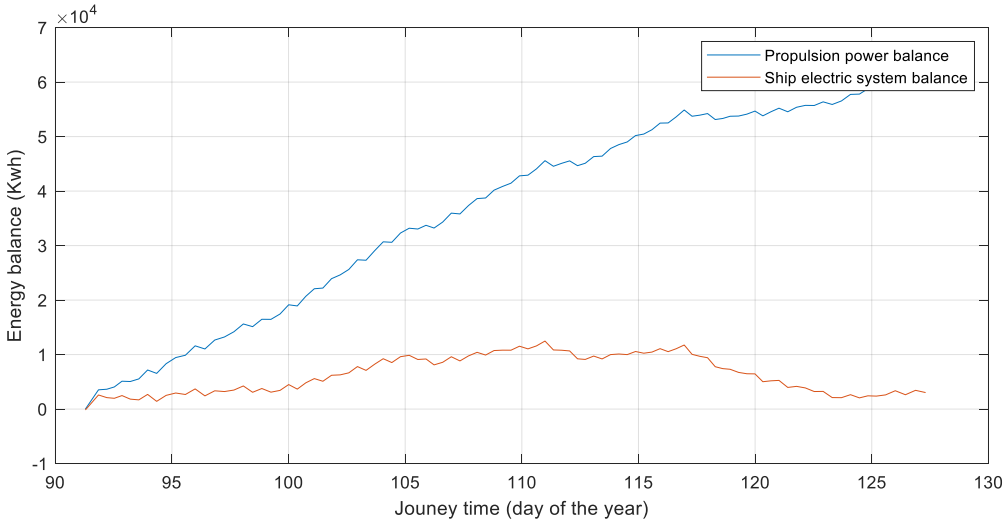

Figure 5.17: Accumulated energy from Los Angeles to Shanghai

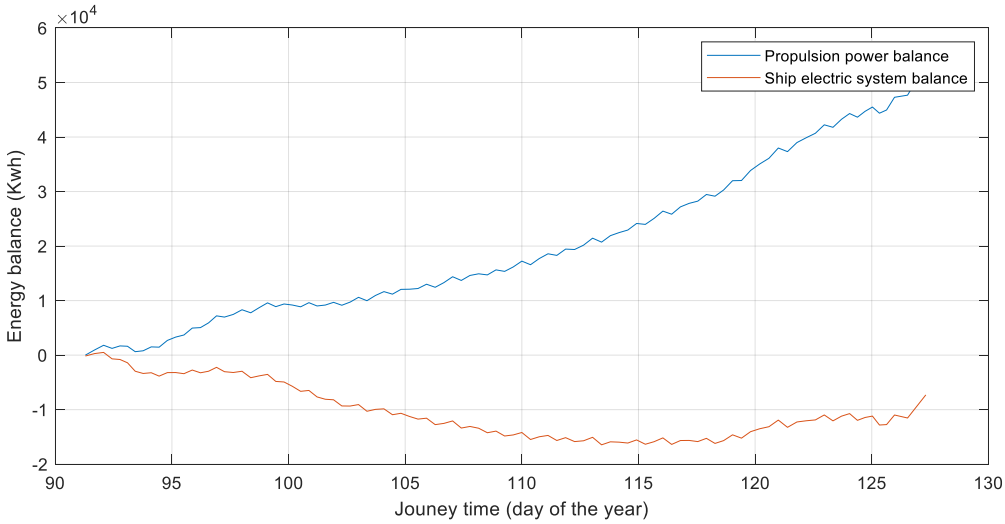

Figure 5.18: Accumulated energy from Shanghai to Los Angeles.

In Figure 5.17 and 5.18 it can be seen that the accumulated power only considering propulsion systems is positive for both journeys. However, considering all systems the accumulated power for the trip from Shanghai to Los Angeles is slightly negative (about -7294 kWh). The trip from Los Angeles to Shanghai results in a power balance close to equilibrium, with an accumulated power of about 3029 kWh.

Results from Figures 5.13 - 5.18 and Appendix E-F show that the concept is close to feasible at this route, with an almost balanced power generation and consumption and average speeds close to the target speed of 8 kn.

Results from the three simulated routes show that the energy consumption of the Flettner rotors is challenging for the concept. Additionally, it was shown that the achieved average speeds can be low for some routes. The results show the need to implement other power generation systems (e.g. hydro- turbines) and propulsion methods (e.g. electric motors) in order to even out the high energy consumption of the rotors in conditions with high ship speeds but also to increase the ship speed in areas with low wind speeds.

6 Conclusions

This thesis aimed to design a concept ship purely powered and operated with renewable energies. The main objective was to promote a sustainable transition of the shipping industry by providing an assessment of the feasibility to operate a cargo ship with the elimination of fossil fuels. With this purpose, the thesis studied the available technologies, developed numerical tools for the evaluation of the systems, and simulated different journeys on defined routes.

Insights from the literature are used to evaluate the renewable energy systems from current studies and to define the bases and requirements for the development of the concept ship. The chosen technologies for further studies were Flettner rotors, Wing sails, PV solar panels, and Wind turbine generators. The selection was based on requirements as non-dependence on the use of fuel, simplicity in operation, availability to install on an existing ship and feasibility from previous research.

In feasibility study, the evaluation of the technologies showed that for propulsion, the Flettner rotors adapts better to the needs of the concept because of the reduction of space required and the simplicity of operation, compared towing sails. Moreover, for energy generation, the PV solar systems and the wind turbines can coexist in the ship together with Flettner rotors in a hybrid solar-wind power system.

A high blockage ship hull was chosen for the concept and the power generation and propulsion systems where arranged on the ship. The final design includes 6 Flettner rotors installed symmetrically to port and starboard as a propulsion system, 1564 PV panels distributed over the entire deck surface and two vertical axis wind turbines in the aft of the ship for electric power production.

Simulation of the ships response is done by the integration of the different numerical models from each system. Three round trip routes are evaluated to face different scenarios.

Simulation results on the first roundtrip route (Rotterdam- Houston) showed a high dependency of the energy consumption of the Flettner rotors on the wind angle. Due to the high wind speeds and thus high power consumption of the Flettner rotors, the concept proved infeasible on this rout, even though the average ship speed was promising. Results on the second route (Rio de Janeiro- Gothenburg) were promising with a positive accumulated energy balance over the route, however on the price of low average ship speeds. Results from the final route (Los Angeles- Shanghai) were in line with the second route, with balanced energy consumption and production but averages speed slightly below the targeted 8kn.

As a general conclusion, a dependency between the power requirement and the speed reached with the sails is shown. Flettner rotors are a beneficial system for merchant ships; however, if the purpose is to go for an entirely renewable ship, its energy consumption can limit the operation of the vessel. The results made it obvious that additional power generation and propulsion systems must be implemented into the concept, along with an energy storage system in order to: (i) overcome the high energy requirement of the Flettner rotors in high wind speeds and high ship speeds and, (ii) to increase the ship speed in areas with low wind strength.

7 Future Work

This master thesis proceeds in an initial step for the design and study of a concept ship powered with renewable energies. Although, to improve the efficiency of the concept and the reliability of the simulations, further work must be done. Below, there is a forecast of the following steps in the thesis.

- It is necessary to investigate wing sails to install in the ship concept. Flettner rotors are a technology that requires power, and the available energy the concept ship is dependent on the renewable sources; a situation without enough energy is provable. The evaluation goes to implement wing sails model to the simulation and compare results with those from Flettner rotors.
- It is necessary to add the shadow effect of the sails to the PV generators in the simulations. By including wing sails in the concept, it would create new challenges. Wing sails create solar radiation shielding on the solar panel surface that reduces the electrical generation. In this case, it is necessary to evaluate the implication of shadows to estimate the energy loses that it could produce.
- Batteries must be assessed and included in the numerical method. Energy balance evaluates the difference between power generated and power consumed without assessing the requires energy storage system. For future work, it is necessary to establish the magnitude of the system to arrange it inside the ship as well as implement the efficiencies of the circuits.
- Electrical auxiliary propulsion will be considered. For a more reliable trade, it is necessary not just to depend on wind for the thrust and afford those situations when the wind cannot provide enough propulsive power with electrical engines.
- Fuel cells must be considered as a support for the electric generation systems. In the situations where there is not enough power stored for the propulsion on for electrical requirements, it would be necessary to include an additional source of energy. For future work, there would be considered electric power from hydrogen fuel cells.
- It is requested to evaluate simulations for different hull types. For the future, it would be interesting to see how the concept behaves with varying types of ship and with modifications in the hull.
- Evaluate and implement wave propulsion foils into the concept. Wave power is a promising technology for a lot of speed ship. It was not considered for the complexity of the system, although, for future work, it would be interesting to evaluate it and incorporate it in the simulations as an additional source of power.
- Including a probabilistic approach with the Monte-Carlo method to define weather conditions would improve the methodology and make the simulations more realistic. The monthly average calculations must be substituted with probabilistic simulations.
- Optimize the simulation with a “captain mode”. With the possibility of propulsion by a wind-assisted system, electrical stored power with batteries and hydrogen it is necessary to include in the simulation a management system that optimizes the best option for propulsion based on the ship requirements.

8 References

Andersson, A., Baxevanis, D., Julià, E., Lemonakis, F., Lee, Y., Taquet, G., Xiao, H. Llop, J., Cerol, J., Zu, M. A. A., Brito, M., Sudhan, N., Patel, S., Siepmann, T., Sugita, T., Raju, V., Dai, Y. (2018) Stena Volta (Thesis). Chalmers University of Technology, Gothenburg, Sweden.

Andrews, R. W., & Pearce, J. M. (2013). The effect of spectral albedo on amorphous silicon and crystalline silicon solar photovoltaic device performance. *Solar Energy*, *91*, 233-241. Available at: https://doi.org/10.1016/j.solener.2013.01.030

Atkinson, G., Nguyen, H., & Binns, J. (2018). Considerations regarding the use of rigid sails on modern powered ships. *Cogent Engineering*, *5*(1), 1543564. Available at:10.1080/23311916.2018.1543564.

Balcombe, P., Brierley, J., Lewis, C., Skatvedt, L., Speirs, J., Hawkes, A., & Staffell, I. (2019). How to decarbonise international shipping: Options for fuels, technologies and policies. *Energy conversion and management*, *182*, 72-88. Available at: https://doi.org/10.1016/j.enconman.2018.12.080.

Becker, R. (1997). MARPOL 73/78: An Overview in International Environmental Enforcement. *Geo. Int'l Envtl. L. Rev.*, *10*, 625. Available at: https://heinonline.org/HOL/LandingPage?handle=hein.journals/gintenlr10&div=28&id=&page=

Bøckmann, E. (2015) Wave Propulsion of Ships (Doctoral thesis). NTNU, Trondheim, Norwey. Available at: http://hdl.handle.net/11250/284142.

Bøckmann, E., & Steen, S. (2011, June). Wind turbine propulsion of ships. In *Second international symposium on marine propulsors, Hamburg, Germany*. Available at: http://www.marinepropulsors.com/smp/files/downloads/smp11/Paper/FA1-2_Bockmann.pdf.

Bøckmann, E., Yrke, A., & Steen, S. (2018). Fuel savings for a general cargo ship employing retractable bow foils. *Applied Ocean Research*, *76*, 1-10. Available at: https://doi.org/10.1016/j.apor.2018.03.015.

Casson, L. (1964). Illustrated history of ships & boats. *Doubleday*. Available at: https://books.google.it/books?id=pE9iQgAACAAJ.

Jo, Y., Lee, H., Choi, S., Kwon, J., & Ahn, S. (2013). Aerodynamic design optimization of wing-sails. In *31st AIAA Applied Aerodynamics Conference* (p. 2524). Available at:10.2514/6.2013-2524.

Clark, R. (2018) The 2020 Global Sulphur Cap : An Overview. *Reed Smith*, pp. 1–8. Available at: https://www.reedsmith.com/en/perspectives/2018/11/the-2020-global-sulphur-cap-an-overview.

Clarson, O. and Nilsson, P. (2015) Wind Turbines on Ships. *Chalmers publication library*. Available at: http://publications.lib.chalmers.se/publication/217076.

D'Ambrosio, M., & Medaglia, M. (2010). Vertical axis wind turbines: History, technology and applications. Available at: http://urn.kb.se/resolve?urn=urn:nbn:se:hh:diva-4986.

Harrould-Kolieb, E. (2008) Shipping Impacts on Climate: a Source with Solution. *Oceana*. Available at: http://www.oceana.ca/sites/default/files/reports/Oceana_Shipping_Report1.pdf

Hesse, H., Schimpe, M., Kucevic, D., & Jossen, A. (2017). Lithium-ion battery storage for the grid—a review of stationary battery storage system design tailored for applications in modern power grids. *Energies*, *10*(12), 2107. Available at: https://doi.org/10.3390/en10122107

Hoffmann, J., Asariotis, R., Assaf, M., Benamara, H. (2017) *UNCTAD Review of Maritime Transport 2017*. Available at: http://unctad.org/en/PublicationsLibrary/rmt2017_en.pdf.

Hong Liang, L. (2017) The 2020 IMO Fuel Sulphur Regulation. *Seatrade Maritime News*, p. 7. Available at: http://www.seatrade-maritime.com/

Hou, J., Sun, J., & Hofmann, H. (2018). Control development and performance evaluation for battery/flywheel hybrid energy storage solutions to mitigate load fluctuations in all-electric ship propulsion systems. *Applied energy*, *212*, 919-930. Available at: https://doi.org/10.1016/j.apenergy.2017.12.098

IMO (2018a) *Next Steps to Deliver IMO HGH Strategy*. Available at: http://www.imo.org/.

IMO (2018b) *RESOLUTION MEPC.308(73)*. Available at: http://www.imo.org/.

Jakobsen, E. (1981). The foil propeller, wave power for propulsion. In *2nd International Symposium on Wave and Tidal Energy, 1981* (pp. 363-369). BHRA fluid Engineering. Available at: https://ci.nii.ac.jp/naid/80001169029/.

Kam, S. K. (2019). Compelling the EPA to Regulate GHG Emissions Under the Act to Prevent Pollution From Ships. *Environmental Claims Journal*, *31*(1), 16-31. Available at: https://doi.org/10.1080/10406026.2018.1546467

Kim, T. K., & Yaakob, O. (2016). Adaptation of wind power for ship essential service system onboard. *Journal of Transport System Engineering*, *1*, 08-19. Available at: https://jtse.utm.my/index.php/jtse/article/view/78.

Korinek, J., & Sourdin, P. (2009). Maritime transport costs and their impact on trade. *Organization for Economic Co-operation and Development TAD/TC/WP (2009)*, *7*. Available at: https://www.etsg.org/ETSG2009/papers/korinek.pdf

Kramer, J. A., Steen, S., & Savio, L. (2016). Drift forces–wingsails vs Flettner rotors. *High performance marine vehicles*. Available at: https://www.researchgate.net/publication/308674535.

Kusuma, I. R., & Pratama, R. (2017). Development of Power Management System for Electric Power Generation in Tanker Ship Based on Simulation. *International Journal of Marine Engineering Innovation and Research*, *1*(3). Available at: http://dx.doi.org/10.12962/j25481479.v1i3.2002

Lan, H., Wen, S., Hong, Y. Y., David, C. Y., & Zhang, L. (2015). Optimal sizing of hybrid PV/diesel/battery in ship power system. *Applied energy*, *158*, 26-34. Available at: https://doi.org/10.1016/j.apenergy.2015.08.031

Lee, T., & Nam, H. (2017). A study on green shipping in major countries: in the view of shipyards, shipping companies, ports, and policies. *The Asian Journal of Shipping and Logistics*, *33*(4), 253-262. Available at: https://doi.org/10.1016/j.ajsl.2017.12.009

Leloup, R., Roncin, K., Behrel, M., Bles, G., Leroux, J. B., Jochum, C., & Parlier, Y. (2016). A continuous and analytical modeling for kites as auxiliary propulsion devoted to merchant ships, including fuel saving estimation. *Renewable Energy*, *86*, 483-496. Available at: https://doi.org/10.1016/j.renene.2015.08.036

Margaritou, M. D., & Tzannatos, E. (2018). A multi-criteria optimization approach for solar energy and wind power technologies in shipping. *FME Transactions*, *46*(3), 374-380. Available at: https://doi.org/10.5937/fmet1803374M

MEPC 53/4/4 (2005) Annex VI - Proposal to initiate a revision process, pp. 1–8. Available at: I:\MEPC\53\4-4.doc.

McKenna, M. F., Katz, S. L., Condit, C., & Walbridge, S. (2012). Response of commercial ships to a voluntary speed reduction measure: are voluntary strategies adequate for mitigating ship-strike risk?. *Coastal Management*, *40*(6), 634-650. Available at: https://doi.org/10.1080/08920753.2012.727749

NASA (2019) *POWER Data Access Viewer*. Available at: https://power.larc.nasa.gov/data-access-viewer

Neoline (2019) *Neoline*. Available at: www.neoline.eu

NYK Grup (2018) *NYK SUPER ECO SHIP 2050*. Available at: https://www.nyk.com/

Platzer, M. F., Sarigul-Klijn, N., Young, J., Ashraf, M. A., & Lai, J. C. S. (2014). Renewable hydrogen production using sailing ships. *Journal of Energy Resources Technology*, *136*(2), 021203. Available at: https://doi.org/10.1115/1.4026200

Politis, G., & Politis, K. (2014). Biomimetic propulsion under random heaving conditions, using active pitch control. *Journal of Fluids and Structures*, *47*, 139-149. Available at: https://doi.org/10.1016/j.jfluidstructs.2012.05.004

Rezaie, B., Esmailzadeh, E., & Dincer, I. (2011). Renewable energy options for buildings: case studies. *Energy and Buildings*, *43*(1), 56-65. Available at: https://doi.org/10.1016/j.enbuild.2010.08.013

Riley, E. F. (2015). The potential energy savings by application of a wave foil on the autonomous container vessel ReVolt (Master thesis). NTNU, Trondheim, Norwey. Available at: http://hdl.handle.net/11250/2350718

Rutkowski, G. (2017) Study of Green Shipping Technologies - Harnessing Wind, Waves and Solar Power in New Generation Marine Propulsion Systems.*TransNav, the International Journal on Marine Navigation and Safety of Sea Transportation*, pp. 627–632. Available at: https://doi.org/0.12716/1001.10.04.12.

Sáiz, V. M. M., & López, A. P. (2007). Future trends in electric propulsion systems for commercial vessels. *Journal of Maritime Research*, *4*(2), 81-100. Available at: https://www.jmr.unican.es/index.php/jmr/article/view/81

Talluri, L., Nalianda, D. K., & Giuliani, E. (2018). Techno economic and environmental assessment of Flettner rotors for marine propulsion. *Ocean engineering*, *154*, 1-15. Available at: https://doi.org/10.1016/j.oceaneng.2018.02.020

Tillig, F., Ringsberg, J., Harilaos, P. and Zis, T. (2019) ShipCLEAN – An integrated model for transport efficiency, economics and CO2 emissions in shipping. *2nd international conference on modelling and optimisation of ship energy systems*

Tröster, E., & Schmidt, J. D. (2012). Evaluating the impact of PV module orientation on grid operation. In *Proceedings of the 2nd International Workshop on Integration of Solar Power into Power Systems, Lisbon, Portugal*. Available at: http://smooth-pv.info/doc/App22_ENA_Evaluating_the_Impact_of_PV_Module_Orientation.pdf.

United Nations (2010) The Copenhagen accord.in, p. 43. Available at:10.1038/news.2009.1156.

Da Rosa, A. V. (2012). Fundamentals of renewable energy processes. *Academic Press.* Available at: https://doi.org/10.1016/B978-0-12-374639-9.00018-X.

Wallenius Wilhelmsen (2005) *E/S Orcelle*. Available at: https://www.2wglobal.com/.

Traut, M., Gilbert, P., Walsh, C., Bows, A., Filippone, A., Stansby, P., & Wood, R. (2014). Propulsive power contribution of a kite and a Flettner rotor on selected shipping routes. *Applied Energy*, *113*, 362-372. Available at: https://doi.org/10.1016/j.apenergy.2013.07.026.

Lan, H., Dai, J., Wen, S., Hong, Y. Y., Yu, D., & Bai, Y. (2015). Optimal tilt angle of photovoltaic arrays and economic allocation of energy storage system on large oil tanker ship. *Energies*, *8*(10), 11515-11530. Available at: https://doi.org/10.3390/en81011515.

Zhang, H. (2016). Towards global green shipping: the development of international regulations on reduction of GHG emissions from ships. *International Environmental Agreements: Politics, Law and Economics*, *16*(4), 561-577. Available at: https://doi.org/10.1007/s10784-014-9270-5.

Appendix A: Results of simulations from Rotterdam to Houston

Distance from the start (nm)	Time (day of the year/ Hour of the day)		Speed (kn)	Generation (kW)	Rotor Consumption (kW)	Balance propulsion systems (kW)	Accumulated balance with electric systems (kWh)
0.0	1	7	8.5	0.0	48.1	2.2	-160.0
82.5	1	16	8.7	909.9	198.1	-101.9	-1625.7
82.5	1	16	9.1	0.0	70.2	-2.7	-1625.7
144.8	1	24	8.8	650.6	209.2	-117.5	-2956.8
207.2	2	6	9.6	576.5	288.8	-199.7	-4702.3
269.6	2	12	9.6	610.6	321.0	-226.6	-6620.8
331.9	2	19	9.7	762.1	327.6	-209.5	-8424.4
394.3	3	1	10.0	641.7	357.4	-254.6	-10452.1
456.7	3	8	9.8	517.9	328.0	-246.7	-12467.7
519.0	3	14	10.1	825.2	354.1	-221.0	-14272.1
519.0	3	14	10.2	0.0	357.9	-219.9	-14272.1
580.7	3	20	10.3	841.6	375.2	-235.0	-16103.3
642.4	4	2	10.3	619.4	370.4	-267.5	-18134.9
704.1	4	8	10.4	566.4	387.5	-292.3	-20291.2
765.8	4	14	10.6	826.6	423.8	-281.8	-22338.4
827.5	4	19	10.7	885.5	439.6	-286.0	-24389.6
889.2	5	1	10.9	693.9	475.1	-352.1	-26771.9
950.9	5	7	10.7	580.8	438.0	-337.3	-29120.8
1012.6	5	12	11.0	780.9	484.3	-345.5	-31458.3
1074.3	5	18	11.1	902.6	510.4	-348.2	-33785.6
1136.0	5	23	11.2	755.1	538.2	-400.9	-36375.2
1197.7	6	5	11.3	627.1	552.0	-437.2	-39146.8
1259.4	6	10	11.2	732.4	521.8	-389.4	-41688.1
1321.1	6	16	11.3	955.1	556.5	-380.9	-44140.1
1382.8	6	21	11.5	913.4	578.2	-408.6	-46717.7
1444.5	7	3	11.6	657.6	606.1	-482.5	-49656.1
1506.2	7	8	11.5	664.7	577.5	-453.8	-52472.4
1567.9	7	13	11.5	974.4	587.9	-405.8	-55017.0
1629.6	7	19	11.6	1041.8	597.2	-401.5	-57527.3
1691.3	7	24	11.6	846.5	603.3	-444.0	-60257.6
1753.0	8	5	11.7	653.0	675.1	-551.5	-63540.2
1814.7	8	11	11.5	822.2	632.0	-478.7	-66482.6
1876.4	8	16	11.6	1046.2	637.5	-441.4	-69210.4
1938.1	8	21	11.6	952.4	624.0	-445.3	-71957.1
1999.8	9	3	11.6	659.1	618.7	-495.1	-74969.4
2061.6	9	8	11.6	659.2	613.3	-489.6	-77953.4
2123.3	9	13	11.5	914.0	605.1	-434.5	-80656.0
2185.0	9	19	11.4	995.8	570.0	-386.5	-83132.8
2246.7	10	1	10.6	878.8	419.1	-268.6	-85110.9
2308.4	10	7	10.1	635.4	355.6	-251.5	-87073.0
2370.1	10	12	10.6	958.3	425.3	-260.4	-88993.5
2431.8	10	18	10.8	954.1	508.8	-341.8	-91345.5
2493.5	10	24	10.9	769.8	511.6	-376.1	-93879.7

2555.2	11	5	10.9	640.2	511.7	-398.5	-96527.6
2616.9	11	11	11.0	855.4	506.7	-354.7	-98918.6
2678.6	11	17	11.2	1011.3	572.1	-387.9	-101433.0
2740.3	11	22	11.2	931.7	548.5	-380.1	-103922.4
2802.0	12	4	10.9	698.8	493.9	-370.2	-106410.6
2863.7	12	9	10.8	622.0	541.6	-432.4	-109271.2
2925.4	12	15	10.8	931.6	519.7	-356.7	-111709.5
2987.1	12	21	10.7	907.9	506.9	-349.2	-114122.1
3048.8	13	3	10.5	624.7	455.9	-349.7	-116589.7
3110.5	13	9	10.3	615.6	415.7	-313.1	-118888.0
3172.2	13	15	10.1	965.5	379.8	-222.2	-120678.5
3233.9	13	21	9.7	1082.7	327.1	-156.6	-122117.1
3295.6	14	4	9.9	659.9	351.3	-245.3	-124079.5
3295.6	14	4	10.1	0.0	78.7	-40.7	-124079.5
3356.4	14	10	9.9	625.0	418.8	-317.2	-126460.0
3417.1	14	16	9.9	951.3	418.8	-264.1	-128514.0
3477.9	14	22	9.7	889.7	402.6	-260.7	-130587.7
3538.7	15	5	9.3	687.5	300.9	-195.5	-132319.5
3599.5	15	11	9.2	704.0	299.4	-192.6	-134050.9
3660.3	15	18	8.9	1148.3	274.4	-106.5	-135257.5
3721.1	16	1	8.5	1032.5	202.1	-57.7	-136170.4
3781.9	16	9	8.3	434.3	190.1	-130.8	-137641.2
3842.7	16	16	8.3	1304.7	182.8	-5.5	-138196.4
3903.5	16	24	7.9	1406.6	160.1	23.4	-138553.8
3964.2	17	8	7.6	344.1	147.1	-104.0	-139941.7
4025.0	17	16	7.2	1523.7	111.8	68.8	-139951.7
4085.8	18	1	7.0	1585.8	24.7	159.0	-139183.5
4146.6	18	10	6.7	119.5	29.1	-15.8	-139957.1
4207.4	18	19	6.3	1882.7	19.3	177.0	-138931.0
4268.2	19	4	6.7	1020.1	29.9	82.2	-138819.6
4329.0	19	13	7.1	316.4	26.4	10.6	-139327.4
4329.0	19	13	6.9	0.0	106.1	156.9	-139327.4
4392.4	19	21	7.4	2101.9	38.0	208.5	-138146.3
4455.8	20	7	6.9	121.1	27.9	-14.8	-138928.0
4519.3	20	15	7.3	1480.3	31.4	138.2	-138332.9
4582.7	20	24	7.5	1669.8	39.5	157.1	-137593.2
4646.1	21	8	7.7	153.9	40.1	-21.4	-138344.1
4709.5	21	16	7.8	1458.4	42.8	136.6	-137802.5
4773.0	22	0	7.9	1371.1	43.4	127.0	-137344.0
4836.4	22	8	7.9	169.8	44.6	-23.5	-138095.7
4899.8	22	16	7.8	1295.8	42.8	116.9	-137715.5
4963.3	23	0	7.9	1216.0	45.9	106.1	-137426.9
5026.7	23	9	7.6	152.7	38.5	-20.3	-138185.4
5090.1	23	17	7.3	1265.1	36.0	109.3	-137843.6
5153.5	24	3	6.6	1116.5	26.3	89.3	-137737.3

Appendix B: Results of simulations from Houston to Rotterdam

Distance from the start (nm)	Time (day of the year/ Hour of the day)		Speed (kn)	Generation (kW)	Rotor Consumption (kW)	Balance propulsion systems (kW)	Accumulated balance with electric systems (kWh)
0.0	1	7	6.9	0.0	106.1	83.8	-160.0
60.8	1	16	6.6	1589.9	85.9	87.6	161.2
121.6	2	2	6.2	1906.6	74.1	121.8	665.5
182.4	2	11	6.7	288.4	85.6	-54.0	-465.3
243.2	2	20	7.0	1964.9	101.3	124.2	6.7
303.9	3	4	7.6	502.4	139.0	-76.3	-1166.5
364.7	3	12	7.8	175.3	36.1	-13.7	-1822.2
425.5	3	19	8.0	1207.1	36.3	123.3	-1419.4
486.3	4	2	8.5	475.6	213.0	-146.9	-2979.2
547.1	4	10	8.4	129.9	44.9	-26.8	-3675.9
607.9	4	16	9.1	904.8	247.0	-112.2	-4899.4
668.7	4	23	9.6	719.7	284.5	-170.7	-6420.6
729.5	5	5	10.2	247.4	323.3	-281.9	-8528.4
790.3	5	10	10.6	460.5	359.3	-278.7	-10519.1
851.0	5	16	11.0	749.1	404.9	-269.0	-12386.5
911.8	5	21	11.2	712.8	428.1	-296.7	-14376.1
972.6	6	3	11.2	439.5	428.1	-347.1	-16638.9
1033.4	6	8	10.9	431.2	389.0	-311.7	-18767.4
1033.4	6	8	10.6	0.0	380.2	-232.2	-18767.4
1095.1	6	14	10.0	611.0	79.7	19.3	-19080.4
1156.8	6	20	10.3	633.6	99.5	6.1	-19463.6
1218.5	7	2	10.5	245.0	78.1	-36.6	-20092.2
1280.2	7	8	10.8	207.1	91.2	-55.2	-20810.5
1341.9	7	14	11.0	490.7	107.8	-20.0	-21313.8
1403.6	7	19	11.1	564.0	109.5	-8.0	-21747.1
1465.3	8	1	11.2	382.0	120.2	-50.9	-22413.8
1527.0	8	6	11.2	295.9	130.7	-76.8	-23220.1
1588.7	8	12	11.4	421.6	112.4	-34.4	-23784.1
1650.4	8	17	11.5	587.7	123.1	-13.3	-24230.2
1712.1	8	22	11.2	442.9	102.1	-21.7	-24735.4
1773.8	9	4	11.2	252.3	113.8	-68.0	-25495.6
1835.5	9	9	11.2	345.9	119.0	-56.4	-26193.7
1897.2	9	15	11.1	614.0	122.0	-11.2	-26643.9
1958.9	9	21	10.9	701.5	118.7	5.1	-27011.7
2020.6	10	3	10.4	296.2	98.5	-48.7	-27718.3
2082.3	10	8	10.8	293.1	118.2	-66.9	-28500.8
2144.0	10	14	11.7	532.7	126.4	-25.7	-29007.5
2205.7	10	19	11.8	591.0	137.2	-24.0	-29498.1
2267.4	11	0	11.9	393.0	132.7	-57.0	-30157.2
2329.1	11	5	11.9	294.3	141.2	-84.5	-30959.4
2390.8	11	10	11.9	465.6	147.8	-58.2	-31625.4
2452.5	11	16	11.9	728.0	160.3	-20.3	-32094.9
2514.2	11	21	11.8	557.5	125.0	-18.3	-32556.9

2575.9	12	2	12.0	313.1	135.6	-74.6	-33300.2
2637.6	12	7	12.0	294.0	141.8	-84.8	-34098.8
2699.3	12	12	11.9	547.8	142.7	-37.0	-34652.8
2761.0	12	18	11.8	707.5	145.1	-9.3	-35066.1
2822.7	12	23	11.8	562.8	144.9	-37.5	-35629.8
2884.4	13	4	11.9	333.4	153.7	-89.4	-36457.0
2946.1	13	9	11.7	383.5	149.6	-76.8	-37229.3
3007.8	13	15	11.6	606.4	144.9	-30.8	-37765.3
3069.5	13	20	11.4	609.5	137.6	-24.8	-38277.7
3131.2	14	1	11.6	379.2	146.8	-75.8	-39056.4
3192.9	14	7	11.5	338.0	143.6	-80.7	-39866.1
3254.6	14	12	11.4	488.7	135.3	-45.4	-40493.5
3316.3	14	18	11.2	622.7	127.0	-13.7	-40953.4
3378.0	14	23	11.0	488.1	112.0	-25.3	-41490.4
3439.7	15	5	11.2	292.5	123.3	-70.3	-42263.8
3501.4	15	10	11.0	359.8	112.6	-48.7	-42931.6
3563.1	15	16	10.9	575.0	107.9	-6.7	-43367.7
3624.8	15	22	10.6	494.3	96.1	-11.2	-43840.3
3686.5	16	4	10.5	220.1	90.5	-53.2	-44566.7
3748.2	16	10	10.5	280.9	92.6	-44.8	-45241.5
3809.9	16	16	10.4	504.9	88.8	-3.9	-45680.8
3809.9	16	16	10.5	0.0	96.1	-13.4	-45680.8
3872.3	16	22	10.0	451.1	74.9	-2.6	-46134.4
3934.7	17	4	10.2	215.8	85.6	-50.2	-46868.0
3997.0	17	10	9.9	252.6	81.6	-41.4	-47566.7
4059.4	17	17	9.9	503.6	78.7	1.2	-48000.5
4121.8	17	23	9.9	461.9	82.0	-8.8	-48497.3
4184.1	18	6	8.9	198.2	62.7	-34.3	-49225.1
4246.5	18	13	8.9	334.0	54.0	-6.2	-49757.7
4246.5	18	13	8.9	0.0	201.9	-92.0	-49757.7
4329.0	18	22	8.8	628.4	52.4	14.3	-50362.1

Appendix C: Results of simulations from Rio de Janeiro to Gothenburg

Distance from the start (nm)	Time (day of the year/ Hour of the day)		Speed (kn)	Generation (kW)	Rotor Consumption (kW)	Balance propulsion systems (kW)	Accumulated balance with electric systems (kWh)
0.0	213	7	3.8	0.0	18.6	129.0	-160.0
72.7	213	18	6.4	1872.3	65.7	99.3	332.1
145.5	214	3	8.1	1370.1	145.2	6.5	-241.6
145.5	214	3	7.5	0.0	132.8	-65.1	-241.6
206.2	214	11	7.7	489.8	155.2	-93.2	-1531.5
267.0	214	20	7.1	2027.4	112.6	124.4	-1066.2
327.7	215	4	7.1	651.1	109.4	-32.8	-1939.8
388.5	215	13	6.8	1007.4	103.3	9.3	-2482.4
449.3	215	23	6.5	2654.5	80.6	204.6	-1229.7
510.0	216	8	6.5	248.3	92.4	-65.9	-2502.7
570.8	216	17	6.6	2382.6	91.4	169.1	-1596.6
631.5	217	2	6.8	2394.4	64.0	203.4	-402.2
692.3	217	10	7.3	336.4	74.2	-33.8	-1266.5
753.0	217	18	7.6	2468.1	77.5	232.3	26.5
813.8	218	2	8.0	1750.2	85.3	145.1	596.7
874.5	218	9	8.2	320.5	84.8	-41.6	-232.0
935.3	218	17	8.3	2360.9	91.1	231.2	949.0
996.0	218	24	8.4	2123.5	88.2	206.8	1933.7
1056.8	219	7	8.7	321.5	91.8	-45.9	1121.8
1117.6	219	14	8.8	1793.9	88.4	170.5	1818.0
1178.3	219	21	8.9	2180.1	92.8	225.4	2882.6
1239.1	220	4	8.9	559.0	91.0	-9.0	2344.2
1299.8	220	10	8.9	453.5	89.6	-22.8	1714.2
1360.6	220	17	8.8	2278.1	87.0	243.0	2908.5
1421.3	221	0	8.7	2012.0	81.6	206.8	3862.7
1482.1	221	7	8.4	257.6	72.8	-37.0	3093.5
1542.8	221	15	8.4	2196.1	72.8	232.6	4262.8
1603.6	221	22	8.1	2475.0	61.8	270.1	5755.0
1664.3	222	6	7.9	194.4	52.2	-26.8	5013.0
1725.1	222	14	7.7	1714.3	42.6	173.5	5834.2
1785.9	222	22	7.5	2401.6	39.0	257.1	7351.7
1846.6	223	6	7.2	125.9	32.0	-17.0	6620.5
1907.4	223	15	7.0	1699.8	31.6	164.7	7440.6
1968.1	223	24	6.8	1911.5	26.4	187.8	8491.9
2028.9	224	9	6.6	91.5	21.9	-12.0	7734.2
2089.6	224	19	6.3	1465.5	22.5	130.6	8313.8
2150.4	225	4	6.2	873.3	19.0	70.7	8320.5
2211.1	225	14	6.2	677.0	19.0	50.5	8130.9
2271.9	225	24	6.2	1447.9	17.9	129.4	8715.0
2332.6	226	10	6.0	74.6	17.0	-9.6	7911.4
2393.4	226	21	5.7	1732.4	15.6	145.7	8724.5

2454.2	227	9	5.0	276.8	12.6	10.2	7998.3
2514.9	227	21	5.0	2400.4	33.8	162.1	9126.8
2575.7	228	10	4.8	690.0	26.4	28.0	8594.9
2636.4	228	23	4.6	2908.0	23.9	197.7	10270.5
2697.2	229	12	4.6	103.6	26.5	-18.6	9112.7
2757.9	230	1	4.8	2440.3	29.8	163.4	10292.2
2818.7	230	13	4.8	106.2	29.8	-21.4	9137.6
2879.4	231	1	5.2	2478.4	38.1	172.8	10345.7
2940.2	231	12	5.7	156.0	47.5	-32.9	9247.6
3000.9	231	21	6.5	2193.8	73.7	159.7	10090.7
3061.7	232	5	7.2	777.4	98.5	-6.6	9442.3
3122.5	232	13	7.9	1629.4	140.9	72.2	9458.8
3183.2	232	21	7.8	1912.0	130.0	114.7	9808.0
3244.0	233	4	8.4	837.3	174.3	-59.1	8869.4
3304.7	233	12	8.1	1196.7	158.3	1.9	8360.7
3365.5	233	19	8.4	2196.1	170.7	132.8	8815.2
3426.2	234	2	8.4	1793.8	171.6	77.2	8867.2
3487.0	234	9	8.4	561.2	171.6	-93.8	7686.6
3547.7	234	17	7.7	2794.1	132.0	224.1	8895.8
3608.5	235	1	7.9	2308.9	142.1	157.9	9572.1
3669.2	235	8	8.1	392.3	150.9	-98.3	8317.0
3730.0	235	16	8.4	2461.0	186.9	154.2	8924.7
3790.8	235	23	8.6	2475.8	196.4	153.0	9513.0
3851.5	236	6	8.1	374.3	156.2	-106.5	8184.8
3912.3	236	14	7.5	2268.6	128.8	150.9	8841.1
3973.0	236	23	7.0	2929.5	97.2	240.5	10320.2
4033.8	237	7	7.2	338.0	101.5	-61.2	9219.8
4094.5	237	16	6.9	2993.6	89.5	249.4	10804.4
4155.3	238	1	7.0	2999.1	92.5	253.7	12395.6
4216.0	238	13	5.0	455.1	31.1	6.4	11623.0
4276.8	239	2	4.6	4086.9	24.2	288.3	14477.9
4337.5	239	16	4.3	695.1	19.3	29.8	13908.7
4398.3	240	8	3.7	4955.0	13.1	292.7	17517.2
4398.3	240	8	3.6	0.0	7.4	293.6	17517.2
4462.2	240	23	4.4	4362.2	21.4	279.8	20555.7
4526.1	241	15	3.9	850.9	15.8	36.1	19999.8
4589.9	242	9	3.5	3735.8	12.3	194.3	22246.8
4653.8	242	21	5.5	3076.6	42.1	224.9	24031.7
4717.7	243	8	6.0	1213.9	54.0	59.9	23924.4
4781.6	243	18	6.3	2378.4	58.5	174.7	24992.2
4845.5	244	7	4.8	2067.8	27.7	128.6	25767.1
4909.3	244	20	4.8	1647.1	30.6	93.7	26080.7
4973.2	245	9	5.2	862.7	44.1	25.8	25534.3
5037.1	245	18	7.0	1331.4	107.5	38.3	25245.0
5101.0	246	3	6.7	966.4	21.0	79.6	25337.6
5101.0	246	3	6.8	0.0	93.9	-16.1	25337.6
5161.6	246	12	6.6	681.5	22.9	51.5	25167.7
5222.1	246	21	7.5	1208.8	31.7	117.2	25551.0
5282.7	247	4	7.8	572.6	34.0	39.4	25311.9

5343.2	247	12	8.1	722.2	37.6	59.1	25230.2
5403.8	247	19	8.3	1090.6	204.1	-53.8	24331.7
5464.3	248	2	8.7	730.3	224.4	-119.4	23014.8
5524.9	248	9	8.6	548.6	216.4	-138.9	21535.4
5585.5	248	16	8.2	1147.6	42.8	113.1	21852.6
5646.0	249	2	6.5	1132.6	20.6	100.9	22140.2
5646.0	249	2	6.8	0.0	87.8	-31.3	22140.2
5716.4	249	13	6.1	751.0	21.8	43.1	21748.7

Appendix D: Results of simulations from Gothenburg to Rio de Janeiro

Distance from the start (nm)	Time (day of the year/ Hour of the day)		Speed (kn)	Generation (kW)	Rotor Consumption (kW)	Balance propulsion systems (kW)	Accumulated balance with electric systems (kWh)
0.0	213	7	5.4	0.0	50.3	110.1	-160.0
60.6	213	16	7.0	1913.9	110.8	109.0	339.6
121.1	214	0	7.2	1900.4	114.3	110.7	683.4
181.7	214	9	7.3	1109.8	117.8	15.2	225.5
242.2	214	17	7.1	1889.6	113.9	106.3	537.0
302.8	215	2	6.9	1699.3	108.5	83.7	658.3
363.4	215	11	6.6	1098.4	94.6	25.0	245.4
423.9	215	21	6.3	2046.8	84.7	128.7	808.1
484.5	216	7	5.8	1431.9	52.1	84.5	959.7
545.0	216	17	5.9	1665.0	60.2	102.8	1295.2
545.0	216	17	6.2	0.0	62.4	94.2	1295.2
608.9	217	4	5.8	2145.3	56.6	137.8	2043.6
672.8	217	19	4.5	1722.7	29.5	92.7	2363.1
736.7	218	10	4.1	2255.3	13.9	131.8	3319.0
800.6	219	0	4.5	2710.0	16.0	175.9	4814.6
864.4	219	10	6.4	805.4	24.2	55.9	4673.3
928.3	219	21	6.1	2580.5	21.6	223.2	6288.5
992.2	220	8	5.6	1649.1	17.0	127.9	6947.7
1056.1	221	2	3.6	3505.8	4.1	192.8	9134.8
1120.0	221	18	4.0	1228.1	5.6	70.5	9143.6
1183.8	222	8	4.5	3880.6	8.9	262.4	11895.8
1247.7	223	2	3.6	5365.9	7.4	297.6	15899.2
1247.7	223	2	3.5	0.0	11.9	63.7	15899.2
1308.5	223	16	4.2	1062.4	10.9	62.8	15795.3
1369.2	224	5	4.7	3787.7	10.0	283.4	18550.1
1430.0	224	17	5.1	2998.2	11.3	238.3	20571.9
1490.7	225	2	7.1	2606.3	28.9	275.9	22332.7
1551.5	225	11	7.0	795.6	32.2	59.0	22237.0
1612.3	225	19	7.4	2607.4	33.1	282.9	23993.8
1673.0	226	3	7.1	1852.7	32.8	184.0	24968.0
1733.8	226	11	7.6	1088.6	33.4	103.3	25233.4
1794.5	226	19	8.2	2188.0	48.3	247.5	26546.4
1855.3	227	2	8.7	1555.6	50.2	173.2	27264.9
1916.0	227	9	8.6	350.0	48.5	1.0	26777.0
1976.8	227	16	8.3	2213.3	45.0	258.1	28150.6
2037.5	227	24	8.0	2302.0	42.2	261.9	29603.6
2098.3	228	7	7.9	129.8	38.3	-21.5	28898.2
2159.0	228	14	8.6	2105.3	48.5	249.8	30167.0
2219.8	228	21	8.6	2226.8	48.5	267.0	31557.4
2280.6	229	5	8.6	474.9	48.9	18.1	31189.6
2341.3	229	12	8.3	1145.4	47.9	108.0	31469.0

2402.1	229	19	8.5	1768.3	53.5	194.1	32355.1
2462.8	230	3	7.9	1226.2	39.1	120.8	32744.6
2523.6	230	10	8.1	302.7	43.7	-3.4	32192.6
2584.3	230	19	7.3	2234.9	31.8	236.8	33580.5
2645.1	231	4	6.6	1775.3	24.2	167.4	34483.3
2705.8	231	14	5.8	739.5	16.3	53.9	34313.6
2766.6	232	2	5.3	2701.9	13.0	221.1	36057.1
2827.3	232	14	4.9	62.7	10.6	-5.6	35115.8
2888.1	233	3	4.9	2813.7	10.6	215.4	36925.7
2948.9	233	16	4.7	55.3	9.2	-4.9	35960.4
3009.6	234	5	4.7	2834.2	9.7	209.1	37762.0
3070.4	234	17	4.8	995.8	13.1	66.2	37714.0
3131.1	235	6	4.6	2500.4	30.9	157.4	38874.4
3191.9	235	19	5.0	2096.7	36.8	134.9	39667.1
3252.6	236	6	5.6	1130.9	47.0	56.8	39523.1
3313.4	236	16	5.9	1310.5	63.3	63.6	39456.9
3374.1	237	2	6.1	1549.2	66.1	89.6	39651.6
3434.9	237	12	6.2	196.7	66.2	-46.2	38503.6
3495.6	237	22	6.2	1229.9	66.2	58.4	38389.0
3556.4	238	7	6.2	234.5	60.7	-36.7	37346.8
3617.2	238	17	6.5	1693.1	69.7	111.1	37731.3
3677.9	239	2	6.7	1838.2	77.1	125.8	38237.0
3738.7	239	11	6.9	233.9	84.8	-58.2	37111.3
3799.4	239	19	7.1	2320.0	92.4	179.8	38047.3
3860.2	240	3	7.4	1348.1	102.2	61.3	37975.8
3920.9	240	11	7.5	522.4	113.3	-48.5	37019.8
3981.7	240	19	7.8	2272.5	124.4	167.4	37778.2
4042.4	241	3	8.0	1297.7	135.0	36.9	37528.6
4103.2	241	10	8.4	285.3	154.9	-115.5	36184.6
4163.9	241	17	8.4	2426.2	154.9	180.0	36981.5
4224.7	242	0	8.7	2027.9	172.4	116.8	37309.5
4285.5	242	7	8.8	301.5	181.0	-137.4	35875.4
4346.2	242	14	8.9	1973.6	188.9	100.6	36084.0
4407.0	242	21	8.9	2159.3	189.0	127.4	36475.9
4467.7	243	4	8.9	467.6	189.6	-121.1	35170.2
4528.5	243	11	8.8	490.4	181.4	-110.5	33920.6
4589.2	243	17	8.8	2151.7	178.6	132.4	34352.3
4650.0	244	1	8.6	1879.6	168.5	97.9	34548.9
4710.7	244	8	8.1	216.5	134.9	-106.2	33221.0
4771.5	244	16	7.9	2223.1	129.0	161.8	33922.9
4832.2	244	23	7.9	2365.7	126.1	180.2	34774.2
4893.0	245	7	7.6	164.6	116.3	-95.6	33454.9
4953.8	245	16	7.4	2041.1	110.4	139.5	34022.7
5014.5	246	0	7.1	2385.7	102.2	177.9	34941.8
5075.3	246	9	7.0	102.7	101.8	-90.1	33543.6
5136.0	246	18	6.8	2333.2	31.8	229.3	34967.4
5196.8	247	2	6.9	1434.5	25.4	138.7	35568.0
5257.5	247	11	7.4	133.1	36.3	-20.1	34826.7
5318.3	247	19	7.7	1641.9	33.0	173.9	35651.1

5379.0	248	3	7.6	743.9	32.4	60.7	35576.8
5439.8	248	10	8.2	172.0	44.2	-20.9	34905.8
5500.5	248	17	8.3	1500.4	45.8	159.9	35561.7
5500.5	248	17	8.7	0.0	78.8	86.7	35561.7
5573.3	249	4	6.8	1186.5	27.1	83.2	35704.2
5646.0	249	20	4.4	731.0	7.9	36.7	35078.8

Appendix E: Results of simulations from Los Angeles to Shanghai

Distance from the start (nm)	Time (day of the year/ Hour of the day)		Speed (kn)	Generation (kW)	Rotor Consumption (kW)	Balance propulsion systems (kW)	Accumulated balance with electric systems (kWh)
0.0	91	7	3.8	0.0	13.5	270.1	-160.0
63.6	91	20	4.7	3975.5	33.0	262.3	2588.7
127.3	92	5	7.4	1234.5	130.7	13.1	2100.3
190.9	92	13	8.3	1797.8	179.0	54.1	1977.9
254.6	92	21	8.1	2565.3	191.9	133.2	2476.7
318.2	93	5	7.5	1165.0	142.9	-6.3	1825.9
381.9	93	14	7.2	1591.9	126.7	54.3	1687.9
445.5	93	23	7.0	2670.5	114.3	181.3	2693.1
509.2	94	8	6.8	326.1	102.4	-67.3	1415.5
572.8	94	18	6.5	2626.0	87.0	182.9	2514.0
636.5	95	4	6.5	1946.8	83.3	114.0	2948.1
700.1	95	14	6.4	1234.8	81.0	42.8	2677.3
763.8	95	24	6.3	2544.3	81.4	172.1	3702.2
827.4	96	10	6.3	256.5	82.9	-57.4	2421.4
891.1	96	20	6.3	2502.4	85.8	162.4	3353.2
954.7	97	6	6.3	1289.4	72.2	56.3	3215.6
1018.4	97	16	6.6	1796.4	86.9	98.3	3490.3
1082.0	98	1	6.6	2333.9	92.9	147.6	4243.3
1145.7	98	11	6.7	313.2	84.2	-51.5	3081.0
1209.3	98	21	6.7	2236.5	93.3	143.2	3773.0
1272.9	99	6	6.8	802.4	87.0	-1.5	3102.4
1336.6	99	15	6.8	1816.7	89.5	104.9	3428.7
1400.2	100	0	7.1	2130.2	49.1	190.0	4497.8
1463.9	100	9	7.2	212.5	48.1	-24.1	3664.1
1527.5	100	18	7.3	2121.2	41.3	201.8	4814.1
1591.2	101	2	7.3	1695.3	34.5	158.7	5592.3
1654.8	101	11	7.2	402.0	30.8	14.7	5104.1
1718.5	101	20	7.2	2026.5	34.3	193.7	6203.7
1782.1	102	5	7.2	1003.1	34.5	78.2	6276.7
1845.8	102	14	7.2	1246.8	28.2	112.0	6649.8
1909.4	102	23	7.2	2074.1	34.2	199.5	7798.8
1973.1	103	8	7.2	175.9	29.0	-9.1	7099.6
2036.7	103	17	7.2	2042.9	33.2	198.0	8230.7
2100.4	104	1	7.2	1889.1	29.6	184.5	9241.0
2164.0	104	10	7.2	227.0	35.3	-9.7	8534.8
2227.7	104	19	7.2	1973.0	30.6	191.2	9613.1
2291.3	105	4	7.1	1150.0	29.8	97.9	9864.3
2355.0	105	13	7.2	909.0	119.3	-16.4	9101.2
2418.6	105	21	7.6	1693.4	120.0	81.1	9194.5
2482.3	106	6	7.7	497.9	120.7	-60.7	8110.9
2545.9	106	15	7.2	1395.5	34.2	123.3	8583.3
2609.5	106	23	7.2	1909.8	30.3	184.7	9602.1
2673.2	107	8	7.2	110.4	28.8	-16.4	8834.6

2736.8	107	17	7.2	1796.6	28.4	174.7	9761.1
2800.5	108	2	7.2	1525.9	29.3	144.2	10413.9
2864.1	108	11	7.3	368.9	29.3	12.8	9913.0
2927.8	108	19	7.3	1691.2	29.2	165.2	10741.0
2991.4	109	4	7.3	981.4	35.2	78.0	10810.5
3055.1	109	13	7.3	924.7	36.6	69.2	10803.6
3118.7	109	22	7.3	1627.1	32.6	153.7	11534.6
3182.4	110	6	7.3	415.9	33.5	14.2	11048.0
3246.0	110	15	7.3	1417.6	29.9	132.1	11591.0
3309.7	110	24	7.2	1744.3	27.0	171.3	12482.4
3373.3	111	8	7.3	111.6	131.5	-118.6	10848.9
3437.0	111	17	7.5	1669.1	133.1	63.9	10796.8
3500.6	112	1	7.7	1575.8	137.0	54.5	10669.5
3564.3	112	9	7.9	256.5	140.3	-108.6	9222.5
3627.9	112	17	8.0	1596.0	144.3	56.0	9110.9
3691.6	113	2	7.3	1480.4	29.8	141.0	9726.2
3755.2	113	11	7.4	329.3	28.6	9.4	9202.0
3818.9	113	19	7.3	1642.1	27.6	161.6	9997.1
3882.5	114	4	7.4	1046.8	38.8	82.7	10106.7
3946.1	114	12	7.4	818.1	38.5	57.0	9995.1
4009.8	114	21	7.5	1499.0	39.0	136.8	10564.5
4073.4	115	5	7.5	627.4	40.6	33.2	10251.8
4137.1	115	14	7.5	1156.8	42.4	94.6	10459.6
4200.7	115	22	7.6	1551.2	40.9	145.3	11087.0
4264.4	116	7	7.7	355.8	39.2	3.7	10537.0
4328.0	116	15	7.7	1427.2	37.4	134.9	11074.8
4391.7	116	23	7.7	1553.3	35.5	152.9	11758.4
4455.3	117	7	7.9	132.1	159.1	-142.8	10043.0
4519.0	117	15	8.0	1452.5	157.2	25.0	9684.5
4582.6	117	23	8.0	1536.1	155.6	37.0	9421.2
4646.3	118	7	8.1	153.7	158.5	-139.0	7772.1
4709.9	118	15	8.2	1413.0	157.6	24.9	7422.6
4773.6	118	22	8.4	1585.0	154.7	54.1	7302.0
4837.2	119	7	7.3	270.4	26.9	4.1	6726.9
4900.9	119	16	7.5	1487.3	133.0	41.2	6481.4
4964.5	119	24	7.7	1642.0	130.5	67.3	6458.6
5028.2	120	8	7.8	175.4	128.9	-107.3	5020.1
5091.8	120	16	7.7	1716.9	118.6	89.8	5183.4
5155.4	121	1	7.6	1664.7	120.1	79.6	5263.2
5219.1	121	10	7.0	172.7	91.9	-72.8	3971.8
5282.7	121	19	7.1	1657.4	92.0	91.6	4167.2
5346.4	122	4	7.0	1162.9	89.5	38.4	3879.8
5410.0	122	13	7.0	793.0	89.6	-2.5	3220.4
5473.7	122	22	6.9	1473.1	87.7	72.5	3243.2
5537.3	123	7	6.8	333.5	87.7	-51.9	2110.1
5601.0	123	17	6.7	1484.4	87.4	68.2	2092.6
5601.0	123	17	6.7	0.0	87.4	69.8	2092.6
5662.7	124	2	6.6	1407.0	22.3	129.1	2641.9
5724.4	124	11	6.7	295.6	26.2	6.0	2054.4

5786.1	124	20	7.1	1276.6	33.5	113.6	2432.9
5847.9	125	5	7.1	840.8	32.1	63.9	2379.5
5909.6	125	14	6.5	1156.6	28.6	93.6	2602.5
5971.3	126	0	6.2	1689.0	22.7	146.5	3366.3
6033.0	126	11	5.9	180.9	17.7	-0.4	2631.1
6094.8	126	21	5.9	1715.5	17.2	147.9	3440.7
6156.5	127	7	6.0	557.4	15.9	38.0	3029.3

Appendix F: Results of simulations from Shanghai to Los Angeles

Distance from the start (nm)	Time (day of the year/ Hour of the day)		Speed (kn)	Generation (kW)	Rotor Consumption (kW)	Balance propulsion systems (kW)	Accumulated balance with electric systems (kWh)
0.0	91	7	6.6	0.0	29.5	119.4	-160.0
61.7	91	17	6.4	1617.1	68.6	100.1	288.4
123.4	92	2	6.8	1536.2	75.4	92.8	497.0
185.2	92	10	7.1	198.6	88.5	-65.6	-684.1
246.9	92	19	7.6	1369.6	112.7	55.6	-800.9
308.6	93	2	8.0	1002.8	137.9	-8.1	-1403.7
370.3	93	10	7.8	132.1	141.8	-125.2	-2955.6
432.1	93	18	7.6	1249.1	132.9	20.1	-3362.4
493.8	94	3	7.4	981.5	31.9	85.8	-3230.5
555.5	94	11	7.6	262.4	38.8	-6.4	-3849.8
555.5	94	11	7.5	0.0	36.3	135.4	-3849.8
619.1	94	19	7.5	1529.6	34.5	145.8	-3206.9
682.8	95	4	7.4	925.8	37.0	71.3	-3195.8
746.4	95	12	7.5	693.9	36.1	45.4	-3404.9
810.1	95	21	7.5	1559.3	34.2	148.3	-2735.8
873.7	96	5	7.6	381.6	35.0	10.2	-3239.6
937.4	96	14	7.6	1181.7	37.5	104.1	-2955.2
1001.0	96	22	7.8	1628.7	41.4	157.3	-2239.6
1064.7	97	6	7.8	218.7	54.6	-27.8	-3037.5
1128.3	97	15	7.0	1467.6	108.3	53.6	-3186.1
1192.0	98	0	7.1	1945.2	120.8	95.2	-2959.1
1255.6	98	9	7.1	394.3	106.0	-62.0	-4142.9
1319.3	98	18	7.2	1991.1	116.8	108.8	-3800.6
1382.9	99	2	7.5	1595.4	86.9	101.5	-3533.8
1446.6	99	11	7.5	508.9	142.0	-82.0	-4823.2
1510.2	99	19	7.5	1763.3	150.0	57.7	-4927.6
1573.9	100	4	7.4	1078.9	148.7	-22.5	-5718.1
1637.5	100	12	7.5	961.5	150.8	-38.1	-6640.5
1701.2	100	21	7.5	1837.8	127.3	89.2	-6477.2
1764.8	101	5	7.6	602.2	143.3	-71.5	-7665.1
1828.4	101	14	7.5	1386.6	144.1	19.6	-8092.4
1892.1	101	22	7.5	1743.3	146.6	58.2	-8192.6
1955.7	102	7	7.5	513.4	122.8	-62.6	-9322.0
2019.4	102	15	7.5	1637.1	123.8	67.9	-9340.1
2083.0	102	24	7.4	1905.5	119.6	101.5	-9068.7
2146.7	103	9	7.3	387.7	116.1	-71.4	-10296.8
2210.3	103	17	7.3	1955.4	114.5	109.7	-9950.2
2274.0	104	2	7.3	1708.1	114.1	81.3	-9851.6
2337.6	104	11	7.3	536.0	114.2	-53.1	-10930.9
2401.3	104	20	7.3	1892.6	115.9	100.1	-10667.2
2464.9	105	4	7.2	1057.3	116.7	3.5	-11251.7
2528.6	105	13	7.3	1262.2	130.2	14.6	-11734.9
2592.2	105	22	7.2	1922.5	129.2	89.2	-11566.1

2655.9	106	7	7.2	580.1	128.4	-63.1	-12747.8
2719.5	106	16	7.1	1793.3	104.2	95.3	-12520.7
2783.2	107	1	7.1	2039.5	107.4	120.2	-12070.6
2846.8	107	10	7.1	340.8	114.6	-76.3	-13374.1
2910.5	107	19	7.1	1978.5	119.2	102.7	-13082.5
2974.1	108	4	7.1	1421.6	125.0	33.7	-13407.7
3037.8	108	13	7.1	902.9	123.1	-22.3	-14234.9
3101.4	108	21	7.2	1882.1	108.1	103.8	-13934.6
3165.0	109	6	7.2	645.2	103.7	-31.1	-14832.5
3228.7	109	15	7.2	1786.0	110.4	92.1	-14638.0
3292.3	110	0	7.2	2037.7	109.1	120.3	-14191.4
3356.0	110	9	7.1	306.1	108.1	-73.8	-15474.6
3419.6	110	18	7.1	2075.1	105.6	125.7	-14974.5
3483.3	111	3	7.1	1827.4	105.2	97.2	-14729.1
3546.9	111	12	7.0	674.7	107.1	-32.6	-15658.6
3610.6	111	21	7.0	2022.7	96.0	127.6	-15137.5
3674.2	112	6	6.9	869.8	102.0	-7.9	-15857.0
3737.9	112	16	6.9	1782.7	107.1	86.0	-15709.5
3801.5	113	1	6.9	2164.5	94.7	138.7	-15072.3
3865.2	113	10	6.9	305.6	112.2	-79.1	-16450.6
3928.8	113	19	7.0	2157.6	107.1	130.6	-15900.6
3992.5	114	4	7.1	1447.9	97.8	63.0	-15963.5
4056.1	114	13	7.1	1396.1	103.8	52.1	-16123.6
4119.8	114	22	7.1	2172.8	107.5	133.6	-15550.5
4183.4	115	7	7.1	692.8	95.6	-18.5	-16345.4
4247.1	115	16	7.1	2001.5	100.2	122.0	-15876.9
4310.7	116	1	7.0	2248.6	101.2	147.2	-15177.8
4374.3	116	10	7.0	336.4	100.0	-62.7	-16377.0
4438.0	116	19	7.1	2214.7	96.5	149.2	-15663.4
4501.6	117	4	7.1	1482.5	93.6	72.0	-15645.2
4565.3	117	13	7.2	1238.7	93.1	46.1	-15858.2
4628.9	117	22	7.2	2062.7	95.4	137.3	-15261.7
4692.6	118	7	7.2	512.7	93.2	-35.2	-16192.7
4756.2	118	16	7.2	1959.2	93.5	127.8	-15680.8
4819.9	119	1	6.9	1988.7	30.6	185.3	-14618.7
4883.5	119	10	6.9	301.0	28.9	3.8	-15227.0
4947.2	119	19	6.8	2059.6	23.4	197.0	-14040.5
5010.8	120	5	6.8	1452.0	27.4	127.1	-13503.8
5074.5	120	14	6.7	1262.5	23.2	109.6	-13127.4
5138.1	120	24	6.6	2169.9	29.1	196.0	-11912.7
5201.8	121	9	6.7	205.4	92.5	-70.8	-13242.7
5265.4	121	19	6.6	2334.4	69.6	171.3	-12261.1
5329.1	122	5	6.6	1573.7	71.2	93.0	-12040.9
5392.7	122	14	6.7	1530.6	75.6	86.7	-11883.4
5456.4	122	23	7.0	2313.2	83.5	169.9	-10971.3
5520.0	123	8	7.1	341.0	89.2	-51.2	-12056.8
5583.7	123	17	7.3	2320.7	96.5	168.4	-11194.8
5647.3	124	1	7.6	2019.3	116.1	126.4	-10725.4
5710.9	124	9	7.9	382.8	130.4	-83.0	-11961.1

5774.6	124	17	8.1	2223.7	147.4	136.8	-11438.4
5838.2	125	1	8.4	2055.3	166.7	104.2	-11179.2
5901.9	125	8	8.8	365.6	207.3	-156.7	-12818.7
5965.5	125	15	8.7	2220.1	222.5	80.9	-12739.1
6029.2	125	23	7.8	2625.0	36.2	285.2	-10981.5
6092.8	126	13	4.7	506.4	8.8	28.9	-11533.7
6156.5	127	8	3.4	5707.6	3.9	300.1	-7294.2